RELATIONSHIP OF VEGETATION INDICES FROM DRONE-BASED PASSIVE OPTICAL

SENSORS WITH CORN GRAIN YIELD AND SUGAR BEET ROOT YIELD AND

QUALITY

A Thesis
Submitted to the Graduate Faculty
of the
North Dakota State University
of Agriculture and Applied Science

By

Daniel Owen Olson

In Partial Fulfillment of the Requirements
for the Degree of
MASTER OF SCIENCE

Major Program:
Soil Science

March 2019

Fargo, North Dakota

North Dakota State University
Graduate School

Title

RELATIONSHIP OF VEGETATION INDICES FROM DRONE-BASED
PASSIVE OPTICAL SENSORS WITH CORN GRAIN YIELD AND SUGAR
BEET ROOT YIELD AND QUALITY

By

Dan Olson

The Supervisory Committee certifies that this ***disquisition*** complies with North Dakota

State University's regulations and meets the accepted standards for the degree of

MASTER OF SCIENCE

SUPERVISORY COMMITTEE:

Dr. Amitava Chatterjee

Co-Chair

Dr. David Franzen

Co-Chair

Dr. Aaron Daigh

Dr. Stephanie Day

Approved:

April 9th 2019	Frank Casey
Date	Department Chair

ABSTRACT

The main goal of this study was to calibrate small unmanned aircraft system (SUAS) based vegetation indices with fertilizer-N application rate and yield for corn and sugar beet. It was hypothesized that canopy reflectance would change with increasing fertilizer-N application rates. The objectives of this study were (i) to determine the crop yield and quality in response to fertilizer application rates at two field sites, (ii) map vegetation indices of the experimental plots using drone-based optical sensors, and (iii) calibration of vegetation indices with crop yield. During 2017 and 2018 growing seasons, field trials were conducted to determine corn and sugar beet response to fertilizer-N application rates. In general, the use of optical sensors for quantitative and qualitative relationships were greater after the V6 growth stage in both corn and sugar beet. Early season moisture deficiency, disease, and crop size could impact the quality of the optical sensing data collection.

TABLE OF CONTENTS

LIST OF TABLES

LIST OF FIGURES

LIST OF ABBREVIATIONS

ANOVA ....analysis of variance

DSM..digital surface map

DTM..digital terrain map

ES .... electromagnetic spectrum

ER ....electromagnetic radiation

GDD.. growing degree days

INSEY ....in season estimate of yield

N... nitrogen

NIR... near infrared electromagnetic radiation

NUE ....nitrogen use efficiency

RNDVI...red normalized difference vegetation index

RENDVI ....red edge normalized difference vegetation index

R...red electromagnetic radiation

RE .... red edge electromagnetic radiation

RSP ....recoverable sugar prediction

SUAS ....small unmanned aircraft system

VI ....vegetation index

YP .... yield prediction

LIST OF APPENDIX TABLES

LIST OF APPENDIX FIGURES

INTRODUCTION

Nitrogen (N) is the most limiting nutrient for crop production world-wide (Lawlor et al., 2001; Raun et al., 2011). Nitrogen fertilizer should be carefully managed in regards to timing, rate, source, and placement to increase crop nitrogen use efficiency (NUE) and to reduce environmental impacts from N losses. Nitrogen loss and tie-up are possible through denitrification, leaching, immobilization, and volatilization, which can reduce the NUE (Jenkinson, 2001).

In agricultural systems around the world excess N fertilizer is being applied and results in wasted resources and damage to ground and surface water and release of the greenhouse gas nitrous oxide into the atmosphere. (Good and Beatty, 2011; Hatfield and Follet, 2008). The amount of N fertilizer applied to agricultural production areas and that is ultimately incorporated into crop biomass is quite low. There has been a decrease in conversion of reactive N into harvested product from 68% in the early 1960s to 47% in the 2000s, meanwhile N fertilizer input have increased by factor of 9 over this same time period (Lassaletta et al., 2014). This could possibly be attributed to increase in food demand, soil degradation, and more marginal soils being exploited for crop production.

Nitrogen fertilizer requirements for corn in the Red River Valley range from 135 to 321 kg ha^{-1} based on production area conditions and market values (Franzen et al., 2017; Khan, 2017). In the Red River Valley, current recommendations are to apply 146 kg N ha^{-1} for sugar beet (Lamb et al., 2001; Franzen et al., 2018). Current yields have averaged about 66 Mg ha^{-1} in 2017 (USDA, ERS, 2017).

The yields for corn and sugar beet have been steadily increasing due to a variety of factors including improved management practices, crop genetics, and pest management. The amounts of N fertilizer being applied globally are 100 Tg N yr^{-1} (Lu and Tian, 2017) and even a small increases in NUE that might be gained with the use of optical sensors is worth examination.

There are a variety of remote optical sensors that have been employed in precision agriculture over the past several decades, including thermal and hyperspectral sensors (Toth and Jóźków, 2016; Zhang et al., 2002). Remote sensing technologies are used to contruct vegetation indices (VIs), which are produced by different light wavelength combinations, and have been employed for nutrient monitoring and producing yield estimations with generally high levels of accuracy and success (Clevers, 1997; Martin, 2012).

The recent advent and rapid advance in small unmanned aircraft systems (SUAS) technology has opened up a new dimension in precision agriculture (Tripicchio et al., 2015). The SUAS can be equipped with a range of remote sensors which capture precision data and make it possible to increase NUE, minimize grower's expenses, and reduce environmental impacts (Malveaux et al., 2014).

The objectives of this research:

- To determine the crop yield and quality in response to fertilizer application rates at multiple field sites.

- To map vegetation indices of the experiment using drone-based optical sensors.

- Calibration of vegetation indices with crop yield.

- During 2017 and 2018 growing seasons, field trials were conducted to determine corn and sugar beet response to incremental fertilizer-N application rates.

These field experiments were the first step in determining and calibrating the relationship between optical reflectance and yield and quality. The relationships might be used to together with data from past and future experiments construct algorithms necessary to develop yield prediction models. Farmers desire accurate yield estimates for a variety of reasons including, crop insurance purposes, delivery estimates, harvest and storage requirements, and cash-flow budgeting (Department of Economic Development, 2017). In addition, yield estimates compared to a N-nonlimiting area may be used as a basis for in-season N fertilization for under fertilized areas to regain yield potential. To produce accurate quantitative and qualitative predictions requires many site-years of data within a specific agricultural production area and knowledge of yield field history. The use of SUAS-based optical sensors may expedite the development of yield prediction model.

The SUAS used in this research was a DJI Matrice 100[TM] (DJI, Shenzhen, China) and it was equipped with a MicaSense Red Edge[TM] (MicaSense Inc., Washington, USA) multispectral optical sensor and they were used to collect optical reflectance data from corn and sugar beet with the objective of assessing N status and predicting yield and quality of the crop in the Red River Valley. The data was analyzed with Pix4D[TM] (Pix4D, Lausanne, Switzerland) and ArcGIS[TM] (ESRI, California, USA). Pix4D[TM] produced the VIs and ArcGIS[TM] was used to generate crop height.

LITERATURE REVIEW

Nitrogen fertilizer use in industrial agriculture

Nitrogen is the most limiting nutrient for crop yield and quality (Hasanuzzaman, 2015; Sale 2010; Novoa and Loomis 1981). Although a large percentage of earth's atmosphere is composed of N (78%), but two N atoms are triple-bonded to form N_2 which renders it inaccessible to plants. (Elser, 2011).

In the early 1900's the Haber-Bosch process was developed to synthesize ammonia (NH_3) at the industrial scale (Ertl, 2012). The Haber-Bosch process made it possible to mass produce the N fertilizer that now feeds half the earth's human population (Erisman et al., 2008). Unfortunately, now that N fertilizer was being mass produced it would also lead to a significant disruption of one of Earth's major chemical cycles along with considerable environmental damage due to excess N fertilizer application (Canfield et al., 2010).

Nitrogen fertilizer can be lost by denitrification, leaching, and volatilization (Figure 1). A significant percentage of the N fertilizer is then ultimately destined for the release into ground and surface water as well as the atmosphere (Gu et al., 2009). Only 2-10% of the synthetic N fertilizer created from the Haber-Bosch ultimately makes it to the human consumer (Fields, 2004). Denitrification produces nitrous oxide (N_2O) which is a powerful greenhouse gas. Leaching of NO_3^- may end up in aquatic environments where it has the potential to cause large algal blooms followed by "dead zones" in surface water which are areas that are low in oxygen and support little aquatic life as a result of decomposition of algae after their death.
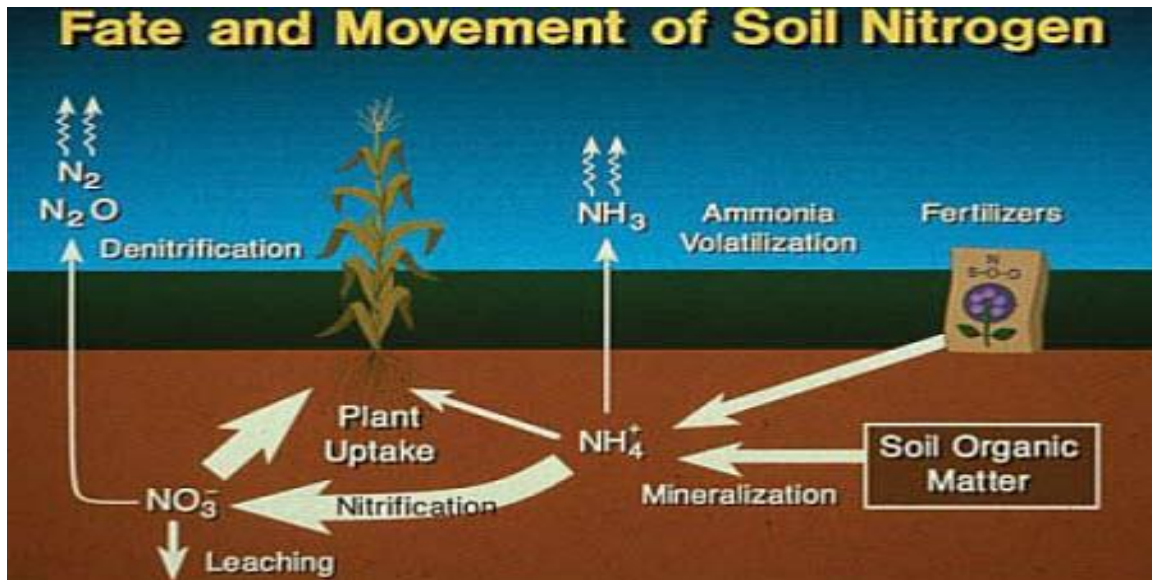
Figure 1. Fate and movement of nitrogen fertilizer
(https://www.pioneer.com/home/site/us/agronomy/nitrogen-losses-corn/).

Crops, like all other organisms require nutrients to grow, reproduce, and complete their

lifecycles. Carbon, hydrogen, and oxygen are the elements that are needed in highest quantities

by plants and are derived from the atmosphere and water (Silva and Uchida, 2000). After these

three elements, N is needed in the highest amounts. Nitrogen is required for many plant

biochemical processes, with one of the most important processes being the relationship between

N and chlorophyll. There is a strong linear relationship between leaf chlorophyll concentration

and leaf N concentration (Lamb et al., 2002; Evans 1989). Due to the unique characteristics of

chlorophyll it is possible to analyze the "optical signature" of the target crop and make

associated assessments and predictions.

Precision agriculture and the use of remote sensing

Precision agriculture is a set of technologies that captures, allows measurement, and

analysis of spatial agronomic data and utilizes it to make informed and optimized management

decisions that would otherwise impossible using conventional agricultural methods and

techniques (Gebbers and Adamchuk, 2010). Precision agricultural technology made steady

advancements in recent years and has been integrated into many kinds of modern agricultural equipment (Lowenberg-DeBoer, 2015). In the past N fertilizer was uniformly applied across agricultural production areas. This meant that some areas received excessive amounts while others were under-fertilized. With precision agricultural technology it has become possible to improve spatial N application rate. When properly utilized precision agriculture has great potential to improve productivity along with minimizing environmental impacts (Bongiovanni and Lowenberg-Deboer, 2004).

The extent of productive agricultural land significantly decreased over the years. Each year more farm land is lost to urbanization, desertification, and a variety of other factors (Foley et al., 2005). For example, 1.8-2.4% loss of global croplands is expected due to urbanization by 2030 (d'Amour et al., 2016). The farmland that exists generally experiences degradation in quality as it is used for industrial agricultural purposes, particularly in Second and Third World countries. Soil degradation is taking place around the world and can come in various forms including erosion, loss of organic matter and nutrients, or from soil compaction (Liu et al., 2010).

Adding further pressure is the ever-rising human population and the demand for food that goes along with it. In 1900 there were approximately 1.6 billion people on earth, with this number increasing to over 6 billion in 2000. Population growth is not expected to slow down into the future (Lutz and Qiang, 2002). According to the department of Economic and Social Affairs, Population Division (2017) estimates that the global human population will exceed 11 billion by 2100. With this unprecedented increase in the human population, demand for food, loss of farm land, and deterioration of soil quality, the development and implementation of precision agriculture systems may be an important approach used to mitigate these monumental pressures.

The art, science, and technology of identification, measurement, and analysis of object features either on, above, or even below the earth's surface without direct contact existing between the sensors and the targets or events being observed is defined as remote sensing (Awange and Kyalo Kiema, 2013; Aggarwal, 2004). In general, there are three types of remote sensing systems: space sensing (satellite imagery), aerial sensing (aerial photography), and ground based sensing (proximal sensor readings) (Mulla, 2013). Each of these has its own distinct advantages and disadvantages.

In addition to the different remote sensing platforms there are also two different types of optical sensing systems, active and passive. Active optical sensors are sensors that produce their own electromagnetic radiation (ER) source and analyze the reflected optical signature (Lamb et al., 2014). Passive optical sensors are reliant on the sun as their ultimate source of ER. Since passive optical sensors are reliant on the sun as their ER source, clouds and intermittent ER conditions can interfere with and degrade the quality of data that they collect. In addition, the optimal time for data collection for passive optical sensors is around solar noon (sun is at its highest point in the sky). Some passive optical sensors can be equipped with down welling ER sensors to compensate for changing ER conditions during data collection. Since active optical sensors produce their own ER source they are not dependent on the ambient ER conditions (Hatfield et al., 2008).

When the optical sensor data is collected and analyzed it becomes possible to indirectly monitor the N status of the target crop. When ER is absorbed and reflected from the crop it creates a unique optical reflectance signature depending on the condition and amount of chlorophyll (Carlson and Ripley, 1997). The returned optical signature can then be transformed

into useful information (VIs or crop height). With the appropriate use of this data, N monitoring

and quantitative and qualitative prediction become possible.

Electromagnetic spectrum and vegetation indices

The electromagnetic spectrum (ES) is broadly classified into categories based on the

wavelength and characteristics of the ER energy (Figure 2). The ES includes radio waves,

microwaves, infrared, visible light, ultraviolet, x-rays, and gamma rays, with the appropriately

named visible region being the only part of the ES that is visible to the human eye (Humboldt

State University, 2014; Sankaran and Ehsani, 201
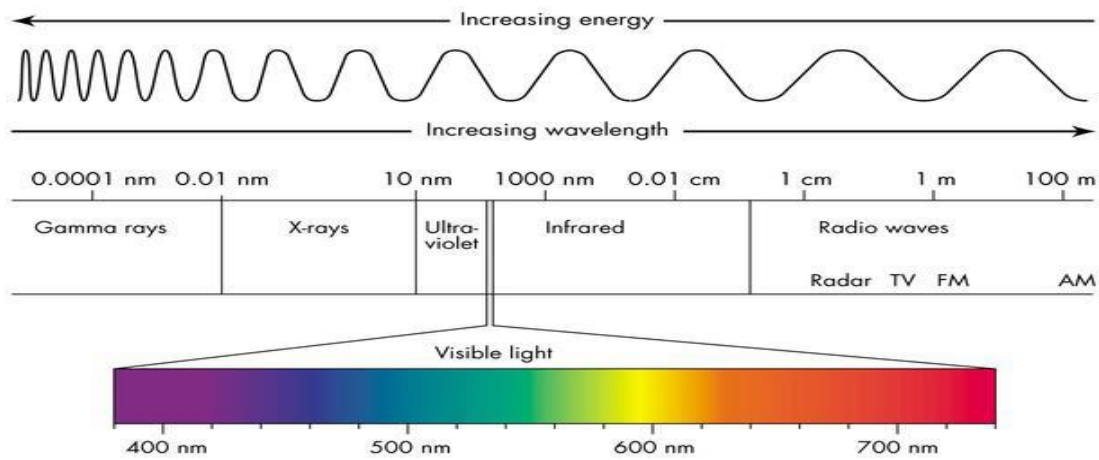
Figure 2. Electromagnetic spectrum (https://sites.google.com/a/coe.edu/principles-of-structural-chemistry/relationship-between-light-and-matter/electromagnetic-spectrum).

When ER impacts matter a portion of the ES is absorbed or reflected. When ER is

absorbed or reflected from an object there are many factors such as shape, size, and material that

dictates the final unique composition of the reflected ER (Dorsey et al., 2008). This is the

phenomenon that is exploited by optical sensors to collect data. The VIs are created by taking

various spectral bands and creating different equations to measure numerous properties of

vegetation (Gutierrez-Rodriguez et al., 2005). The MicaSense Red Edge camera that was

employed in this research is capable of capturing blue, green, red, near infrared (NIR), and red

edge wavelengths (Table 1).

Table 1. Wavelengths captured by the MicaSense Red Edge camera.

Wavelength	Electromagnetic Radiation Spectrum
Blue	475 nm
Green	560 nm
Red	668 nm
Red Edge	717 nm
Near Infrared	840 nm

Dozens of different VIs have been developed with a vast range of purposes (Table 2). In

this study, the two VIs were red NDVI (RNDVI) and red edge NDVI (RENDVI), which have

previously been most examined in the field of precision agriculture. Also crop height from

optical sensor data calculation was also employed in this research.

Table 2. Published vegetation indices.

Index	Algorithm	Source
RNDVI	(NIR-R)/(NIR+R)	Rouse et al., (1973)
RENDVI	(NIR-RE)/(NIR+RE)	Gitelson and Merzyak, (1994)
Crop Height	DSM-DTM	-
GNDVI	(NIR-G)/(NIR+G)	Gitelson and Merzyak, (1998)
GRVI	NIR/G	Sripada et al., (2006)
SR	NIR/R	Jordan, (1969)
ISR	R/NIR	Gong et al., (2003)

(Red normalized difference vegetation index (RNDVI); Red edge normalized difference red edge
index (RENDVI); Green normalized difference vegetation index (GNDVI); Green ratio
vegetation index (GRVI); Simple ratio (SR); Inverted simple ratio (ISR). (NIR=near infrared;
R=red; RE=red edge; DSM=digital surface model; DTM=digital terrain model; G=green)).

In addition to the choice of VI, there are a number of factors that can confound and

change the reliability of the predictive ability of VI algorithms. Some of the variables include

leaf area, soil characteristics, ambient light conditions, disease, amount of accumulated growing

degree days (GDD), or the growth stage that the sensing was done. Furthermore it is possible to obtain the in-season estimate of yield (INSEY) which is the VI divided by the GDD that can act as a normalization of the VI over limited crop growth stages (Raun et al., 2001). Moreover, height can also be used as a component of the predictive algorithm, or it can be used as a stand-alone variable (Sharma and Franzen, 2014; Grenzdörffer, 2014). Figure 3 shows some of the possible methods for obtaining qualitative and quantitative predictions. There can be a wide range of variation in predictive ability depending on what VI or algorithm is employed.
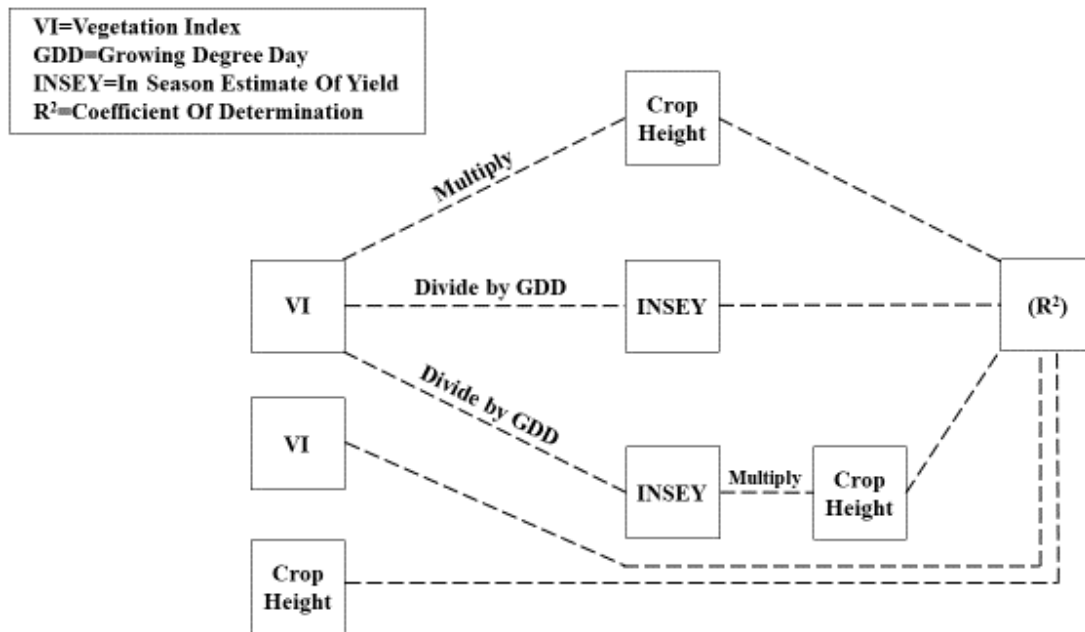
Figure 3. Interactive work flow among yield prediction and vegetation indices.

RNDVI

The red (R) normalized difference vegetation index is an algorithm which uses the NIR and red wavelength of the ES. RNDVI is computed as follows:

$$RNDVI = \frac{Near\ Infrared\ - Red}{Near\ Infrared + Red}$$

The RNDVI value for crops will generally fall into the range of 0.3 to 0.9, with higher values indicating a larger and biologically fit crop with higher levels of chlorophyll. Chlorophyll has the properties of absorbing red and blue ER while reflecting green and infrared ER (Blankenship, 2008.) Exploiting this phenomena it becomes possible to assess the "health" of the crop by taking the reflected ES wavelengths that have been captured by the optical sensor and creating the above algorithm.

The RNDVI was proposed in 1978, by D.W. Deering, and became the most popular VI for studying vegetation health and productivity (Atzberger, 2013). At present there have been many studies that have shown a strong relationship for RNDVI and N status and potential use is revealed (Mkhabela et al., 2011; Huang et al., 2014; Bu et al., 2016). The downside of RNDVI are saturation of RNDVI values over the growing period due to increase in canopy density and diminishing level of clarity (Asrar et al., 1984). Therefore, RNDVI is most useful during the early and mid-development of crop development.

RENDVI

The red edge (RE) normalized difference vegetation index (RENDVI) is similar to RNDVI, but RENDVI uses red edge wavelength (717nm) instead of the red wavelength (668 nm). The RENDVI is computed as follows:

$$RENDVI = \frac{Near\ Infrared\ -\ Red\ Edge}{Near\ Infrared\ +\ Red\ Edge}$$

The RENDVI value for crops will generally fall between 0.1 and 0.3.

RENDVI has been investigated for assessing chlorophyll content in plants since the early 1980s (Horler, 1983). The RENDVI has been employed in agricultural uses with high levels of success (Sharma et al., 2015; Viña, et al., 2011; Li, 2014). The RENDVI is a useful VI early-season, but its use increase as the canopy architecture fill progresses through the season, as the RENDVI is able to function independently of the leaf area index (Horler and Dockray, 1983). Where the RNDVI is associated with leaf area index, RENDVI is more related to the tint, dark compared to light, of the leaves, particularly from the chlorophyll content, although the RENDVI does not measure greenness directly. Therefore RENDVI will retain higher levels of sensitivity than RNDVI during mid to late season periods.

Crop Height

Although crop height is not a VI it can be used in a similar fashion for N monitoring and predictive purposes. Crop height can be calculated by finding the difference between the digital surface model (DSM) and the digital terrain model (DTM) and is calculated as follows:

$$Crop\ Height = \text{Digital Surface Model} - \text{Digital Terrain Model}$$

A DSM is the optical return of the highest points captured in a data set (Crops) and a DTM is the bare earth optical returns of the data set. The DTM can be captured when no crop vegetation is present, or if crop vegetation is present Pix4D^{TM} is capable of extrapolating the elevations under the crop and producing a DTM by the use of various complex algorithms (Unger et al., 2009).

Crops that have attained sufficient N levels will generally have greater have greater biomass and are more vigorous than crops deficient in N. In the same regard crops that are

larger will generally produce higher yield levels. Crop height has been used as a standalone variable for N monitoring and prediction with some high levels of accuracy and success that explained as much as 80% yield variability (Yin et al., 2011; Maresma et al., 2016). In addition, crop height has also been incorporated into monitoring and predictive algorithms with generally positive results that were able to explain as much as 78% of yield variability (Sharma et al., 2016; Yue et al., 2017).

Quantitative and qualitative prediction using optical sensors

Table 3 summarizes results from selected studies using a variety of VIs for N monitoring and predictive purposes (Yin and McClure, 2013; Li et al., 2014; Teal et al., 2006; Sharma et al., 2015; Yin et al., 2011; Tagarakis and Ketterigs, 2017; Bu, 2014; Subedi, 2016; Bu et al., 2016). These studies varied by sensing times, type of remote sensor, soil conditions, temperatures, rainfall, algorithm combinations, mathematical model type, or combinations of pooled site/year data among other factors.

In corn, Yin and McClure found that RNDVI combined (multiplied) with crop height enhanced the R^2 value for N monitoring. RNDVI multiplied by crop height in general had the highest explanatory power during the V6 to the V12 growth stages. In agreement with numerous other studies, Li et al. found that RENDVI in corn had a higher degree of explanatory power for N monitoring than RNDVI after the V6 stage and beyond due to canopy and chlorophyll saturation.

Teal et al. (2006) found in corn the highest degree of explanatory power for yield occurred at the V8 growth using RNDVI. Teal et al (2006) attempted to normalize RNDVI with GDD, but normalization did not improve the explanatory power, contradicting a number of studies. Sharma et al. found in corn that RENDVI normalized with GDD (REINSEY) had the

highest degree of explanatory power at the V12 growth stage for yield. Yin et al. examined the relationship between corn height and yield and found stronger relationships later in the season during the V6, V10, and V12 growth stages. In general V10 and V12 offered the highest explanatory power for corn yield. Tagarakis and Ketterigs used RNDVI and found that RNDVI normalized with GDD (RINSEY) produced a higher degree of explanatory power than RNDVI did in regards to explaining corn yield.

Bu (2014) found in sugar beet that RENDVI normalized with GDD could explain 97% of the variation in N status in sugar beet. Subedi (2016) used both RNDVI and RENDVI normalized with GDD and found a high degree of explanatory power in sugar beet yield at the V13 growth stage compared with the early growth stages of V7. The explanatory power for yield was often strengthened by incorporating crop height into the algorithm. Bu et al. (2016) normalized RNDVI and RENDVI with growing degree days over serval sites and found that that the V13 sensor readings had a higher degree of explanatory power than V6 readings for sugar beet yield prediction, which is in agreement with much of the other literature. Bu (2014) found that the explanatory power for sugar beet quality was higher at the V13 compared to the V6.

Table 3. Various studies using optical sensor data for N monitoring and yield and quality predictions.

Crop	Algorithm	Growth Stage	Objective	R^2	Source
Corn	RNDVI	V6	N monitoring	0.40	Yin and McClure, (2013)
	RENDVI	V6	N monitoring	0.40	Li et al., (2014)
	RNDVI	V8	Quantitative prediction	0.73	Teal et al., (2006)
	INSEY[1]	V12	Quantitative prediction	0.58	Sharma et al., (2015)
	Height	V12	Quantitative prediction	0.74	Yin et al., (2011)
	INSEY[2]	V7	Quantitative prediction	0.78	Tagarakis and Ketterigs, (2017)
Sugar Beet	INSEY[3]	V13	N monitoring	0.97	Bu, (2014)
	RNDVI	V12	Quantitative prediction	0.72	Subedi, (2016)
	RENDVI	V12	Quantitative prediction	0.57	Subedi, (2016)
	INSEY[4]	V13	Quantitative prediction	0.43	Bu et al., (2016)
	INSEY[5]	V13	Quantitative prediction	0.68	Bu et al., (2016)
	INSEY[6]	V13	Qualitative prediction	0.41	Bu, (2014)

([1]: RENDVI/GDD, [2]: RNDVI/GDD, [3]: RENDVI/GDD, [4]: RNDVI/GDD, [5]: RENDVI/GDD, [6]: RNDVI/GDD).

Remote sensors used for N monitoring and qualitative and quantitative prediction in general have moderate to high levels of accuracy depending on the conditions. Rainfall, soil type, temperature, and growth stage will have large impacts on the accuracy of the algorithm. In general the accuracy of the model in explaining N status and yield and quality increases with the accumulation of GDD throughout the crops life cycle.

Small unmanned aerial systems for precision agriculture

Drones or small unmanned aircraft systems (SUAS), have been increasingly making their way into the agricultural sector and are poised for strong growth during the next decade (Research And Markets, 2018).

There are two main categories of SUAS: fixed wing airplane and rotary motor helicopter. Each has its own advantage and disadvantage. Fixed wing airplanes have greater ranges and speeds while the rotary motor helicopters are capable of hovering and focusing on specific

targets (Puri et al., 2017). Flight plans are prepared by control stations that are wirelessly paired

up with the SUAS. SUAS control stations come in a number of forms including computers,

tablets, and controllers that are assisted by GPS aboard the SUAS. Flight plans can be executed

manually or automatically. Automatic flight plans are carried out with the help of multiple GPS

satellites that help the SUAS pinpoint its position.

The data captured by SUAS is then transferred to an image processing service where it is

processed, interpreted and can be acted upon. There are currently multiple image processing

services that are available and can be either PC or cloud based processing. Each image

processing service generally has the same set of features, with some minor differences.

SUAS can be used for many different agricultural purposes including: weed detection,

disease detection, water stress, N monitoring, and soil classification among others (Zhang et al.,

2012). One of the most promising application SUAS is for directing in season application of

fertilizers. After scanning the target field nutrient deficiencies can be located and addressed with

the use of prescription maps generated by image processing services (Figure 4). This reduces

fertilizer input, cost to the producer, and environmental impacts, while maximizing yield and

profit.
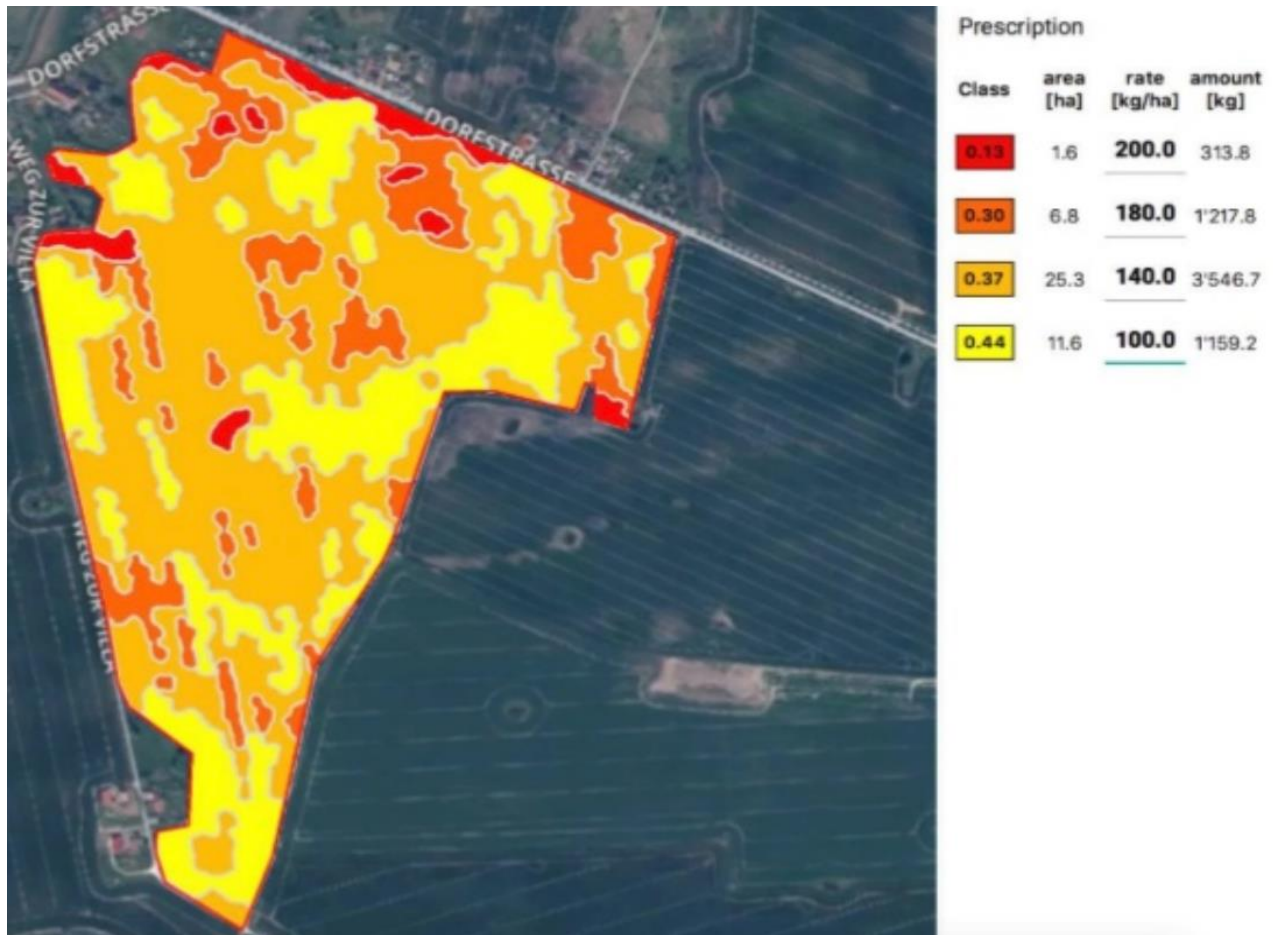
Figure 4. Nitrogen fertilizer prescription map created with Pix4D
(https://www.slideshare.net/valeriiiakovenko/pix4d-agro-innovations-forum-2018-by-droneua).

Effect of nitrogen on corn yield and quality

The United States has the highest corn production in the world. During the 2017 season
the United States produced approximately 371 million Mg with China following with
approximately 216 million Mg (Statista, 2017). Corn is grown in most states in the U.S. but the
majority is grown in the traditional Corn Belt region. This area includes Illinois, Iowa, Indiana,
South Dakota, Nebraska, Kentucky, Ohio, and Missouri (USDA, ERS, 2018). Corn is grown
and used for many purposes including feed and residual, ethanol, export, or for food, seed, or
industrial purposes (Ranum et al., 2014). The majority of the corn that is produced is used for
animal feed, ethanol production, or exported to other countries.

17

Corn, like most crops has experienced significant gains in yield in recent decades. In the United States corn produced grew from 234 million Mg in 1997 to 371 million Mg produced in 2017 (USDA, NASS, 2018). This increase in corn yield can be attributed to numerous factors including disease resistance, genetically modified varieties, precision agriculture, cultural practices, and other management decisions (Egli, 2008).

Corn accumulates about 80% or more of its N requirements after the V6 growth stage (Bender et al., 2013; Mathews, 2001). Therefore it is critical to apply N so that it is available for rapid uptake by corn before or soon after the V6 growth stage. The amount of N applied for corn (ranging between 168 - 280 kg N ha^{-1}) can vary greatly in the Red River Valley based on many different aspects including previous crop, field yield history, and N cost/corn price. In North Dakota N rates of 168 kg to 280 kg ha^{-1} yielded 2.6 million mg in 2000 and by 2017 the yield had risen to 11.4 million Mg (USDA, NASS, 2017).

There are four main sources of N in the soil environment: organic matter and residue decomposition and N release (mineralization), biological N fixation, fertilizer/manure N, and residual synthetic applied N (Ramakrishnan et al., 2015; Pisani et al., 2017). Nitrogen mineralization from organic matter depends on soil moisture, soil temperature, microbial activity, and tillage (Paul, 2016).

Fertilizer N is generally the largest contribution to available N pool that crops draw upon. Crops uptake N in the form of ammonium (NH_4^+) or nitrate (NO_3^-) (Witte, 2011; Von Wiren et al., 1997). The applied N will be taken up as ammonium directly, or go through a microbial conversion pathway and be taken up as nitrate. Under optimum N supply, crop will have earlier canopy closure to reduce weed competition, resulting in higher yield (Hanway, 1962; Alley, 2009).

The effect of N on the yield of corn has been exhaustively examined and confirmed by many experiments in different areas, soil types, harvest dates, N fertilization timing, and N fertilization type, among other factors as briefly summarized in Table 4 (Albus et al., 2008; Bu, 2014; Jokela and Randall, 1989; Mamo et al., 2003; Gehl et al., 2005).

Table 4. Various studies of corn yield response to N fertilizer at different locations and harvest dates.

Source	Location	N kg ha^{-1}	Yield Mg ha^{-1}
Albus et al., (2008)	Carrington, ND	13	4.7
		56	6.0
		112	8.8
		168	10.7
		224	11.5
Bu, (2014)	Valley City, ND	0	8.3
		45	7.5
		90	7.4
		135	8.5
		180	8.3
		225	8.8
Gehl et al., (2004)	Rossville, KS	0	7.9
		250	12.4
		300	12.6
Jokela and Randall, (1989)	Mt. Carroll, MN	0	5.0
		75	7.2
		150	8.0
		225	8.2
Mamo et al., (2003)	Revere, MN	0	8.7
		67	10.5
		134	10.7
		202	11.2

Albus et al found an increase in grain yield, test weight, chlorophyll meter readings, stalk nitrate-N, and grain protein content as the N rate increased. In addition corn silking dates were earlier as N rates increased. Bu (2014) found that that fertilizer N resulted in no statistical difference in yield, but this was heavily influenced by unfavorable weather conditions. Gehl et al (2005) findings were in agreement with much of the literature that as fertilizer N rates increased yields increased. They also found that split application of fertilizer N produced higher yields as opposed to single applications, which lends support for in-season fertilizer applications. Jokela and Randall (1989) found increasing yields as N rates increased. Split fertilizer N

applications failed to produce statistically significantly higher yields in this particular study and could be possibly explained by drier than average conditions experienced during the experiment. Mamo et al (2003) found that increasing levels of fertilizer N offered statistically significant yield increases on an entire field scale level. The experiment broke the field down into individual units and it was found that there was a yield increase on only half of the landscape. This lends support for the use of site specific precision fertilizer use compared to uniform fertilizer application.

A goal of fertilization is achieving the quantitative and qualitative maximum return on investment (Figure 5). In addition, optimum fertilization could help minimize the environmental impacts (Kanter et al., 2015; Zhang et al., 2015).

Nitrogen produces significant effects on the chemical composition of leaves, plant height, and number of leaves (Amin, 2011). In corn, N has positive significant effects on number of cobs, weight of cobs, number of kernels and weight of kernels.
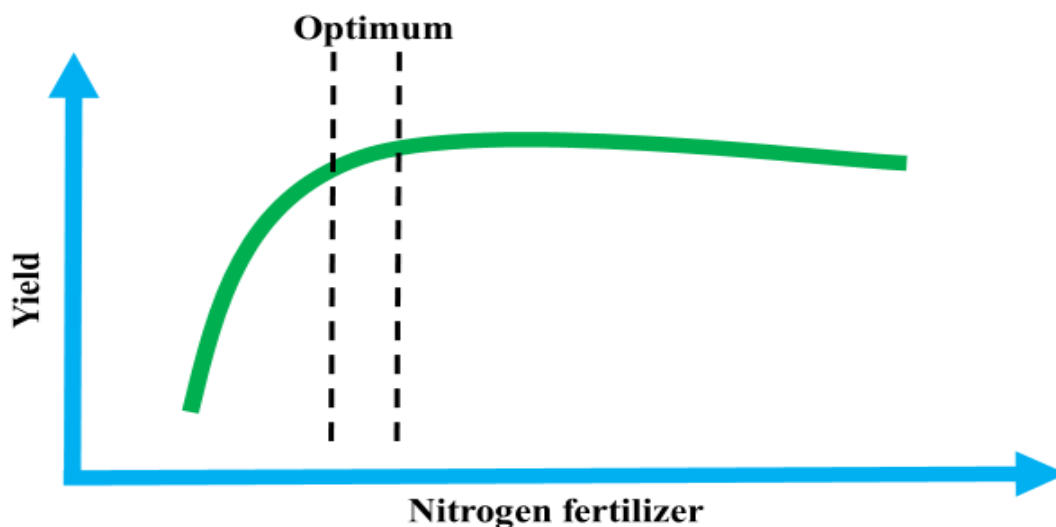
Figure 5. Generalized yield and quality response to N diagram.

Lodging can occur when the corn plants produces too much biomass in higher parts of the corn plant and the stalks are unable to support this added weight. Lodging can increase harvest times and losses, and also increase drying costs. Increasing amounts of N positively affect protein content and mineral compositions (Oktem and Emeklier, 2010). The condition of 'green-snap' is also increased by excessive N application. Green-snap is caused by high winds, usually between V8 and V12 stages, when the corn is growing rapidly and cell walls are not completely developed.

Effect of nitrogen on sugar beet yield and quality

Sugar beet accounts for between 55 and 60% of the US sugar production (USDA, ERS, 2017). In 2001 there were approximately 225 million Mg of sugar beet produced and by 2017 this had risen to around 315 million Mg (Statista, 2017). Increases in sugar beet yields can be attributed to improved disease resistance, development of genetically modified varieties, and precision agriculture.

Nitrogen management is critical in sugar beet production. Less N will reduce the root yield, but excess N can reduce the sucrose concentrations and increase impurities, increasing the cost of processing, which reduces processor profit of independent sugar companies and farmer profitability of production as sugar cooperative members (Malnou et al., 2006; Campbell and Fugate, 2002). Ideally the sugar beet will have adequate N through most of the growing season and will begin to reach a state of deficiency around six weeks prior to harvest (University of Minnesota Extension, 2018). In the Red River Valley there should be no application of N after the first week of July due to risks of increased impurities and reducing sucrose concentrations. This is important because producers are paid through a formula that includes the sucrose

concentration in the sugar beet yield, and reduced by the impurity content of the roots. Therefore it is critical to have the right rate, type, placement, and timing of N.

In the Red River Valley the recommended N rate is 146 kg N ha^{-1} before considering the residual soil N of 120 cm soil depth (Franzen, 2018). The use of the recommended rate of N application resulted in an average of sugar beet yield of 66 Mg in 2017 (USDA, ERS, 2017).

Fertilizer N is generally the largest contribution to available N pool that crops draw upon. Nitrogen will be taken up by sugar beet in the form of ammonium or nitrate (Witte, 2011; Von Wiren et al., 1997). The applied N will be taken up as ammonium directly or go through a microbial conversion pathway and be taken up as nitrate. Sugar beet that has adequate N will have more vigorous growth, be more resistant to pathogens, and will have earlier canopy closure to reduce weed competition resulting in higher yields and greater sucrose yield (Hergert, 2010; Freckelton, 1999).

The effect of N on the yield and quality of sugar beet has been exhaustively examined and confirmed by many experiments in different areas, soil types, harvest dates, N fertilization timing, and N fertilization type, among other factors as briefly summarized in Table 5 (Bu, 2014; Chatterjee et al., 2017; Subedi, 2016; Tarkalson et al., 2012; El-Sarag and Moselhy, 2013).

Table 5. Various studies of sugar beet yield and quality response to N fertilizer at different locations harvest dates.

Source	Location	N kg ha^{-1}	Yield Mg ha^{-1}	Recoverable Sucrose Mg ha^{-1}
Bu et al, (2016)	Thompson, ND	0	56.9	8.4
		34	57.7	8.2
		67	75.5	11.2
		101	64.0	9.4
		135	66.1	8.9
		168	70.3	9.3
Chatterjee et al., (2017)	Sabin, MN	0	69.9	5.0
		112	75.0	4.0
		146	78.3	9.0
		179	78.3	5.0
		213	80.0	3.0
Subedi, (2016)	Crookston, MN	0	48.3	7.7
		112	59.9	9.5
		146	60.4	9.4
		179	67.2	10.2
		213	58.9	8.9
Tarkalson et al., (2012)	Kimberly, ID	0	53.8	7.2
		62	71.3	9.8
		112	74.7	10.4
		157	79.5	11.0
		230	80.7	10.9
El-Sarag and Moselhy, (2013)	North Sinai, Egypt	105	27.6	5.2
		141	35.9	6.7
		176	43.5	8.0
		211	49.5	8.9

Bu et al (2016) found an increase in both yield and recoverable sucrose up until 67 kg of

N hectare, although this experiment was exposed to significant moisture deficiency and sugar

beet root maggot (*Tetanops myopaeformis*). Greater N rates resulted in no additional response,

while yield and recoverable sucrose actually declined with increasing amounts of fertilizer N.

Chatterjee et al (2017) found that the economic rate of return for yield and sucrose were

optimized at 112 kg N ha^{-1}. Increasing rate of fertilizer N beyond 179 kg ha^{-1} could have

potential to reduce recoverable sucrose. Subedi (2016) found that 179 kg ha^{-1} of fertilizer N

produced the highest yield, although this was not statistically significant. Beyond 179 kg N ha^{-1}

yield and recoverable sucrose declined. Tarkalson et al (2012) found increasing yields with the

application of fertilizer N, although higher rates had very little increase in yield. The highest rate

of recoverable sucrose was produced with the application of 157 kg ha^{-1}. Rates above this became detrimental. El-Sarag and Moselhy (2013), found increases for both yield and recoverable sugar to 211 kg ha^{-1}. The goal is to aim for the qualitative and quantitative maximum return on investment (Figure 5). This is extremely critical due to production costs rising faster than the prices of sugar beet commodities (Campbell, 2002). In addition, optimum fertilization could help reduce the environmental impacts (Kanter et al., 2015; Zhang et al., 2015).

As previously explained, too much N late in the growth cycle of sugar beet will result in impurities. The entire focus of sugar beet production is directed toward the 12-20% sucrose mass that is produced by the plant and optimizing the quality and reducing the impurities. Sucrose concentration generally goes up to a certain point. Adding excessive N will lower the sucrose content of the sugar beet, resulting in economic and environmental costs.

MATERIALS AND METHODS

Site description and experimental design

In 2017 corn and sugar beet experiments were located near Ada, MN and Downer, MN. The 2018 corn experiments were located near Ada, MN and Sabin, MN and sugar beet experiments were located near Ada, MN and Downer, MN. Locations, site descriptions, and initial soil properties are presented in Table 6. Figures 6-12 illustrates the experimental site layouts and N fertilization rate that were applied.

Table 6. Location and selected information for experimental sites used in corn and sugar beet experiments in 2017 and 2018.

Characteristic	Ada 2017	Downer 2017	Ada 2018	Downer 2018	Sabin 2018
Location	47°21'20.5" 96°25'43.0"	46°51'55.8" 96°30'55.0"	47°19'41.9" 96°23'48.5"	46°51'52.2" 96°31'05.8"	46°46'18.8" 96°32'51.4"
Crop(s)	Corn Sugar Beet	Sugar Beet	Corn Sugar Beet	Sugar Beet	Corn
Soil Series	Augsburg	Lamoure	Augsburg	Lamoure	Glyndon
Texture	Loam	Silt Loam	Loam	Sandy Loam	Sandy Loam
NO_3-N (kg ha^{-1}) 0-60 cm	41	60	22	26	22
Olsen-P (ppm) 0-15 cm	9	8	5	5	8
Available K (ppm) 0-15 cm	74	98	67	74	110
pH (1:1)	7.0	7.2	8.4	-	8.2
EC (mmhos cm^{-1})	1.15	0.60	0.95	0.65	-
OM (g kg^{-1})	31	46	24	-	26
Previous Crop	Soybean†	Soybean	Spring Wheat	Sugar Beet	Sugar Beet

† Soybean (*Glycine max,*L.,Mer); Spring Wheat (*Triticum aestivum,* L.
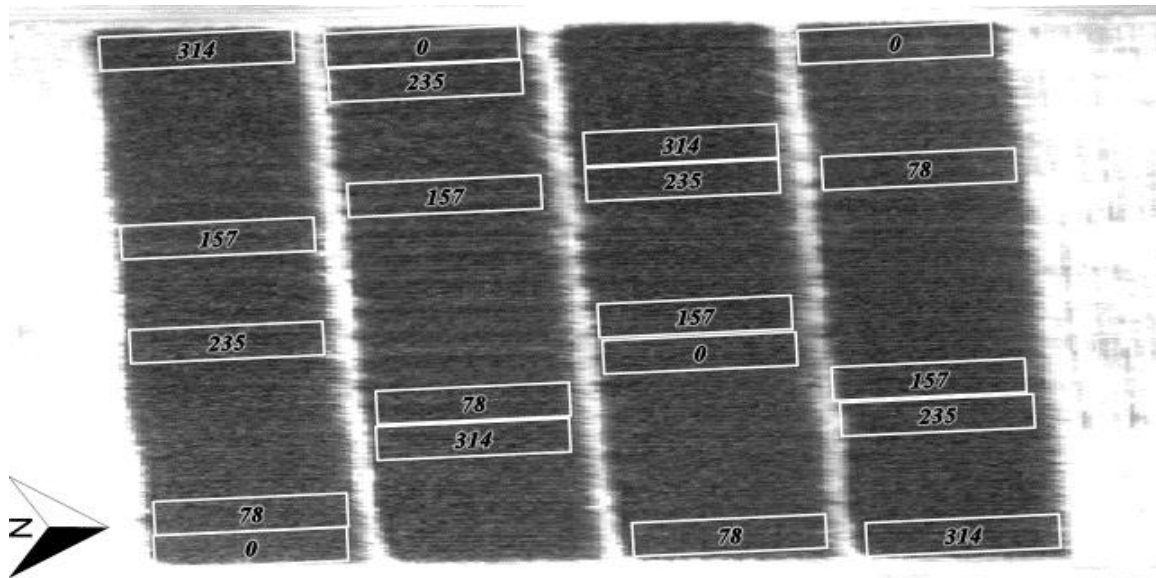
Figure 6. Aerial view of corn experiment at Ada 2017 with N application rates (Units in kg ha^{-1}).
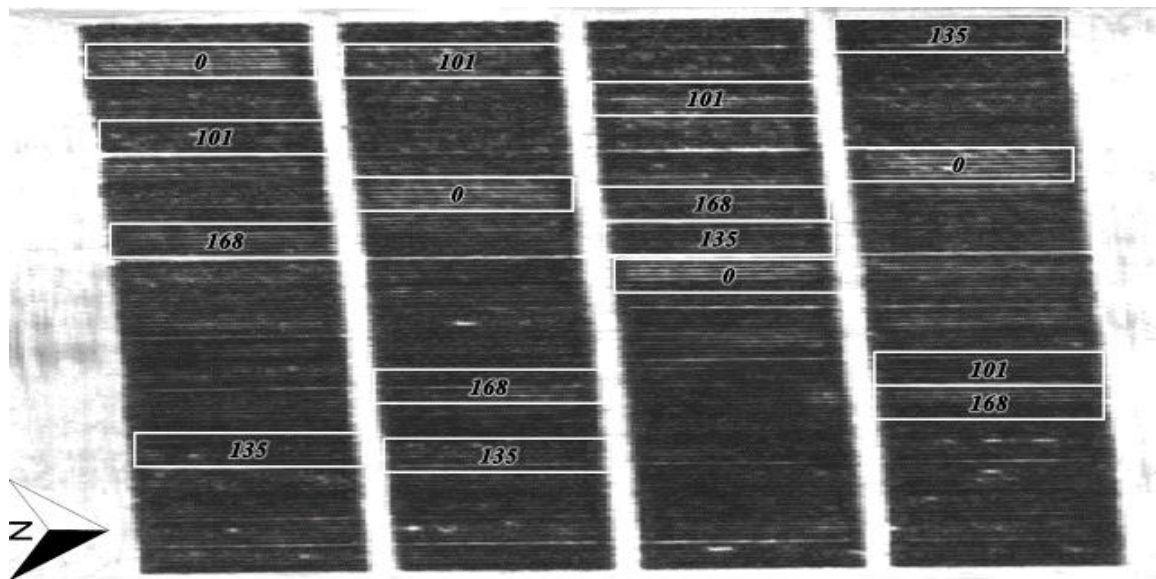
Figure 7. Aerial view of sugar beet experiment at Ada 2017 with N application rates (Units in kg ha^{-1}).
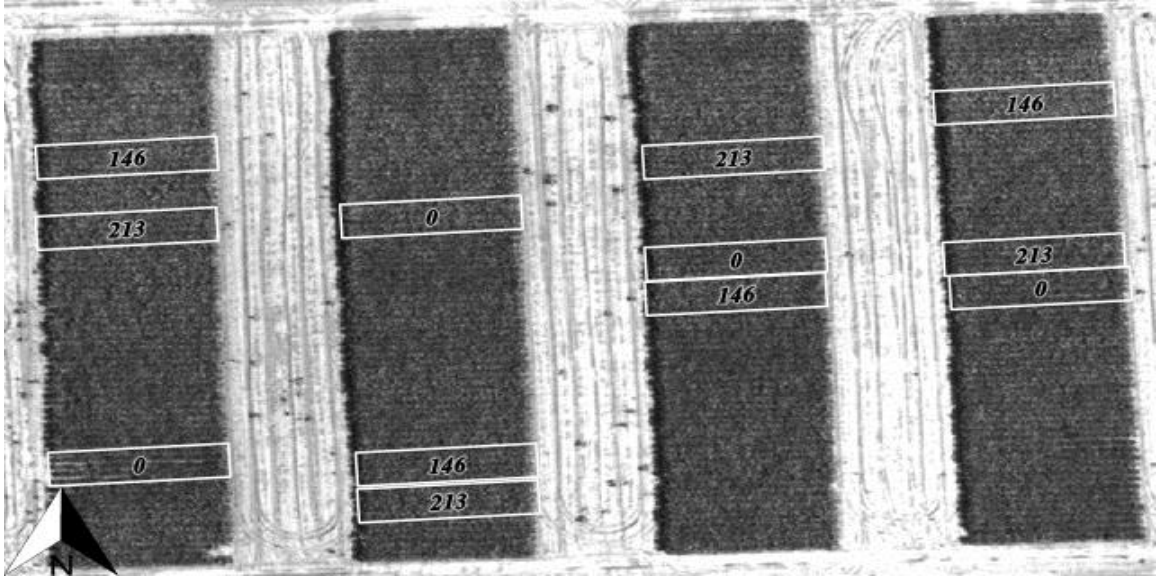
Figure 8. Aerial view of sugar beet experiment at Downer 2017 with N application rates (Units in kg ha^{-1}).
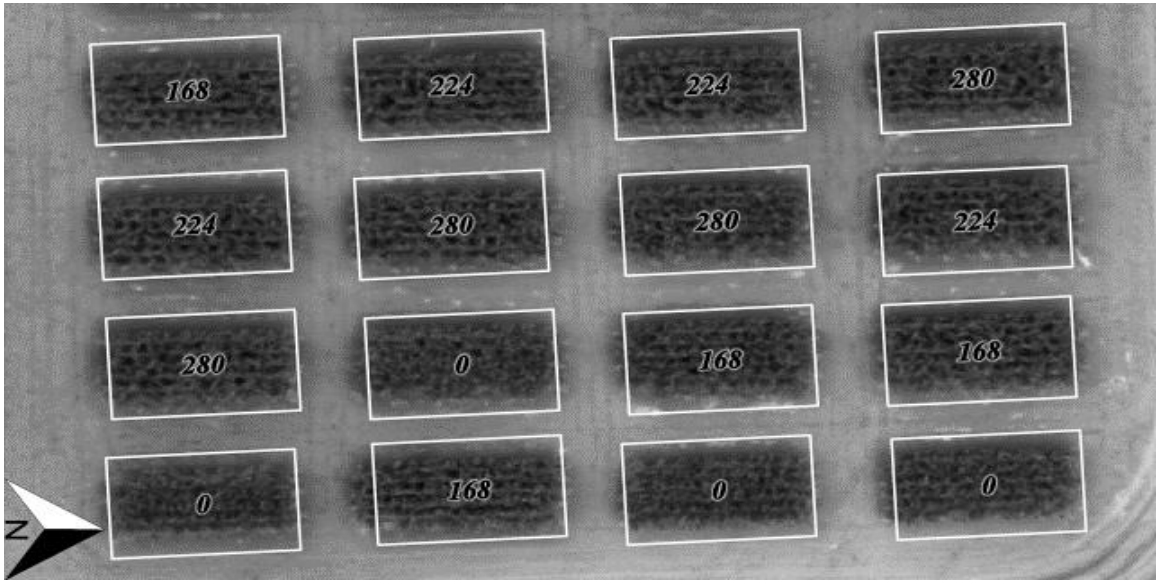
Figure 9. Aerial view of corn experiment at Ada 2018 with N application rates (Units in kg ha^{-1}).
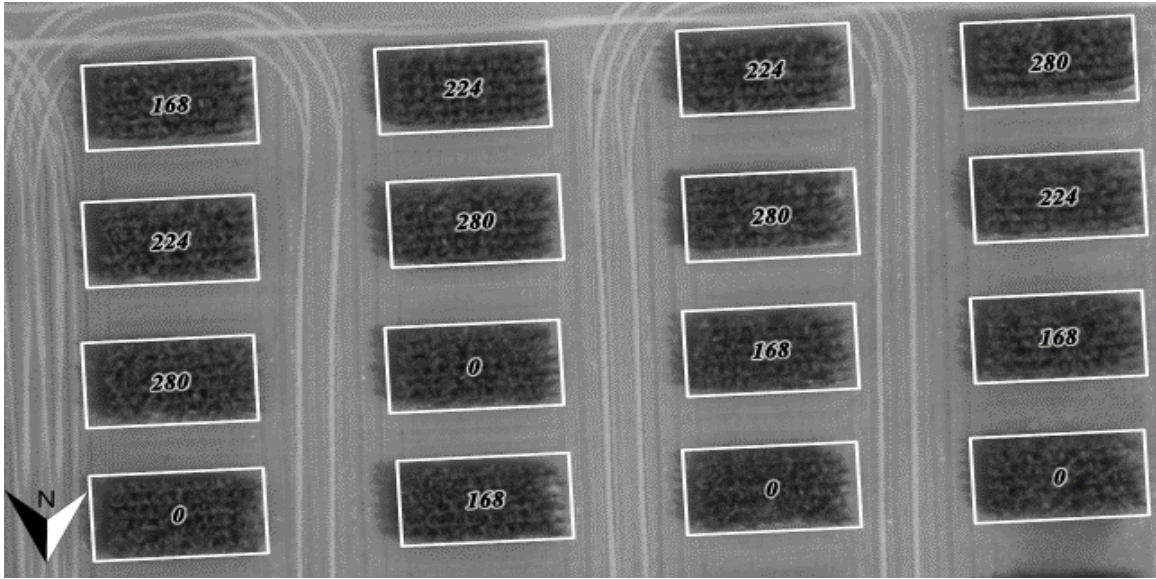
Figure 10. Aerial view of corn experiment at Sabin 2018 with N application rates (Units in kg ha^{-1}).
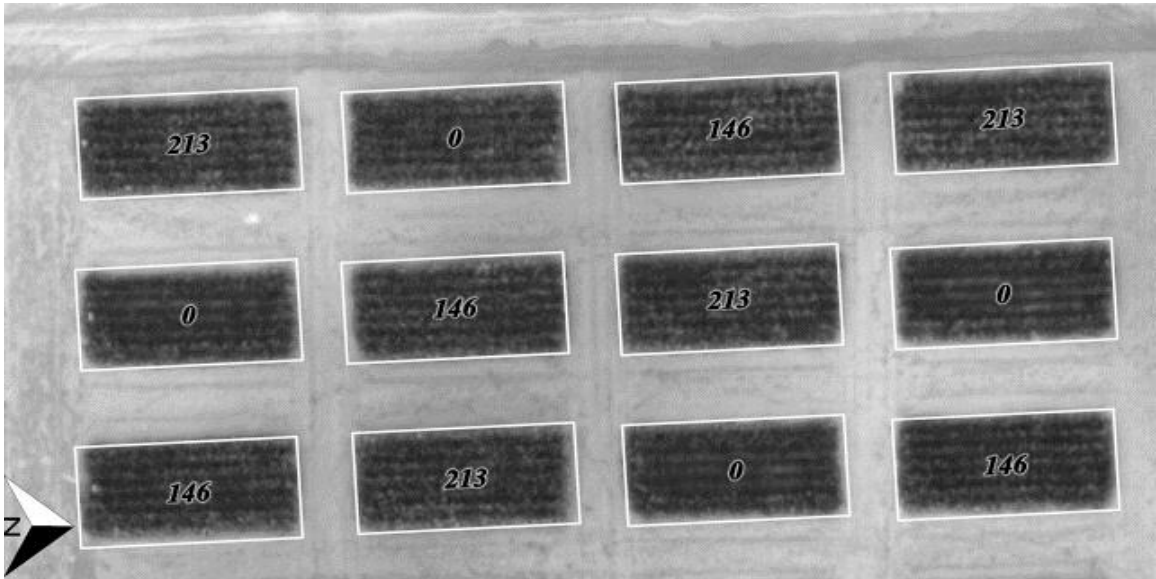
Figure 11. Aerial view of sugar beet experiment at Ada 2018 with N application rates (Units in kg ha^{-1}).
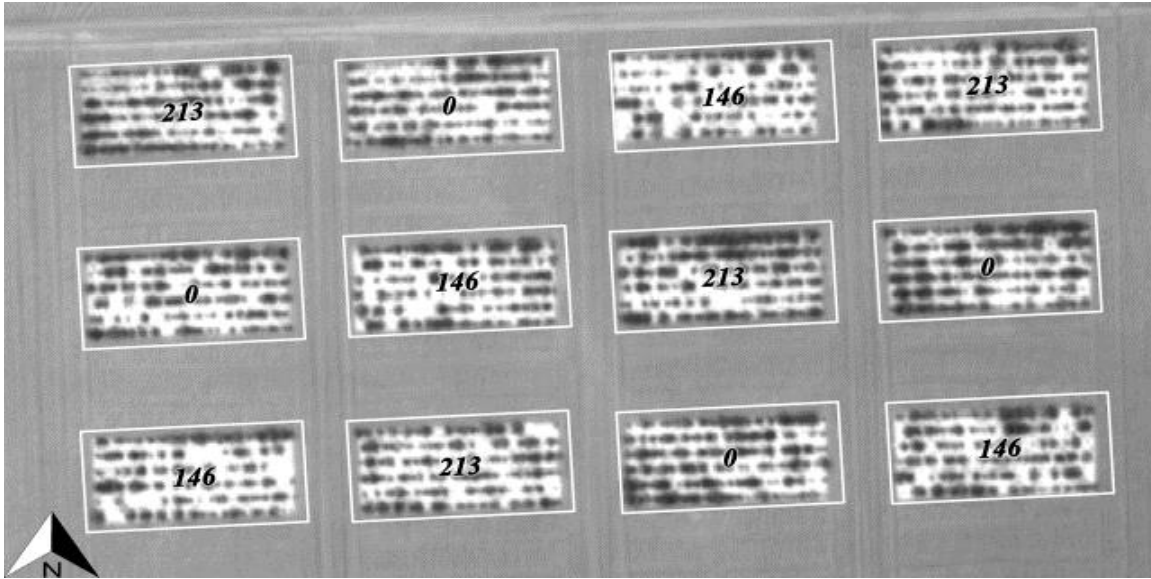
Figure 12. Aerial view of sugar beet experiment at Downer 2018 with N application rates (Units in kg ha^{-1}).

General plot information

Treatments were arranged in a randomized complete block design with four replications. Each experimental unit was 3.35 m wide and 9.14 m in length and consisted of six 0.56 m wide rows. The N treatments were hand applied as granular urea immediately before spring tillage and seeding.

To determine residual soil NO$_3$-N content soil cores of 2 cm diameter were collected to a depth of 0 to 60 cm from each area. Combined soil cores representing one sample were prepared using three cores per plot and were transferred to a laboratory at 5° C, and stored at -20° C, with analysis completed within one week of collection. Prior to analysis, soils were then thawed and homogenized. A 6.5 g weight of soil was then mixed with 25 mL of 2M KCl and then shaken for 30 minutes (NCR 221, 1998). A Timberline^{TM} TL2800 Ammonia Analyzer (Timberline Instruments, Boulder CO, USA) was used to analyze the KCl extract for NO$_3$-N.

Corn and sugar beet were planted at 84,000 and 148,200 plants per ha^{-1}, respectively, using a John Deere MaximEmerge 2^{TM} / 7300 planter 0.56 m wide seed drill for each of the experimental plots. Roundup Weather Max® (isopropylamine salt of glyphosate) 25 ml liter^{-1} and Class Act® with ammonium sulfate 10 ml^{-1} were applied twice post-emergence; the last week of May and the third week of June. Quadris® (azoxystrobin) fungicide was applied at the rate 73 ml liter^{-1} (g a.i. ha^{-1}) was applied at the 4 to 6 leaf stage and again 3 weeks later to control Rhizoctonia root rot in sugar beet. The three fungicides Inspire^{TM} (difenoconazole), Topsin^{TM} (thiophanate methyl), and Headline^{TM} (pyraclostrobin) were applied at rates of 512 ml liter^{-1}, 555 ml liter^{-1}, and 730 ml liter^{-1} to sugar beet at three different times through the growing seasons.

Corn experiments

The 2017 corn trial near Ada, MN consisted of fertilizer N rates that were hand applied at rates of 0, 157, 235, and 314 kg ha^{-1} immediately before spring tillage and seeding. The 2018 corn trials near Ada, MN and Sabin, MN consisted of fertilizer rates that were hand fertilized as urea at 0, 168, 224, and 280 kg N ha^{-1} immediately before spring tillage and seeding. In 2017, the hybrid Dekalb C39-27 RIB was planted with a May 5 at Ada, MN and the center two rows of each experimental unit were harvested with a plot combine October 18. In 2018 hybrid Dekalb 36-28 RIB was planted May 14 at Ada and May 2 at Sabin and the center two rows of each experimental unit were harvested with a plot combine October 23 at Sabin and October 24 at Ada.

Sugar beet experiments

At Ada 2017 N treatments were 0, 101, 135, and 168 kg N ha^{-1} hand applied as urea immediately before spring tillage and seeding. The N treatments near Downer 2017 were 0, 146, and 213 kg N ha^{-1} hand applied as urea immediately before spring tillage and seeding. The 2018 season sugar beet experiments were located near Ada, MN and Downer, MN. At both sites N treatments were 0, 145, and 179 kg N ha^{-1}.

In 2017 the sugar beet cultivar "Crystal 093" was planted using a John Deere MaximEmerge 2 / 7300 planter on April 29 at Downer and May 4 at Ada. Downer was harvested September 19 and Ada was harvested on October 9. The center two rows of each experimental unit were harvested using a modified Heston sugar beet lifter. In 2018 the sugar beet cultivar "Crystal 7538" was planted May 3 at Downer and May 7 at Ada. Downer was harvested September 17 and Ada was harvested September 26.

Sugar beet harvest date experiments

The sugar beet harvest date experiments were different than the N rate experiments previously explained. In 2017, experiments were located near Ada, MN, Downer, MN, and Prosper, ND (Table 7). Sugar beet at Ada was planted on May 1, and Downer and Prosper were planted on May 2. There were two harvest dates in 2017 at September 19 (Harvest Date I) and October 3 (Harvest Date II). The 2018 sugar beet harvest date experiments were located near Ada, MN, Casselton, ND, and Glyndon, MN. Glyndon was planted on May 2, Ada was planted on May 3, and Casselton was planted on May 21. There were three harvest dates of August 21 (Harvest Date I), September 4 (Harvest Date II), and September 18 (Harvest Date III). At harvest, four yield subsamples consisting of the beet roots in randomly selected 1.5 m lengths were hand-pulled, the tops removed with a machete-like tool, and the roots were placed in leather harvest bags with an identity tag and sent to the American Crystal Sugar Laboratory in East Grand Forks, MN for analysis.

Table 7. Site characteristics for the sugar beet harvest date experiments, 2017 and 2018.

Characteristic	Ada 2017	Downer 2017	Prosper 2017	Ada 2018	Casselton 2018	Glyndon 2018
Location	47°21'20.5" 96°25'43.0"	46°51'55.8" 96°30'55.0"	47°0'7.0" 96°6'32.4"	47°19'39.6" 96°23'40.4"	46°56'54.3" 97°11'58.6"	46°53'54.1" 96°39'13.2"
Soil Series	Augsburg	Lamoure	Kindred-Bearden	Augsburg	Glyndon	Bearden
Texture	Loam	Silt loam	Silty clay loam	Loam	Silt loam	Silt loam
N (kg ha^{-1}) 0-60 cm	12	12	50	14	4	14
P (ppm) 0-15 cm	8	5	11	13	28	19
K (ppm) 0-15 cm	106	52	138	86	192	297
pH (1:1)	8.0	8.2	8.1	8.2	7.8	8.0
OM (g kg^{-1})	29	32	36	45	40	53
Planting Date	1 May 2017	2 May 2017	2 May 2017	3 May 2018	21 May 2018	2 May 2018
Harvest Date I (GDD°C)	19 Sep 2017 (2309)	19 Sep 2017 (2374)	19 Sep 2017 (2300)	21 Aug 2018 (1991)	21 Aug 2018 (1752)	21 Aug 2018 (2089)
Harvest Date II (GDD°C)	3 Oct 2017 (2483)	3 Oct 2017 (2552)	3 Oct 2017 (2469)	4 Sept 2018 (2226)	4 Sept 2018 (1988)	4 Sept 2018 (2325)
Harvest Date III (GDD°C)	-	-	-	18 Sep 2018 (2449)	18 Sep 2018 (2222)	18 Sep 2018 (2559)

Optical reflectance data collection, work flow, and analysis

In 2017, SUAS platform optical sensor data was acquired at two dates; June 30 and July 26 at approximately the V6 and VT (tasseling) growth stages in corn and V10 and V15 growth stages in sugar beet. In 2018, SUAS platform optical sensing was performed weekly from the V4 in sugar beet and corn, and until V15 in sugar beet and the R2 growth stage (kernel blister stage) in corn. The SUAS was a DJI Matrice 100^{TM} (DJI, Shenzhen, China) shown in Figure 13. The flight plan for each optical sensing data acquisition was produced and executed through the use of DJI-supported DJI GS Pro^{TM} software (DJI, Shenzhen, China). The optical sensor mounted on the SUAS was a MicaSense Red Edge^{TM} (MicaSense Inc., Washington State, USA) passive light optical sensor (Figure 13). The passive optical sensor measures five wavelengths: blue (475 nm), green (560 nm), red (668 nm), NIR (840 nm), and red edge (717 nm). Two

software packages were utilized to provide data download and manipulation with a GIS platform. These software packages were Pix4D^{TM} (Pix4D, Lausanne, Switzerland) and ArcGIS^{TM} (ESRI, California, USA). The workflow that was used in this research is shown in Figure 14.

Figure 13. DJI Matrice 100 (left) and MicaSense Red Edge (right) (https://www.dji.com/matrice100) (https://support.micasense.com).
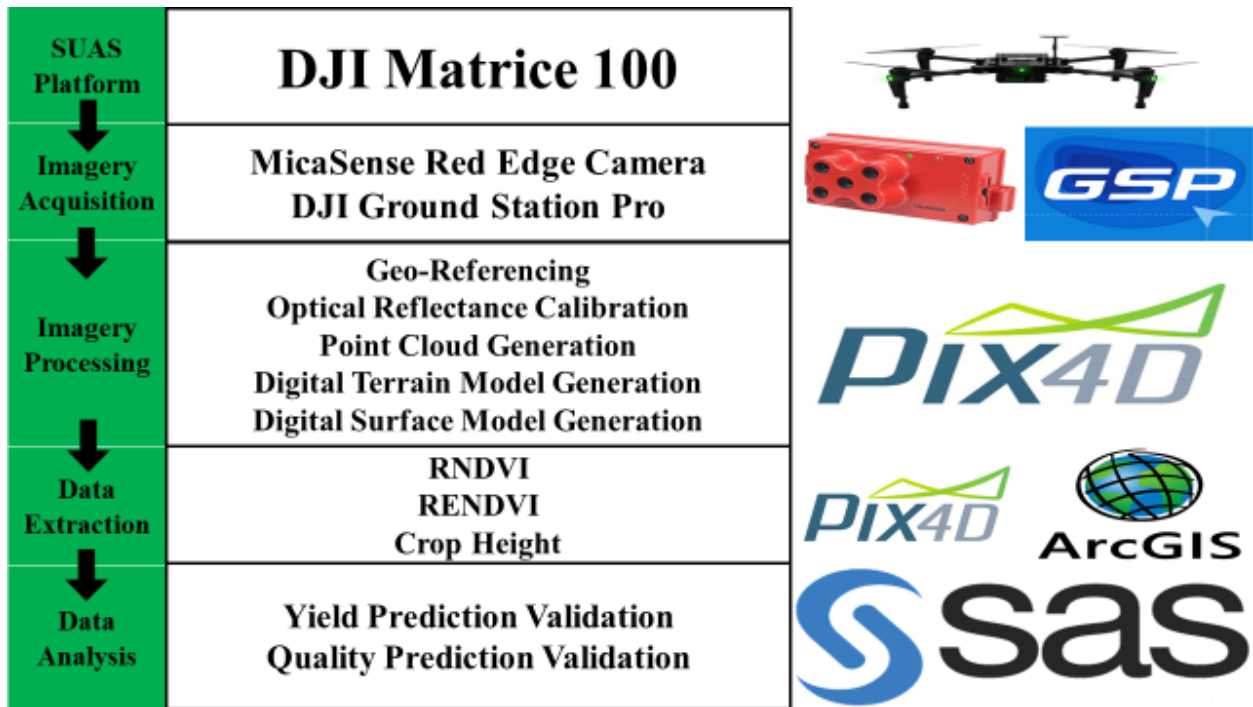
Figure 14. Workflow diagram of SUAS based optical reflectance and crop height extraction methodology.

The SUAS was flown at a constant elevation of 121 meters, at a speed of five m s^{-1}, with 90% side and frontal image overlap, and calibrated reflectance panel images taken pre- and post-flight. The methodology was trial and error. Many different flight elevations and overlap were tried. It was found that only with the maximum height allowed by the Federal Aviation Administration of 121 meters, combined with frontal and side overlap of 90% would produce viable imagery. Many of the suboptimal flight parameters would produce imagery that Pix4D was incapable of successfully processing. It was also advised by Pix4D to use these parameters to guarantee a successful capture of imagery as crop land is often a challenging environment to capture imagery in due to low "anchor points", which are significant land scape features. The flight was executed using DJI Ground Station Pro software which automatically performs the flight plan and keeps the flight at the desired height and image overlap. The calibrated reflectance panel has known reflectance values across the visible and near-infrared light

spectrum. The images are taken pre- and post-flight to provide an accurate representation of light conditions during crop sensing. The optical reflectance data was calibrated by taking pre- and post-flight images of a calibrated reflectance panel. The calibrated reflectance panel's unique optical reflectance factor values were obtained from MicaSense and were entered into the Pix4D software package prior to image processing. The SUAS is equipped with a down-welling light sensor that works with the MicaSense Red Edge camera and compensates for changing ambient light intensity that occurs during flight.

Time of SUAS data acquisition was between 10:00 and 14:00 on days with consistent light conditions. The majority of days experienced clear, cloudless conditions. Optical sensor reflectance data analysis was performed using Pix4D which averaged out all of the pixel values obtained in the center two rows of each experimental plot (Figure 15). Crop height data analysis was performed with the use of Pix4D and ArcGIS. First a DSM, which represents the crop, and a DTM, which represents the soil, were generated with Pix4D. The DSM and DTM generated with Pix4D were then imported into ArcGIS as "TIF" files. The "minus" tool was then used to find the difference between the two layers (Figure 16). The difference layer was then analyzed with the "construction tools" rectangle and "zonal statistics" tool. This tool averages out all of the pixel values obtained in the two center rows of each experimental plot. The final result is a proportional approximation of crop height (Figure 17).
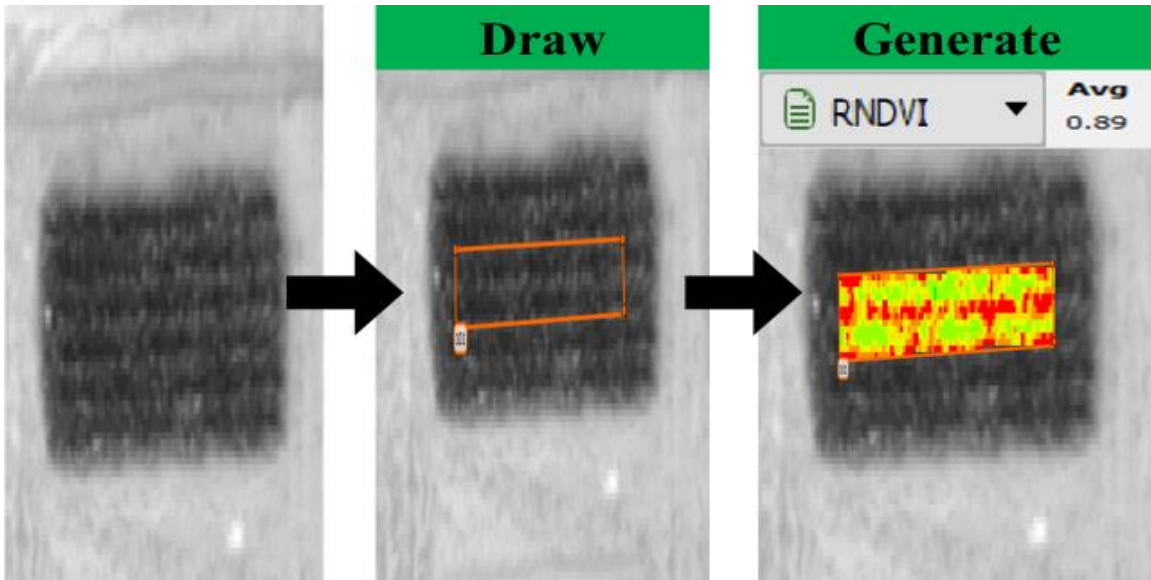
Figure 15. Pix4D optical reflectance data generator.
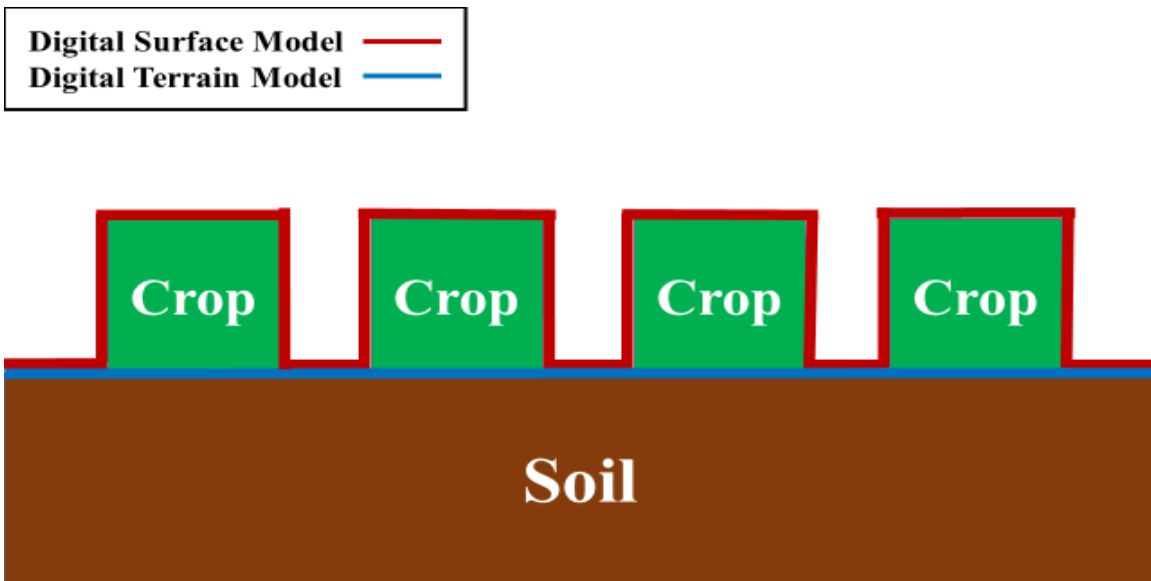
Figure 16. A schematic diagram to show the digital surface model (DSM) and digital terrain model (DTM) layers produced for a cropland.
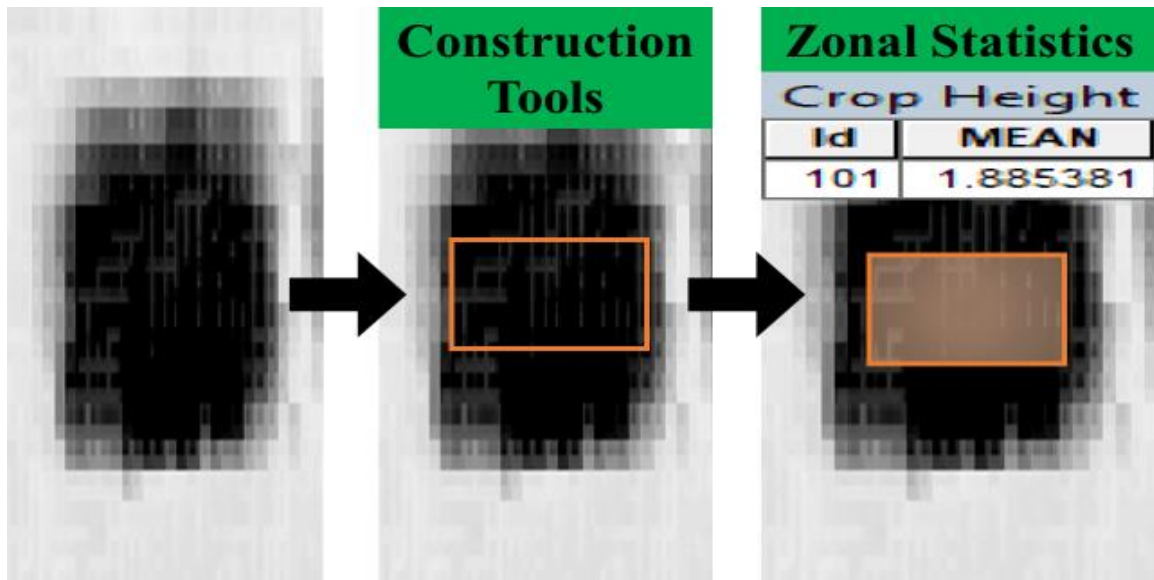
Figure 17. ArcGIS crop height generation.

Crop height generation that was used for this research utilized an automated DTM generation feature provided with the Pix4D software package. The DTM generator uses a series of complex algorithms which extrapolate the approximate elevation value of the soil surface under the crop canopy by the way of surrounding known elevations (Unger et al., 2009). The difference between the DSM and the DTM is then calculated using ArcGIS, which produces a crop height approximation, as previously explained.

Statistical analysis

SAS 9.4 (SAS Institute, Cary, NC) was used to conduct ANOVA mean yield separation and linear regression for optical reflectance and yield on corn and sugar beet yield and sugar beet quality. Means were compared using least significant difference at $P<0.05$. Optical reflectance (RNDVI, RENDVI, and crop height) were related to N fertilization level, yield, and recoverable sucrose using a linear regression model. Relationship between yield/quality/RNDVI/RENDVI/crop height with N rate were considered significant if $P<0.05$.

RESULTS AND DISCUSSION

Growing conditions

Growing season temperature and rainfall for each month at experimental sites in 2017 and 2018, obtained from the nearest North Dakota Agricultural Weather Network (NDAWN) station are presented in Table 8. During 2017 temperature was nearly average and mean temperatures were similar between sites. Both sites started the season drier than average (-50 mm rainfall deficit) and the soil remained relatively dry through the growing season compared to average, although Ada received a significant amount of rainfall during the September. The western area of the 2017 Ada site had a relatively thick residue cover and suffered from early season water-logging from a single large rainfall event which slowed corn emergence.

During 2018 temperatures were near or slightly lower than average at the three experimental locations. Soil was relatively dry at planting, with Ada tending to be drier than average through the entire growing season. Downer and Sabin received relatively large rainfall events after June 1, which helped maintain these sites at near normal soil moisture most of the season. At Downer sugar beets were adversely affected by dry early-growing conditions and the presence of rhizoctonia root rot. The Downer site also showed signs of 'sand syndrome', which is a stunting of the sugar beet beginning at about V6, and which has been shown to be caused in large part by sub-phenotypic infection by Aphenomyces root rot organisms. The eastern side of the Sabin site had received sugar beet tailings, which although previously incorporated, were shallow enough that their presence appeared to slow corn emergence. The corn at Downer also showed signs of early season phosphorous deficiency and dry early growing conditions that affected the corn's emergence and early growth stages.

Table 8. Monthly precipitation and average temperature during the growing season at each experimental site with deviation from the five-year average deviation.

Month	Ada 2017 Temp. (°C)	Ada 2017 Precip. (mm)	Ada 2018 Temp. (°C)	Ada 2018 Precip. (mm)	Downer 2017 Temp. (°C)	Downer 2017 Precip. (mm)	Downer 2018 Temp. (°C)	Downer 2018 Precip. (mm)	Sabin 2018 Temp. (°C)	Sabin 2018 Precip. (mm)
Apr	7	26.5	2	4.6	7	36.9	2	4.3	2	4.3
	0*	-9.3	-4	-31.2	0	-3.5	-5	-36.1	-5	-36.1
May	13	34.4	17	62.8	14	36.3	18	14.0	18	14.0
	0	-47.9	3	-19.5	0	-43.9	3	-66.6	3	-66.6
June	19	73.9	20	78.3	20	60.5	21	148.4	21	148.4
	0	-39.9	2	-35.5	0	-44.4	2	43.5	2	43.5
July	21	68.1	21	62.5	22	36.1	21	116.9	21	116.9
	0	-25.1	0	-30.7	0	-45.5	-1	35.4	-1	35.4
Aug	18	32.2	19	66.6	19	59.7	20	92.0	20	92.0
	-2	-37.4	-1	-3.0	-3	-8.1	-2	24.2	-2	24.2
Sep	16	146.4	14	73.7	16	63.0	14	63.0	14	63.0
	1	79.3	-1	6.7	1	-11.6	-1	-11.7	-1	-11.7
Average	16	63.6	15	58.1	16	48.8	16	73.1	16	73.1
	0	-13.4	0	-18.9	0	-26.2	-1	-1.8	-1	-1.8

* Bottom value for each monthly temperature (Temp.) and precipitation (Precip.) indicates difference from the five-year average deviation.

Corn N rate experiments 2017

Corn yield response to N at Ada 2017 is shown in Table 9. Yields increased with N fertilization up to the 235 kg N ha^{-1} rate. Ada 2017 was subjected to drier than average conditions (Table 8). Suzuki et al., (2014) found that drought stress can have negative impacts especially in the early growing stages in corn. Thick crop residue was also observed which presumably impeded the corn seedlings emergence and delayed the soil warming. In addition, a several day ponding event due to excessive rainfall occurred when the corn was at the V4 to V6 stage. The rate of 235 kg N ha^{-1} produced the greatest yield.

Table 9. Corn yield means for N fertilization response at Ada 2017 trial ANOVA results.

Treatment N kg ha^{-1}	Yield Mg ha^{-1} *
0	8.54c
78	10.00bc
157	10.73b
235	14.02a
314	13.99a
LSD ($\alpha = 0.05$)	1.95

* N treatments significant at the P<0.05. (N=20).

Corn yield at Ada, 2017, increased with N rate. The relationship of yield and N rate was significant, with a coefficient of determination of determination (R^2) value of 0.76 (Figure 18).
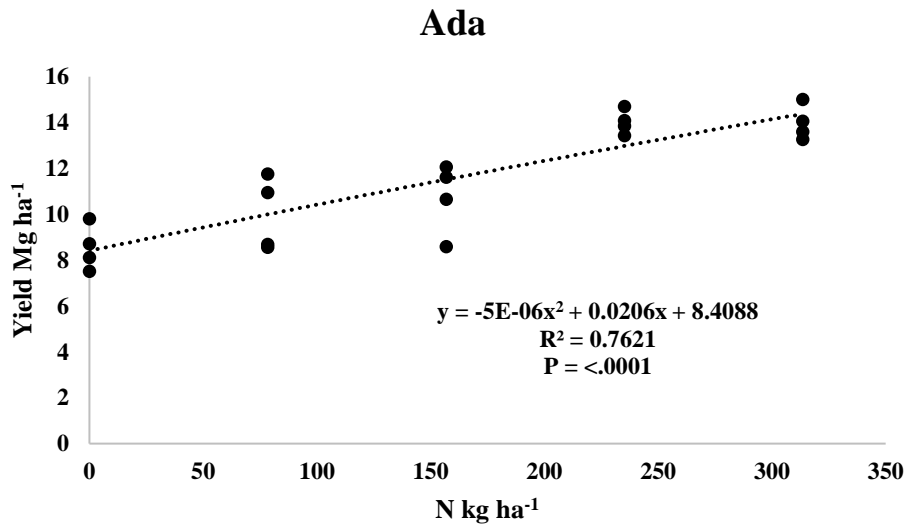
Figure 18. Corn yield Ada 2017 response to N fertilization rates.
Corn Ada 2017 sensor analysis.

Corn Ada 2017 sensor analysis

Drone (SUAS) sensing was performed two times during the 2017 growing season at the V6 (730 GDD, June 30) and the VT (1219 GDD, July 26) growth stages.

Table 10 shows the regression analysis results for yield prediction (YP), which is the relationship between optical sensor data and yield. The R^2 of the VT sensing was significantly

higher than that of the V6 sensing for both N monitoring and yield prediction in all cases. All three VIs performed similarly, with crop height having a slightly greater R^2. This could be due to the fact that corn height is related to total biomass of a tall crop, which is not provided with the 2-D RNDVI (leaf area index) and RENDVI, which is related to tint. The RNDVI multiplied by crop height had the greatest R^2 value, which is logical, since height multiplied by leaf area index (RNDVI) is essentially biomass. The V1 through the V5 growth stages of corn are particularly sensitive to drought, which reduces growth rate and prolongs the vegetative growth stages (Hajibabaee et al., 2012). Ada 2017 likely had less soil moisture available early in the season due to a thin residue cover, which in would result in higher soil temperature and greater evaporation of soil moisture, negatively impacting germination and early season development. Rainfall later in the season allowed corn growth to recover to a sufficient level that sensing relationships had higher R^2 values.

Table 11 shows the optical sensor reflectance value means by sensing date. The RNDVI at the V6 did not differentiate between N treatments, but it did so at the VT growth stage. The RENDVI at the V6 did not differentiate between the N treatments, but it did so at the VT in an inverse relationship. Crop height at the V6 failed to differentiate between the N treatments, but did so at the VT growth stage.

Table 10. Regression coefficient (R^2 value) for the relationship between yield and three sensor readings for corn at Ada 2017.

Model	Growing Degree Days	Growth Stage	RNDVI	RNDVI X Crop Height	RENDVI	RENDVI X Crop Height	Crop Height
YP 1	730	V6	0.006	0.003	0.055	0.000	0.004
YP 2	1219	VT	0.544*	0.557*	0.518*	0.036	0.544*

*Regression significant at the P<0.05. (N=20).

Table 11. Optical reflectance value means for the corn Ada 2017 sensing by sensing date, growing degree days (GDD), and growth stage.

Treatment N kg ha^{-1}	RNDVI June 30 730 GDD V6 Growth Stage	RNDVI July 26 1219 GDD VT Growth Stage*
0	0.71a	0.84b
78	0.76a	0.86a
157	0.70a	0.86a
235	0.70a	0.87a
314	0.74a	0.87a
LSD (α = 0.05)	0.30	0.02
Treatment N kg ha^{-1}	RENDVI June 30 730 GDD V6 Growth Stage	RENDVI July 26 1219 GDD VT Growth Stage*
0	0.15a	0.11a
78	0.15a	0.10a
157	0.15a	0.08b
235	0.14a	0.07b
314	0.15a	0.08b
LSD (α = 0.05)	0.01	0.02
Treatment N kg ha^{-1}	Crop Height June 30 730 GDD V6 Growth Stage	Crop Height July 26 1219 GDD VT Growth Stage*
0	0.56a	1.40b
78	0.64a	1.67a
157	0.58a	1.69a
235	0.53a	1.82a
314	0.58a	1.89a
LSD (α = 0.05)	0.27	0.26

* RCBD significant at the P<0.05. (N=20).

Sugar beet N rate experiments 2017

The Ada 2017 sugar beet experiment N treatments of 0 to 168 kg ha^{-1} resulted in root yields of 67 and 85 Mg ha^{-1} respectively (Table 12). Sugar beet yields at Ada, 2017, increased with N rate. Recoverable sugar concentration was not affected by N rate at Ada, 2017. At Downer, 2017, with N treatments of 0 and 213 kg ha^{-1} root yields were 60 and 78 Mg ha^{-1}

respectively. Sugar beet yield at Downer, 2017, increased with N rate. Increasing N rate

resulted in decreased recoverable sugar concentration at Downer.

Table 12. Sugar beet yield, net sugar %, and recoverable sugar yield means for N fertilization
response at Ada 2017 and Downer 2017 trials ANOVA results.

Site	Treatment N kg ha^{-1}	Yield Mg ha^{-1}	Net Sugar %	Recoverable Sugar Yield Mg ha^{-1}
Ada 2017	0	67.23b	17.68a	12.54a
	101	74.84ab	17.65a	12.85a
	135	80.96a	17.58a	13.55a
	168	84.77a	17.70a	12.82a
	LSD (α = 0.05)	9.99	0.66	2.078
Downer 2017	Treatment N kg ha^{-1}	Yield Mg ha^{-1}	Net Sugar %	Recoverable Sugar Yield Mg ha^{-1}
	0	60.10b	19.55a	11.20b
	146	77.22a	19.18ab	14.05a
	213	77.64a	18.73b	13.63ba
	LSD (α = 0.05)	12.58	0.52	2.493

* N treatments significant the 0.05 level. (N=16; 12).

Ada, 2017 and Downer, 2017 yields were related to N rates, with a coefficient of

determination (R^2) values of 0.62 at Ada 2017and 0.59 at Downer 2017 (Figure 19).
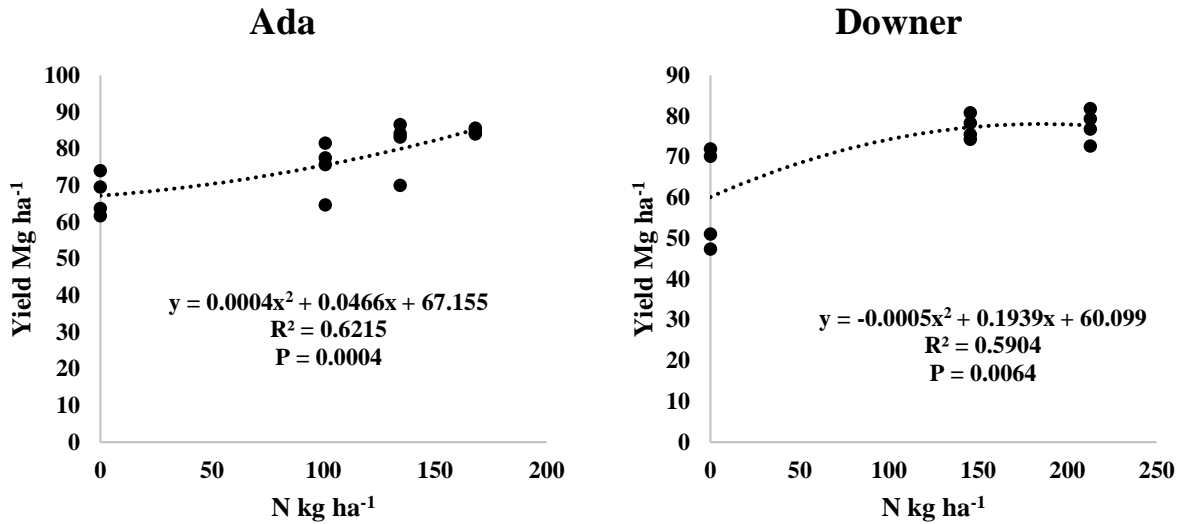
Figure 19. Sugar beet yield Ada 2017 and Downer 2017 response to N fertilization rates. Sugar beet Ada 2017 sensor analysis.

Sugar beet Ada 2017 sensor analysis

The SUAS sensing was performed two times during the 2017 growing season at V10 (1548 GDD, June 30) and the V15 (2450 GDD, July 26) growth stages.

Table 13 shows the regression analysis relationship with YP and recoverable sugar prediction (RSP). The Ada 2017 experimental site experienced droughty soils at planting, followed by a high rainfall event resulting in several days of standing water. There were a wide range of results for each of the models. The V10 was better for yield and recoverable sugar prediction. The RNDVI was the highest performing VI, with crop height following closely. It is unknown why RENDVI performed so poorly at the July 26 date while the RNDVI performed so well. It could be due to SUAS flight conditions, environmental conditions, or the sugar beet physiology at the time of sensing. Changing ambient light conditions could possibly be a cause of the RENDVI low R^2. The RENDVI relationships might be enhanced by combining with canopy structure data (Gabriel et al., (2017). Crop height performed well at both sensing times.

RNDVI produced the greatest R^2 values. Despite the poor growing conditions the sensing results were generally positive, with RENDVI having some setbacks.

Table 14 shows the optical sensor reflectance value means by sensing date. The RNDVI was able to differentiate the N treatments at the V10 and the V15 growth stages. The RENDVI was able to differentiate the N treatments at the V10, but failed to do so at the V15 growth stage. Crop height was not able to differentiate the N treatments at the V10 stage, but was able to do so at the V15 growth stage.

Table 13. Regression coefficient (R^2 value) for the relationship between yield and recoverable sugar and three sensor readings for sugar beet at Ada 2017.

Model	Growing Degree Days	Growth Stage	RNDVI	RNDVI X Crop Height	RENDVI	RENDVI X Crop Height	Crop Height
YP 1	1548	V10	0.745*	0.816*	0.184	0.676*	0.656*
YP 2	2450	V15	0.655*	0.512*	0.424*	0.163	0.498*
RSP 1	1548	V10	0.706*	0.788*	0.202	0.659*	0.633*
RSP 2	2450	V15	0.626*	0.443*	0.371*	0.132	0.426*

*Regression significant at the $P < 0.05$. (N=16).

Table 14. Optical reflectance value means for the sugar beet Ada 2017 sensing by sensing date, growing degree days (GDD), and growth stage.

Treatment N kg ha^{-1}	RNDVI June 30 1548 GDD V10 Growth Stage*	RNDVI July 26 2450 GDD V15 Growth Stage*
0	0.68c	0.76c
101	0.75b	0.82b
135	0.81a	0.87a
168	0.82a	0.86a
LSD (α = 0.05)	0.05	0.02
Treatment N kg ha^{-1}	RENDVI June 30 1548 GDD V10 Growth Stage*	RENDVI July 26 2450 GDD V15 Growth Stage
0	0.18b	0.10a
101	0.19a	0.11a
135	0.19a	0.10a
168	0.19a	0.088a
LSD (α = 0.05)	0.01	0.04
Treatment N kg ha^{-1}	Crop Height June 30 1548 GDD V10 Growth Stage	Crop Height July 26 2450 GDD V15 Growth Stage*
0	0.19a	0.04c
101	0.28a	0.15b
135	0.27a	0.21a
168	0.26a	0.26a
LSD (α = 0.05)	0.10	0.06

* RCBD significant at the P<0.05. (N=16).

Sugar beet Downer 2017 sensor analysis

SUAS sensing was performed at Downer 2017 two times, the V10 (1680 GDD, June 30) and the V15 (2637 GDD, July 26).

Table 15 shows the regression analysis relationship with YP and RSP. The V10 sensing generally had better explanatory power for all three of the models. RNDVI had positive performance for the first sensing, with poor results for the second sensing. RENDVI had poor R^2 values for both sensing times. Crop height was related to N treatment at both of the sensing times. RENDVI had performed well in other studies (Li et al., 2014, Sharma et al., 2015). The

lack of relationship to N rate in this experiment could not be explained. RENDVI might be

enhanced by combining it with canopy structure data (Gabriel et al 2017). Crop height

performed well at both sensing times. Crop height and RNDVI multiplied by crop height

resulted in the greatest R^2 at Downer 2017. Although there were poor growing conditions the

sensing results were generally positive for RNDVI and crop height. However, RENDVI

relationships were not significant and had very poor explanatory power for yield and recoverable

sugar prediction.

Table 16 shows the optical sensor reflectance value means by sensing date. The RNDVI

and RENDVI failed to differentiate the N treatments at both the V10 and V15 growth stages.

Crop height was able to differentiate the N treatments at both the V10 and V15 growth stages.

Table 15. Regression coefficient (R^2 value) for the relationship between yield and recoverable
sugar and three sensor readings for the sugar beet at Downer 2017 sensing.

Model	Growing Degree Days	Growth Stage	RNDVI	RNDVI X Crop Height	RENDVI	RENDVI X Crop Height	Crop Height
YP 1	1680	V10	0.760*	0.711*	0.143	0.661*	0.676*
YP 2	2637	V15	0.224	0.638*	0.042	0.446*	0.653*
RSP 1	1680	V10	0.715*	0.660*	0.083	0.543*	0.629*
RSP 2	2637	V15	0.176	0.529*	0.041	0.376*	0.543*

*Regression significant at the $P<0.05$. (N=12).

Table 16. Optical reflectance value means for the sugar beet Downer 2017 sensing by sensing date, growing degree days (GDD), and growth stage.

Treatment N kg ha^{-1}	RNDVI June 30 1680 GDD V10 Growth Stage	RNDVI July 26 2637 GDD V15 Growth Stage
0	0.84b	0.89a
146	0.90a	0.90a
213	0.89a	0.90a
LSD (α = 0.05)	0.04	0.01
Treatment N kg ha^{-1}	**RENDVI June 30 1680 GDD V10 Growth Stage**	**RENDVI July 26 2637 GDD V15 Growth Stage**
0	0.22a	0.26a
146	0.25a	0.28a
213	0.27a	0.26a
LSD (α = 0.05)	0.07	0.04
Treatment N kg ha^{-1}	**Crop Height June 30 1680 GDD V10 Growth Stage***	**Crop Height July 26 2637 GDD V15 Growth Stage***
0	0.27b	0.25b
146	0.35a	0.36a
213	0.35a	0.36a
LSD (α = 0.05)	0.06	0.09

* RCBD significant at the P<0.05. (N=12).

Corn N rate experiments 2018

Corn yield response to N rate at Ada and Sabin for 2018 are shown in Table 17. The N fertilization treatments of 0 and 280 kg ha^{-1} yielded 10.78 and 16.35 Mg ha^{-1} respectively at Ada 2018. The N rate treatments at of 0 and 280 kg ha^{-1} yielded 10.55 and 14.07 Mg ha^{-1} respectively at Sabin 2018. Yield increased with N rate at both sites. Ada 2018 and Sabin 2018 were experienced less than average rainfall (Table 8). Suzuki et al., (2014) found that drought stress can have negative corn growth impacts in early growing stages. Despite the adverse conditions that were present at the Ada and Sabin 2018 sites, yields were respectable. The rate of 280 kg N ha^{-1} produced the greatest yield.

Table 17. Corn yield means for N fertilization response at Ada 2018 and Sabin 2018 trials ANOVA results.

Site	Treatment N kg ha^{-1}	Yield Mg ha^{-1}*
Ada 2018	0	10.78c
	168	14.41b
	224	15.09ba
	280	16.35a
	LSD (α = 0.05)	1.54
	Treatment N kg ha^{-1}	Yield Mg ha^{-1}*
Sabin 2018	0	10.55b
	168	13.11a
	224	13.69a
	280	14.07a
	LSD (α = 0.05)	2.68

* N treatments significant the 0.05 level. (N=16).

Corn yield at Ada 2018 and Sabin 2018 increased with N rate. Corn yield was related to N rate at both sites, with a coefficient of determination (R^2) values of 0.77 and 0.76 respectively (Figure 20). The relationship of corn yield to N rate at Ada 2018 was nearly linear, suggesting that N was unavailable to the plants through immobilization by residues, or poor availability to the plants due to low soil moisture. Low soil moisture and drought limits the availability of N to plants (Suzuki et al., 2014).
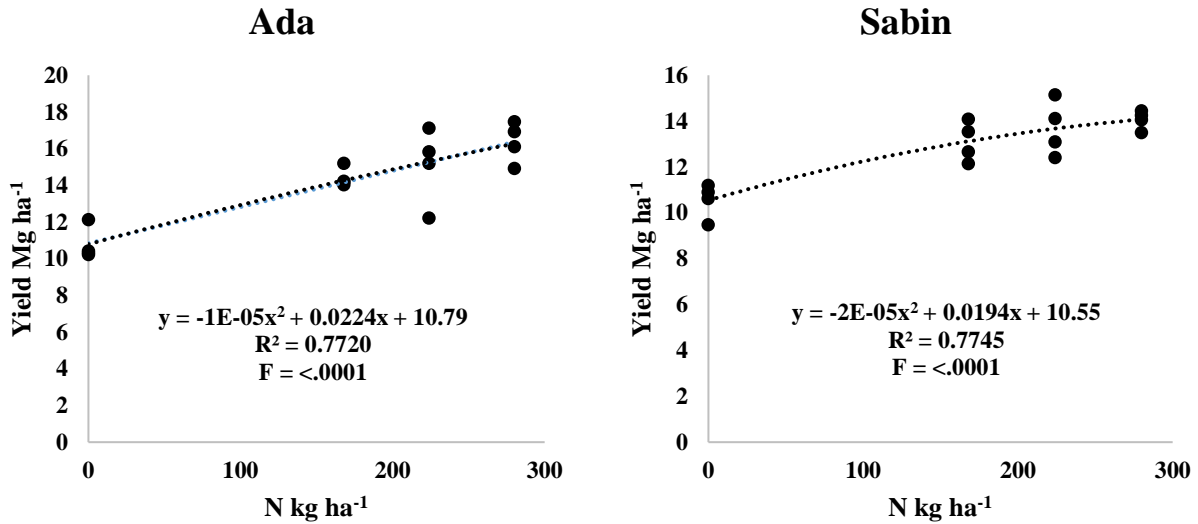
Figure 20. Corn yield Ada 2018 and Sabin 2018 response to N fertilization rates.
Corn Ada 2018 sensor analysis.

Corn Ada 2018 sensor analysis

The SUAS sensing at Ada 2018 for corn was performed roughly weekly from V4 (312 GDD) to the R2 (1387 GDD) growth stage. The sensing dates were on May 31 (V4), June 7 (V5), June 15 (V6), June 21 (V7), June 28 (V10), July 5 (V11), July 12 (R1), July 18 (R1), and July 27 (R2).

Table 18 shows the regression analysis relationship between N rate and yield prediction. Figure 21 graphically depicts how the regression coefficient (R^2) fluctuated throughout the season. At V4, yield was related to crop height and RENDVI multiplied by crop height. At V5 and V6, the relationships of sensor readings with yield were nonsignificant. At V7, yield was related to RENDVI and RENDVI multiplied by crop height. At V10, yield was related to RNDVI, RNDVI multiplied by crop height, RENDVI, RENDVI multiplied by crop height and crop height. At V11, yield was related to all readings except for RENDVI. At R11129 GDD, yield was related to RNDVI and RENDVI, but not crop height. At R1 1239 and yield was related to all sensor readings except RENDVI alone. In general the sensing's R^2 for the relationship

51

between sensor readings YP increased through the season. Previous studies have found that as biomass and leaf area index increase, the sensing data accuracy generally increases to a certain threshold and then reaches diminishing returns particularly RNDVI due to row closure and subsequent saturation (Xia et al., 2016; Li et al., 2014). In this study, the R^2 increased until the R2 stage at the last sensor data acquisition date. In addition RENDVI outperformed RNDVI. As the corn leaves cover the rows, the RENDVI is often superior to RNDVI (Erdle et al., 2011, Nguy-Robertson et al., 2012). In this experiment combining optical reflectance values with crop height reduced R^2 compared to sensor values alone. This could be caused by poor height estimation. To improve the height accuracy it may be advisable to use the "minus method" as opposed to using the automated digital terrain generation where inaccuracies can be introduced. The "minus method" is where a bare earth DTM is captured prior to crop emergence. This DTM then can be compared with the crop DSM upon emergence later in the crop growing cycle.

Table 19 shows the optical sensor reflectance value means by sensing date. Figure 22 graphically depicts how the VIs and crop height fluctuated throughout the season. The RNDVI was able to start differentiating the N treatments at the V10 growth stage, but was unable to before this growth stage was reached. The RENDVI and crop height was able to start differentiating the N treatments at the V7 growth stage, but was unable to before this growth stage was reached. Crop height calculated that corn height dipped at around the V11 and R1 growth stage. This may be explained by leaf wilt or the silhouette scattering of the corn silks.

Table 18. Regression coefficient (R^2 value) for the relationship between yield and three sensor readings for corn at Ada 2018.

Model	Growing Degree Days	Growth Stage	RNDVI	RNDVI X Crop Height	RENDVI	RENDVI X Crop Height	Crop Height
YP 1	312	V4	0.111	0.221	0.171	0.293*	0.254*
YP 2	413	V5	0.064	0.129	0.048	0.159	0.149
YP 3	567	V6	0.047	0.005	0.183	0.013	0.000
YP 4	680	V7	0.026	0.062	0.621*	0.379*	0.142
YP 5	831	V10	0.300*	0.567*	0.633*	0.510*	0.587*
YP 6	972	V11	0.506*	0.285*	0.749*	0.048	0.278*
YP 7	1129	R1	0.688*	0.156	0.740*	0.009	0.132
YP 8	1239	R1	0.611*	0.274*	0.768*	0.042	0.257*
YP 9	1387	R2	0.594*	0.626*	0.760*	0.002	0.596*

*Regression significant at the P<0.05. (N=16).
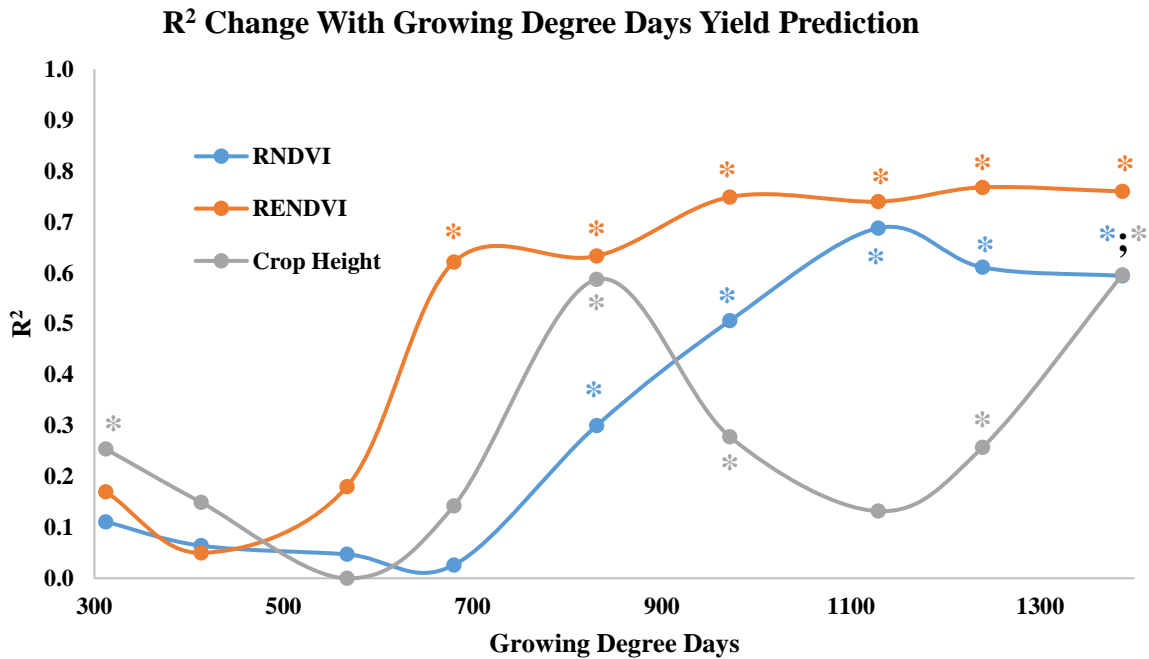
Figure 21. Changes in R^2 for RNDVI, RENDVI, and crop height with yield prediction change through the 2018 corn growing season Ada.
* Regression significant at the P<0.05. (N=16).

53

Table 19. Optical reflectance value means for corn at Ada 2018 sensing by date, growing degree days (GDD), and growth stage.

Treatment N kg ha⁻¹	RNDVI May 31 312 GDD V4 Growth Stage	RNDVI June 7 413 GDD V5 Growth Stage	RNDVI June 15 567 GDD V6 Growth Stage	RNDVI June 21 680 GDD V7 Growth Stage	RNDVI June 28 831 GDD V10 Growth Stage*	RNDVI July 5 972 GDD V11 Growth Stage*	RNDVI July 12 1129 GDD R1 Growth Stage*	RNDVI July 18 1239 GDD R1 Growth Stage*	RNDVI July 27 1387 GDD R2 Growth Stage*
0	0.27b	0.25a	0.50b	0.68c	0.82b	0.87b	0.88b	0.87b	0.85b
168	0.28ba	0.26a	0.53a	0.75a	0.87a	0.89a	0.90a	0.88a	0.87a
224	0.29a	0.25a	0.52ba	0.73ba	0.86a	0.89a	0.90a	0.89a	0.87a
280	0.28ba	0.24a	0.48b	0.69bc	0.85a	0.89a	0.90a	0.89a	0.87a
LSD (α = 0.05)	0.01	0.21	0.05	0.05	0.02	0.01	0.004	0.01	0.01
Treatment N kg ha⁻¹	RENDVI May 31 312 GDD V4 Growth Stage	RENDVI June 7 413 GDD V5 Growth Stage	RENDVI June 15 567 GDD V6 Growth Stage	RENDVI June 21 680 GDD V7 Growth Stage*	RENDVI June 28 831 GDD V10 Growth Stage*	RENDVI July 5 972 GDD V11 Growth Stage*	RENDVI July 12 1129 GDD R1 Growth Stage*	RENDVI July 18 1239 GDD R1 Growth Stage*	RENDVI July 27 1387 GDD R2 Growth Stage*
0	0.075a	0.18a	0.21a	0.16a	0.18a	0.18a	0.23a	0.22a	0.21a
168	0.075a	0.17a	0.20ba	0.15b	0.15b	0.14b	0.17b	0.18b	0.17b
224	0.070a	0.17a	0.19b	0.14b	0.15b	0.14b	0.16c	0.17c	0.16cb
280	0.070a	0.17a	0.20ba	0.15b	0.15b	0.13b	0.16c	0.16c	0.15c
LSD (α = 0.05)	0.01	0.01	0.02	0.01	0.01	0.01	0.01	0.01	0.01
Treatment N kg ha⁻¹	Crop Height May 31 312 GDD V4 Growth Stage	Crop Height June 7 413 GDD V5 Growth Stage	Crop Height June 15 567 GDD V6 Growth Stage	Crop Height June 21 680 GDD V7 Growth Stage*	Crop Height June 28 831 GDD V10 Growth Stage*	Crop Height July 5 972 GDD V11 Growth Stage*	Crop Height July 12 1129 GDD R1 Growth Stage	Crop Height July 18 1239 GDD R1 Growth Stage*	Crop Height July 27 1387 GDD R2 Growth Stage*
0	0.018a	0.0037a	0.040a	0.091ba	0.20b	0.42c	0.50b	0.86b	1.47b
168	0.010a	0.0056a	0.050a	0.10a	0.30a	0.79a	0.74ba	1.51a	1.93a
224	0.012a	0.0076a	0.042a	0.092ba	0.30a	0.71ba	0.66ba	1.46a	1.97a
280	0.010a	0.0064a	0.040a	0.079b	0.29a	0.64b	0.78a	1.37a	1.96a
LSD (α = 0.05)	0.01	0.01	0.01	0.01	0.02	0.09	0.25	0.34	0.18

* RCBD significant at the P<0.05. (N=16).
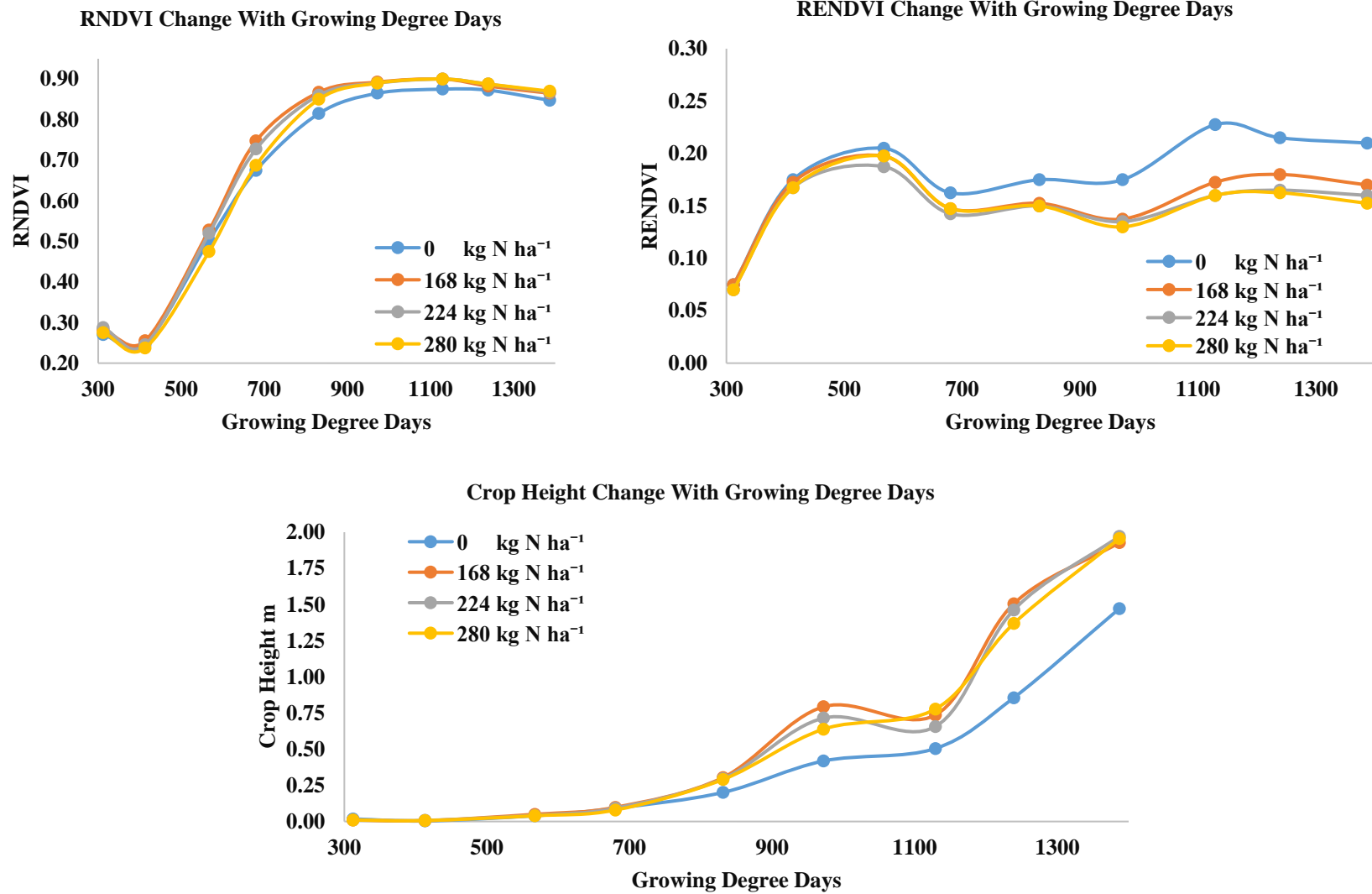
Figure 22. Changes in RNDVI, RENDVI, and crop height through the 2018 corn growing season Ada.

Corn Sabin 2018 sensor analysis

The SUAS sensing for corn at Sabin 2018 was performed on a roughly weekly basis from the V4 (483 GDD) to the R2 (1632 GDD). The sensing dates were on May 31 (V4), June 7 (V4), June 15 (V6), June 21 (V6), June 28 (V8), July 5 (V9), July 12 (VT), July 18 (R1), and July 27 (R2).

Table 20 shows the regression analysis relationship with YP. Figure 23 graphically depicts how the regression coefficient (R^2) fluctuated throughout the season. The experimental site was exposed to early season moisture deficiency, early season phosphorous deficiency in some experimental plots, and thick sugar beet tailings in some of the experimental plots (Table 8). In general the sensing's explanatory power for yield prediction increased through the growing season in corn, with RNDVI having a high R^2 early season and RENDVI having a higher R^2 late season. Existing studies have found that as biomass and leaf area index increase, the sensing data accuracy generally increases to a certain threshold and then reaches diminishing returns (Xia et al., 2016; Li et al., 2014). In this case, the sensing accuracy increased until nearly the end of the corn's life cycle when the kernel fill had begun. RNDVI performed better early season with RENDVI performing better late season. As the corn leaves cover the rows, the RENDVI is often superior to RNDVI (Erdle et al., 2011, Nguy-Robertson et al., 2012). In addition RENDVI generally outperformed the other VIs. In this experiment combing optical reflectance with crop height produced unexpected results for explanatory power. This could be caused by poor height estimation. To improve the height accuracy it may be advisable to use the "minus method" as opposed to using the automated digital terrain generation where inaccuracies can be introduced.

Table 21 shows the optical sensor reflectance value means by sensing date. Figure 24 graphically depicts how the VIs and crop height fluctuated throughout the season. The RNDVI was able to differentiate between the N treatments at the V6, V9, VT, and R1 growth stages, although there was an inverse relationship that appeared with higher N treatments producing lower RNDVI readings. The RENDVI was able to differentiate the N treatments starting at the V8 until the R2 growth stage. An inverse relationship appeared with the N treatments and the RENDVI like the RNDVI. Crop height was only able to differentiate the N treatments at the V8 growth stage and was an inverse relationship.

Table 20. Regression coefficient (R^2 value) for the relationship between yield and three sensor readings for corn at Sabin 2018.

Model	Growing Degree Days	Growth Stage	RNDVI	RNDVI X Crop Height	RENDVI	RENDVI X Crop Height	Crop Height
YP 1	483	V4	0.079	0.047	0.015	0.041	0.038
YP 2	594	V4	0.005	0.014	0.097	0.017	0.007
YP 3	755	V6	0.074	0.024	0.131	0.041	0.067
YP 4	878	V6	0.128	0.190	0.000	0.242	0.281*
YP 5	1037	V8	0.121	0.110	0.124	0.165	0.111
YP 6	1189	V9	0.109	0.100	0.181	0.151	0.087
YP 7	1360	VT	0.296*	0.207	0.629*	0.288*	0.195
YP 8	1478	R1	0.000	0.086	0.790*	0.307*	0.084
YP 9	1632	R2	0.001	0.049	0.780*	0.316*	0.049

* Regression significant at the $P<0.05$. (N=16).

R² Change With Growing Degree Days Yield Prediction
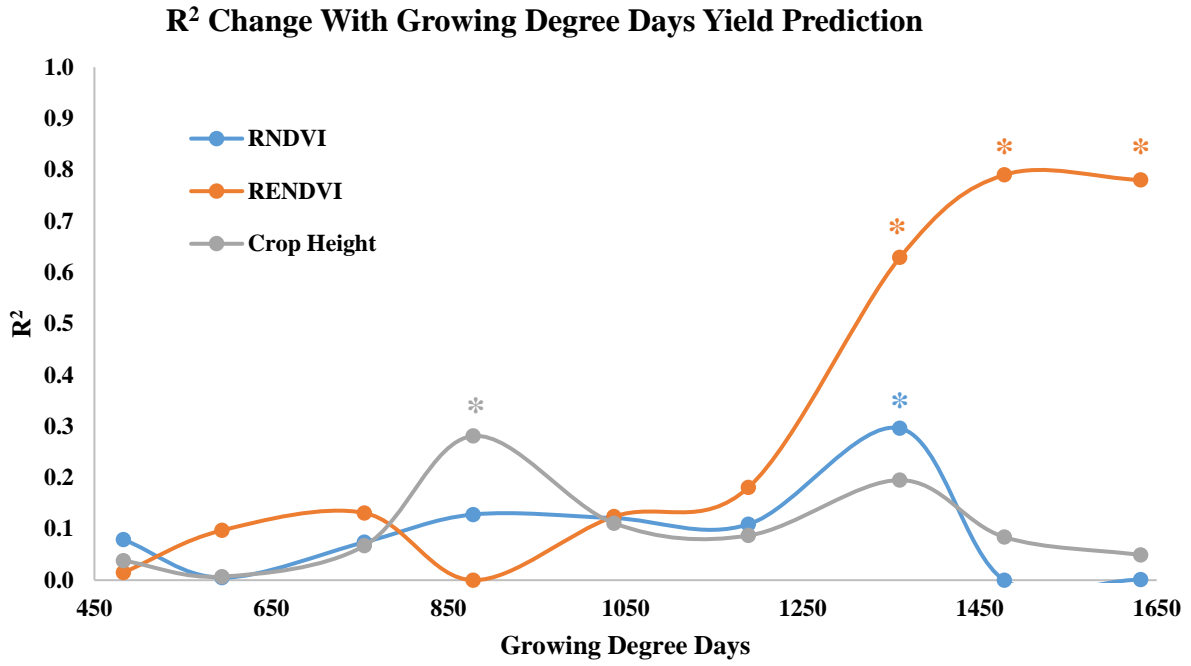
Figure 23. Changes in R^2 for RNDVI, RENDVI, and crop height with yield prediction change through the 2018 corn growing season Sabin.
* Regression significant at the P<0.05. (N=16).

Table 21. Optical reflectance value means for corn at Sabin 2018 sensing by date, growing degree days (GDD), and growth stage.

Treatment N kg ha⁻¹	RNDVI May 31 483 GDD V4 Growth Stage*	RNDVI June 7 594 GDD V4 Growth Stage	RNDVI June 15 755 GDD V6 Growth Stage*	RNDVI June 21 878 GDD V6 Growth Stage*	RNDVI June 28 1037 GDD V8 Growth Stage*	RNDVI July 5 1189 GDD V9 Growth Stage*	RNDVI July 12 1360 GDD VT Growth Stage	RNDVI July 18 1478 GDD R1 Growth Stage*	RNDVI July 27 1632 GDD R2 Growth Stage
0	0.26a	0.23a	0.43a	0.54a	0.77a	0.85a	0.88a	0.86a	0.85a
168	0.25a	0.23a	0.38b	0.47b	0.73ba	0.83b	0.87b	0.85a	0.85a
224	0.26ba	0.23a	0.37cb	0.46b	0.71b	0.83b	0.87b	0.86a	0.85a
280	0.25b	0.21a	0.35c	0.43b	0.70b	0.83b	0.86b	0.85a	0.85a
LSD (α = 0.05)	0.01	0.04	0.02	0.04	0.04	0.02	0.01	0.01	0.02
Treatment N kg ha⁻¹	RENDVI May 31 483 GDD V4 Growth Stage*	RENDVI June 7 594 GDD V4 Growth Stage	RENDVI June 15 755 GDD V6 Growth Stage	RENDVI June 21 878 GDD V6 Growth Stage	RENDVI June 28 1037 GDD V8 Growth Stage*	RENDVI July 5 1189 GDD V9 Growth Stage*	RENDVI July 12 1360 GDD VT Growth Stage*	RENDVI July 18 1478 GDD R1 Growth Stage*	RENDVI July 27 1632 GDD R2 Growth Stage*
0	0.12a	0.22a	0.22a	0.18a	0.21a	0.15a	0.19a	0.19a	0.27a
168	0.12a	0.19a	0.20a	0.18a	0.21a	0.15a	0.17b	0.16b	0.23b
224	0.12a	0.18a	0.20a	0.18a	0.21a	0.15a	0.16b	0.15b	0.23b
280	0.11a	0.20a	0.21a	0.19a	0.21a	0.15a	0.16b	0.16b	0.22b
LSD (α = 0.05)	0.01	0.05	0.02	0.02	0.01	0.01	0.01	0.01	0.02
Treatment N kg ha⁻¹	Crop Height May 31 483 GDD V4 Growth Stage	Crop Height June 7 594 GDD V4 Growth Stage	Crop Height June 15 755 GDD V6 Growth Stage	Crop Height June 21 878 GDD V6 Growth Stage	Crop Height June 28 1037 GDD V8 Growth Stage*	Crop Height July 5 1189 GDD V9 Growth Stage	Crop Height July 12 1360 GDD VT Growth Stage	Crop Height July 18 1478 GDD R1 Growth Stage	Crop Height July 27 1632 GDD R2 Growth Stage
0	0.010a	0.0073a	0.0067a	0.0091b	0.24a	0.47a	0.70a	0.83a	1.06a
168	0.0085a	0.0064a	0.0072a	0.013ba	0.17b	0.40a	0.52ba	0.66a	0.92a
224	0.0080a	0.011a	0.0067a	0.014ba	0.17b	0.33a	0.43b	0.65a	0.88a
280	0.0076a	0.0074a	0.0076a	0.017a	0.11c	0.35a	0.50b	0.72a	0.90a
LSD (α = 0.05)	0.003	0.01	0.004	0.01	0.05	0.16	0.20	0.20	0.31

* RCBD significant at the P<0.05. (N=16).
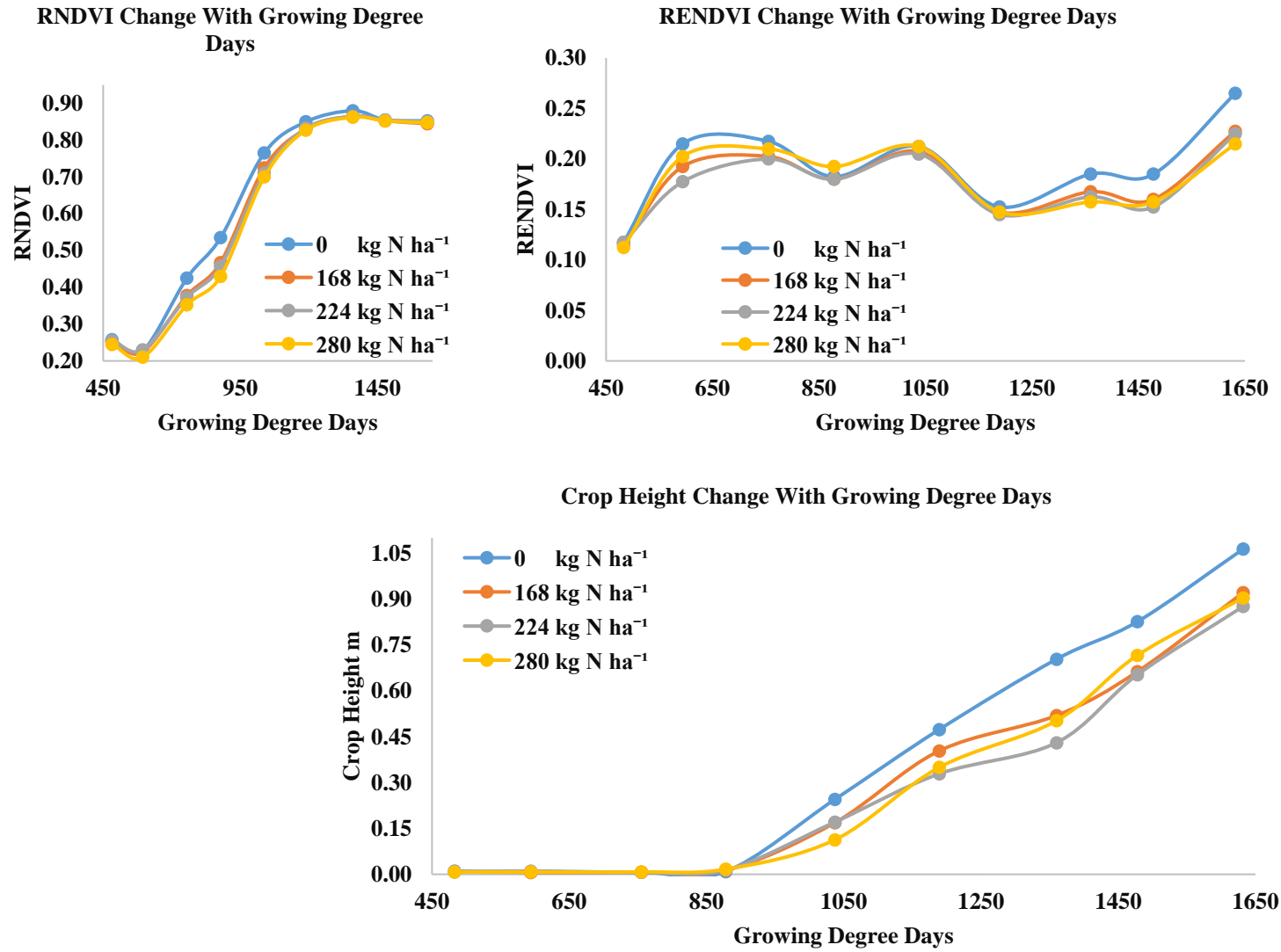
Figure 24. Changes in RNDVI, RENDVI, and crop height through the 2018 corn growing season Sabin.

Sugar beet N rate experiments 2018

Sugar beet yield Ada and Downer for 2018 are shown in Table 22. The N treatments of 0 and 179 kg ha^{-1} yielded 76.90 and 85.77 Mg ha^{-1} respectively at Ada. The N treatments of 0 and 179 kg ha^{-1} yielded 46.80 and 43.67 Mg ha^{-1} respectively at Downer. Nitrogen treatments at both sites failed to produce statistically significant yield increases. This could have occurred for a variety of reasons including residual nitrates and N mineralization that were present in the soil environment. Ada and Downer were generally less than average rainfall (Table 8). Drought stress has a deleterious effect on root dry weight and virtually every biological structure and function of the sugar beet plant (Moosavi et al., 2017). The Downer site was also affected by sand syndrome and rhizoctonia root rot which caused marked yield reduction. The Ada site produced yield that were respectable. The rate of 146 kg N ha^{-1} produced the greatest amount of recoverable sugar.

Table 22. Sugar beet yield, net sugar %, and recoverable sugar yield means for N fertilization response Ada 2018 and Downer 2018 trials ANOVA results.

Site	Treatment N kg ha^{-1}	Yield Mg ha^{-1}	Net Sugar %	Recoverable Sugar Yield Mg ha^{-1}
Ada 2018	0	76.90b	17.78a	12.92b
	146	84.96a	17.68a	14.35a
	179	85.77a	17.38a	13.90ba
	LSD ($\alpha = 0.05$)	6.55	0.59	1.39
Downer 2018	Treatment N kg ha^{-1}	Yield Mg ha^{-1}	Net Sugar %	Recoverable Sugar Yield Mg ha^{-1}
	0	46.80a	13.98a	6.09a
	146	49.56a	13.80a	6.34a
	179	43.66a	13.50a	5.44a
	LSD ($\alpha = 0.05$)	8.65	0.71	1.24

* N treatments significant the 0.05 level. (N=12).

Ada 2018 had significant yield response to different N fertilization rates with coefficient of determination (R^2) value of 0.60, while Downer 2018 had no response due to extremely detrimental plot conditions (Figure 25).

Ada

Downer

$$y = -0.0005x^2 + 0.13x + 76.894$$
$$R^2 = 0.6430$$
$$F = 0.0031$$

$$y = -0.0011x^2 + 0.1769x + 46.801$$
$$R^2 = 0.1876$$
$$F = 0.7758$$
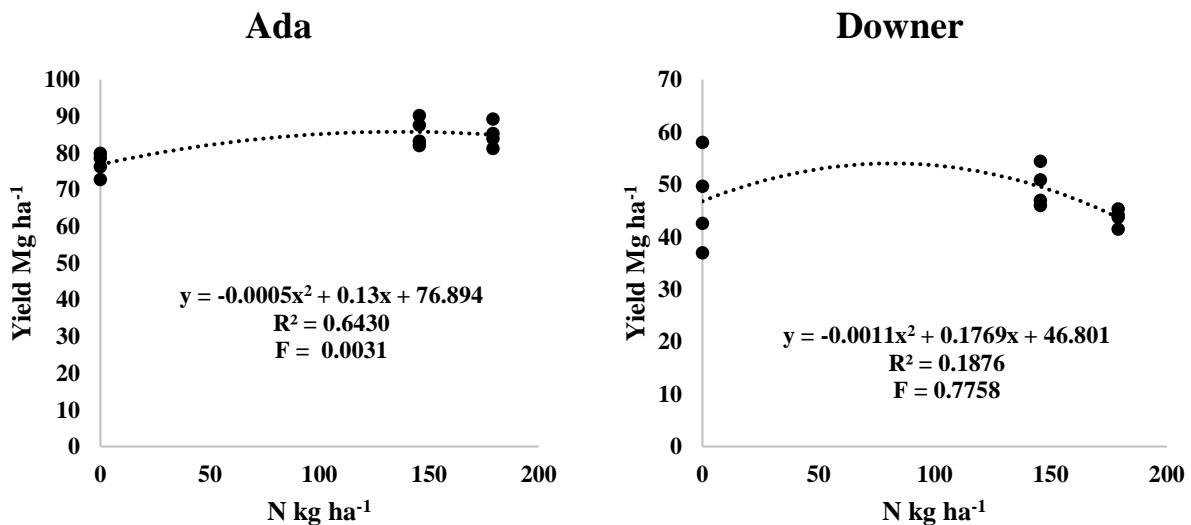
Figure 25. Sugar beet yield Ada 2018 and Downer 2018 response to N fertilization rates. Sugar beet Ada 2018 sensor analysis.

Sugar beet Ada 2018 sensor analysis

SUAS sensing was performed on a weekly basis with the growth stages ranging from the V4 (704 GDD) to the V15 (2679 GDD). The sensing dates for sugar beet at Ada 2018 were on May 31 (V4), June 7 (V6), June 15 (V7), June 21 (V8), June 28 (V10), July 5 (V12), July 12 (V14), July 18 (V15), and July 27 (V15).

Table 23 shows the regression analysis relationship with YP and RSP. Figure 26 graphically depicts how the regression coefficient (R^2) fluctuated throughout the season. The experimental site received less than average rain (Table 8). In general the sensing's R^2 for YP and RSP reached a peak at the V7 and plateaued. Previous studies have found that as biomass and leaf area index increase, the sensing data accuracy generally increases to a certain

threshold and then reaches diminishing returns (Xia et al., 2016; Li et al., 2014). Which is in agreement with what was found in this experiment. RNDVI performed better than RENDVI did throughout the majority of the growing season. In this experiment combing optical reflectance with crop height produced mixed results for the R^2. This could be caused by poor height estimation. To improve the height accuracy it may be advisable to use the "minus method" as opposed to using the automated digital terrain generation where inaccuracies can be introduced. In addition heat stress and moisture deficiency can cause wilting which would further impact on the height generation accuracy. Both YP and RSP had generally poor R^2 that were not statistically significant.

Table 24 shows the optical sensor reflectance value means by sensing date. Figure 27 graphically depicts how the VIs and crop height fluctuated throughout the season. The RNDVI was able to differentiate the N treatments at the V8, V10, and V14 growth stages. The RENDVI and crop height were unable to differentiate the N treatments at any of the growth stages throughout the season. Crop height calculated that sugar beet height decreased at the V14 and V15. This is likely due to leaf wilt due to high heats and moisture deficiency.

Table 23. Regression coefficient (R^2 value) for the relationship between yield and recoverable sugar and three sensor readings for the sugar beet at Ada 2018 sensing.

Model	Growing Degree Days	Growth Stage	RNDVI	RNDVI X Crop Height	RENDVI	RENDVI X Crop Height	Crop Height
YP 1	704	V4	0.156	0.103	0.013	0.059	0.056
YP 2	914	V6	0.002	0.014	0.001	0.018	0.019
YP 3	1191	V7	0.510*	0.101	0.505*	0.050	0.027
YP 4	1400	V8	0.447*	0.367*	0.566*	0.350*	0.313
YP 5	1663	V10	0.311	0.013	0.075	0.000	0.005
YP 6	1916	V12	0.233	0.007	0.024	0.001	0.001
YP 7	2185	V14	0.336*	0.053	0.045	0.058	0.068
YP 8	2389	V15	0.346*	0.162	0.067	0.138	0.193
YP 9	2679	V15	0.267	0.153	0.028	0.107	0.145
RSP 1	704	V4	0.161	0.078	0.018	0.051	0.035
RSP 2	914	V6	0.008	0.000	0.014	0.000	0.001
RSP 3	1191	V7	0.558*	0.261	0.515*	0.169	0.130
RSP 4	1400	V8	0.364*	0.387*	0.451*	0.377*	0.348*
RSP 5	1663	V10	0.177	0.029	0.057	0.009	0.002
RSP 6	1916	V12	0.161	0.009	0.001	0.024	0.040
RSP 7	2185	V14	0.211	0.077	0.010	0.083	0.092
RSP 8	2389	V15	0.198	0.123	0.044	0.102	0.144
RSP 9	2679	V15	0.108	0.040	0.055	0.020	0.036

* Regression significant at the P<0.05. (N=12).
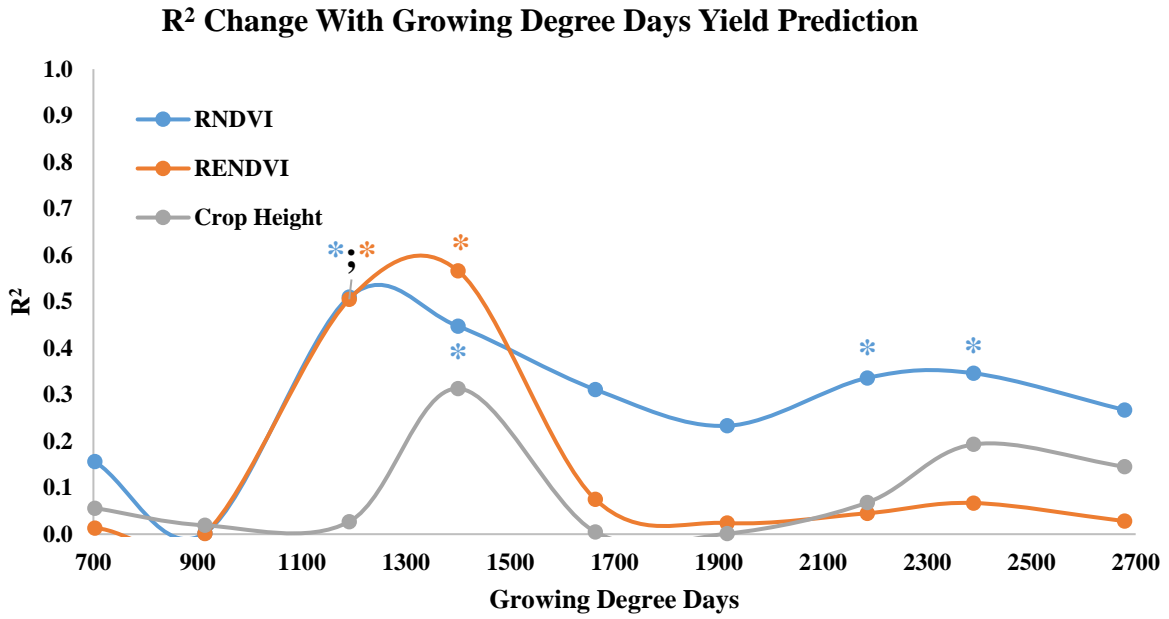
R² Change With Growing Degree Days Yield Prediction

Figure 26. Changes in R^2 for RNDVI, RENDVI, and crop height with yield prediction change through the 2018 sugar beet growing season Ada.
* Regression significant at the P<0.05. (N=12).

Table 24. Optical reflectance value means for sugar beet at Ada 2018 sensing by date, growing degree days (GDD), and growth stage.

Treatment N kg ha⁻¹	RNDVI May 31 703 GDD V4 Growth Stage	RNDVI June 7 914 GDD V6 Growth Stage	RNDVI June 15 1191 GDD V7 Growth Stage	RNDVI June 21 1400 GDD V8 Growth Stage*	RNDVI June 28 1663 GDD V10 Growth Stage*	RNDVI July 5 1916 GDD V12 Growth Stage	RNDVI July 12 2185 GDD V14 Growth Stage*	RNDVI July 18 2389 GDD V15 Growth Stage*	RNDVI July 27 2679 GDD V15 Growth Stage
0	0.25a	0.24a	0.50b	0.66b	0.79b	0.83b	0.88b	0.87b	0.87b
146	0.24a	0.24a	0.56a	0.75a	0.87a	0.86a	0.90a	0.89a	0.89a
179	0.25a	0.24a	0.55ba	0.74a	0.87a	0.86a	0.90a	0.89a	0.89a
LSD ($\alpha = 0.05$)	0.03	0.03	0.06	0.05	0.05	0.03	0.02	0.02	0.01
Treatment N kg ha⁻¹	RENDVI May 31 703 GDD V4 Growth Stage	RENDVI June 7 914 GDD V6 Growth Stage	RENDVI June 15 1191 GDD V7 Growth Stage	RENDVI June 21 1400 GDD V8 Growth Stage	RENDVI June 28 1663 GDD V10 Growth Stage	RENDVI July 5 1916 GDD V12 Growth Stage	RENDVI July 12 2185 GDD V14 Growth Stage	RENDVI July 18 2389 GDD V15 Growth Stage	RENDVI July 27 2679 GDD V15 Growth Stage
0	0.070a	0.20a	0.23a	0.19b	0.25a	0.22b	0.27a	0.25b	0.30a
146	0.065a	0.19a	0.24a	0.20a	0.27a	0.24a	0.28a	0.27a	0.30a
179	0.065a	0.19a	0.24a	0.20a	0.27a	0.24a	0.28a	0.27a	0.30a
LSD ($\alpha = 0.05$)	0.01	0.01	0.02	0.01	0.02	0.03	0.01	0.01	0.02
Treatment N kg ha⁻¹	Crop Height May 31 703 GDD V4 Growth Stage	Crop Height June 7 914 GDD V6 Growth Stage	Crop Height June 15 1191 GDD V7 Growth Stage	Crop Height June 21 1400 GDD V8 Growth Stage	Crop Height June 28 1663 GDD V10 Growth Stage	Crop Height July 5 1916 GDD V12 Growth Stage	Crop Height July 12 2185 GDD V14 Growth Stage	Crop Height July 18 2389 GDD V15 Growth Stage	Crop Height July 27 2679 GDD V15 Growth Stage
0	0.0071a	0.0057a	0.015a	0.029a	0.063a	0.060ba	0.14a	0.094a	0.067b
146	0.0061a	0.0086a	0.015a	0.043a	0.053a	0.058b	0.14a	0.091a	0.087ba
179	0.0051a	0.012a	0.013a	0.050a	0.062a	0.067a	0.15a	0.090a	0.010a
LSD ($\alpha = 0.05$)	0.003	0.02	0.01	0.02	0.02	0.01	0.10	0.06	0.02

* RCBD significant at the $P<0.05$. (N=12).

RNDVI Change With Growing Degree Days

RENDVI Change With Growing Degree Days
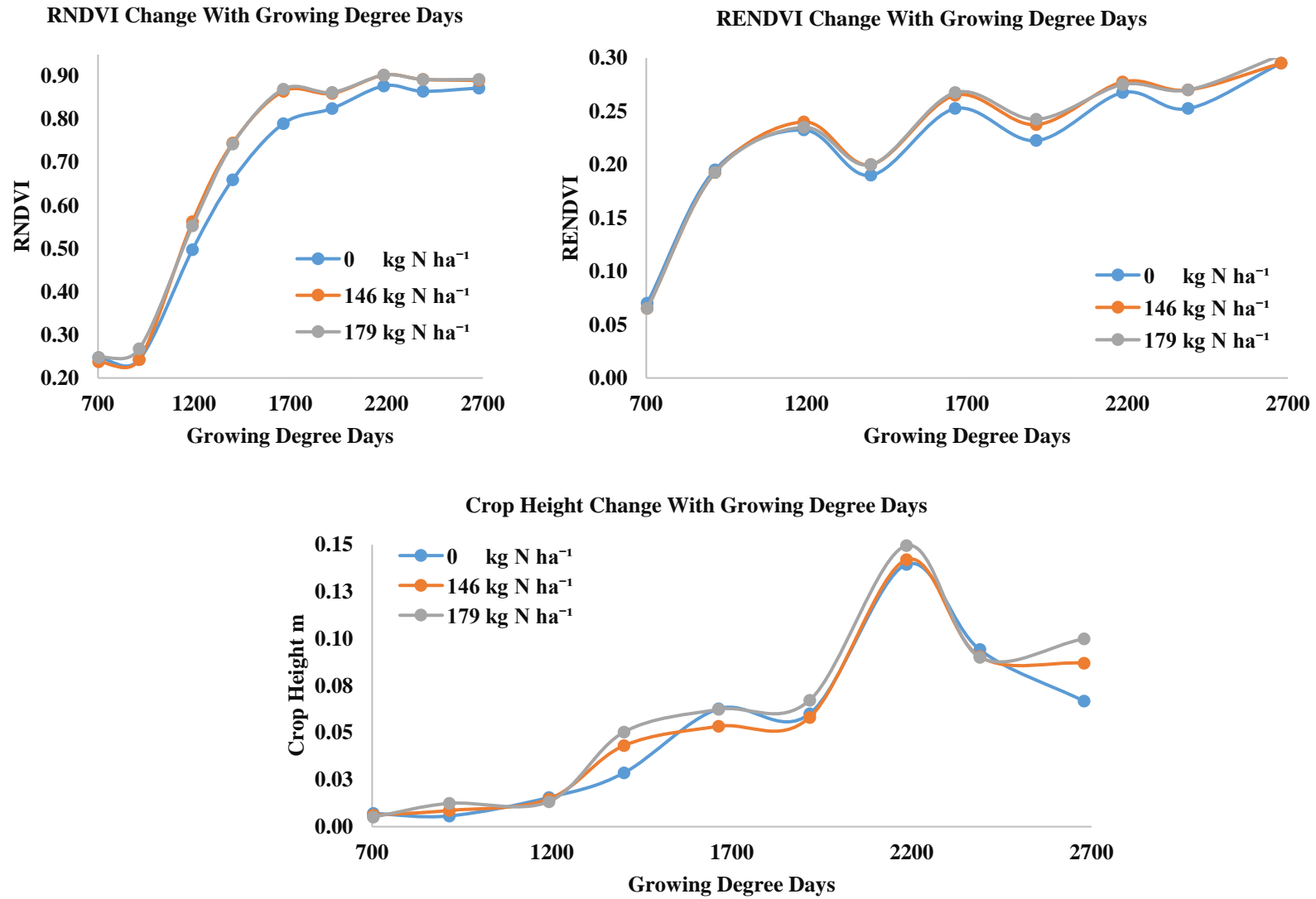
Crop Height Change With Growing Degree Days

Figure 27. Changes in RNDVI, RENDVI, and crop height through the 2018 sugar beet growing season Ada.

Sugar beet Downer 2018 sensor analysis

SUAS sensing was performed on a weekly basis with the growth stages ranging from the V4 (862 GDD) to the V15 (2921 GDD). The sensing dates for sugar beet at Downer 2018 were on May 31 (V4), June 7 (V5), June 15 (V7), June 21 (V8), June 28 (V8), July 5 (V10), July 12 (V14), July 18 (V15), and July 27 (V15). Table 25 shows the regression analysis relationship with YP and RSP. Figure 28 graphically depicts how the regression coefficient (R^2) fluctuated throughout the season. The experimental site was exposed to early season moisture deficiency, sand syndrome, and rhizoctonia root rot (Table 8). In general the sensing's R^2 for YP and RSP were poor throughout the entire season. All VIs performed extremely poorly. Out of the different VIs RNDVI had the highest R^2. In this experiment combing optical reflectance with crop height produced mixed results for the R^2. This could be caused by poor height estimation. To improve the height accuracy it may be advisable to use the "minus method" as opposed to using the automated digital terrain generation where inaccuracies can be introduced. In addition heat stress and moisture deficiency can cause wilting which would further impact on the height generation accuracy. The previously mentioned growing condition had very significant effects on the health, vigor, and canopy of the sugar beet. These conditions had extremely detrimental effects on the R^2 for YP and RSP with the results being very poor in the majority of cases.

Table 26 shows the optical sensor reflectance value means by sensing date. Figure 29 graphically depicts how the VIs and crop height fluctuated throughout the season. The RNDVI, RENDVI, and crop height were unable to differentiate the N treatments at any of the sensing dates, with the exception of RENDVI at the V8 growth stage. This can be explained by the very poor growing conditions that were experienced at the Downer 2018 experimental site.

Table 25. Regression coefficient (R^2 value) for the relationship between yield and recoverable sugar and three sensor readings for the sugar beet at Downer 2018 sensing.

Model	Growing Degree Days	Growth Stage	RNDVI	RNDVI X Crop Height	RENDVI	RENDVI X Crop Height	Crop Height
YP 1	862	V4	0.004	0.114	0.025	0.118	0.114
YP 2	1085	V5	0.008	0.075	0.008	0.069	0.064
YP 3	1373	V7	0.134	-	0.027	-	-
YP 4	1592	V8	0.225	0.418*	0.059	0.307	0.335*
YP 5	1863	V8	0.166	0.158	0.081	0.073	0.101
YP 6	2127	V10	0.154	0.000	0.089	0.005	0.004
YP 7	2410	V14	0.015	0.241	0.272	0.214	0.252
YP 8	2624	V15	0.036	0.158	0.188	0.103	0.136
YP 9	2921	V15	0.151	0.000	0.074	0.012	0.007
RSP 1	862	V4	0.012	0.104	0.019	0.104	0.103
RSP 2	1085	V5	0.009	0.144	0.010	0.134	0.126
RSP 3	1373	V7	0.167	-	0.058	-	-
RSP 4	1592	V8	0.250	0.315	0.049	0.225	0.245
RSP 5	1863	V8	0.180	0.135	0.046	0.060	0.081
RSP 6	2127	V10	0.260	0.008	0.064	0.000	0.000
RSP 7	2410	V14	0.045	0.183	0.302	0.134	0.174
RSP 8	2624	V15	0.085	0.122	0.182	0.066	0.092
RSP 9	2921	V15	0.235	0.005	0.074	0.004	0.001

* Regression significant at the $P < 0.05$. (N=12).

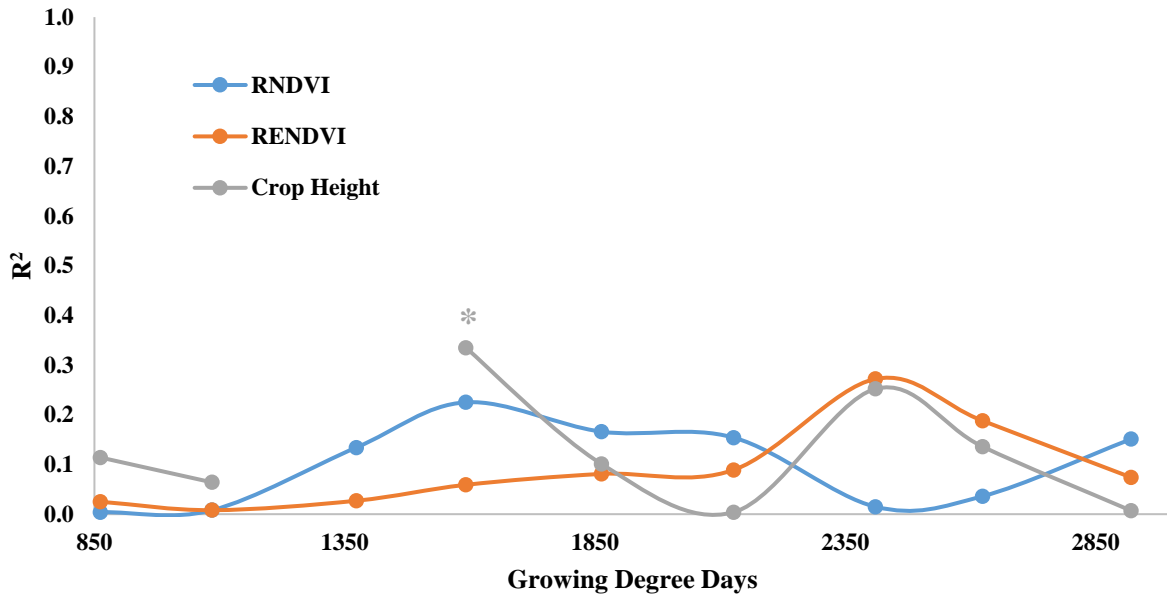**R² Change With Growing Degree Days Yield Prediction**

Figure 28. Changes in R^2 for RNDVI, RENDVI, and crop height with yield prediction change through the 2018 sugar beet growing season Downer.
* Regression significant at the $P<0.05$. (N=12).

Table 26. Optical reflectance value means for sugar beet at Downer 2018 sensing by date, growing degree days (GDD), and growth stage.

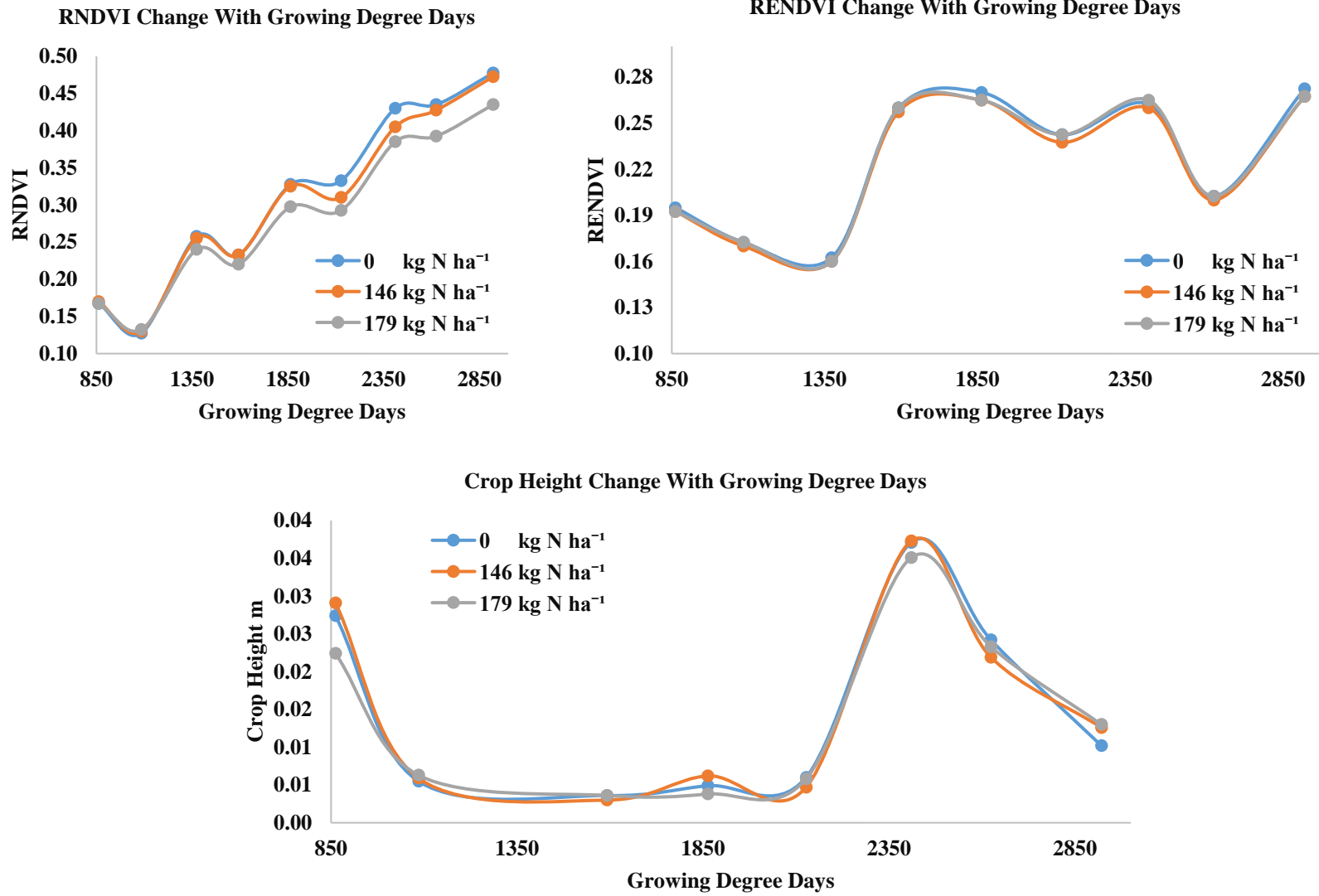| Treatment N kg ha^{-1}	RNDVI May 31 862 GDD V4 Growth Stage	RNDVI June 7 1085 GDD V4 Growth Stage	RNDVI June 15 1373 GDD V7 Growth Stage	RNDVI June 21 1592 GDD V8 Growth Stage	RNDVI June 28 1863 GDD V8 Growth Stage	RNDVI July 5 2127 GDD V10 Growth Stage	RNDVI July 12 2410 GDD V14 Growth Stage*	RNDVI July 18 2624 GDD V15 Growth Stage	RNDVI July 27 2921 GDD V15 Growth Stage
0	0.17a	0.13a	0.26a	0.23a	0.33a	0.33a	0.43a	0.44a	0.48a
146	0.17a	0.13a	0.26a	0.23a	0.33a	0.31ba	0.41ba	0.43a	0.47a
179	0.17a	0.13a	0.24a	0.22a	0.30a	0.29b	0.39b	0.39b	0.44a
LSD (α = 0.05)	0.01	0.02	0.03	0.02	0.04	0.03	0.03	0.04	0.06
Treatment N kg ha^{-1}	RENDVI May 31 862 GDD V4 Growth Stage	RENDVI June 7 1085 GDD V4 Growth Stage	RENDVI June 15 1373 GDD V7 Growth Stage	RENDVI June 21 1592 GDD V8 Growth Stage	RENDVI June 28 1863 GDD V8 Growth Stage*	RENDVI July 5 2127 GDD V10 Growth Stage	RENDVI July 12 2410 GDD V14 Growth Stage	RENDVI July 18 2624 GDD V15 Growth Stage	RENDVI July 27 2921 GDD V15 Growth Stage
0	0.20a	0.17a	0.16a	0.26a	0.27a	0.24a	0.26a	0.20a	0.27a
146	0.19a	0.17a	0.16a	0.26a	0.27a	0.24a	0.26a	0.20a	0.27a
179	0.19a	0.17a	0.16a	0.26a	0.27a	0.24a	0.27a	0.20a	0.27a
LSD (α = 0.05)	0.01	0.01	0.01	0.01	0.01	0.01	0.01	0.11	0.01
Treatment N kg ha^{-1}	Crop Height May 31 862 GDD V4 Growth Stage	Crop Height June 7 1085 GDD V4 Growth Stage	Crop Height June 15 1373 GDD V7 Growth Stage	Crop Height June 21 1592 GDD V8 Growth Stage	Crop Height June 28 1863 GDD V8 Growth Stage	Crop Height July 5 2127 GDD V10 Growth Stage	Crop Height July 12 2410 GDD V14 Growth Stage	Crop Height July 18 2624 GDD V15 Growth Stage	Crop Height July 27 2921 GDD V15 Growth Stage
0	0.027a	0.0055a	-	0.0036a	0.0049a	0.0060a	0.037a	0.024a	0.010a
146	0.029a	0.0059a	-	0.0030a	0.0062a	0.0047a	0.037a	0.022a	0.013a
179	0.022a	0.0063a	-	0.0036a	0.0038a	0.0058a	0.035a	0.023a	0.013a
LSD (α = 0.05)	0.03	0.003	-	0.003	0.003	0.004	0.02	0.02	0.01

* RCBD significant at the P<0.05. (N=12).

Figure 29. Changes in RNDVI, RENDVI, and crop height through the 2018 sugar beet growing season Downer.

Ada 2017 harvest study

Ada 2017 was planted on May 1 and was harvested on the two dates of September 19 and October 3. The yield and recoverable sugar yield both increased substantially during the second harvest with the results being statistically significant. Net sugar percent was similar between the first and second harvest dates. The yield, recoverable sugar, and net sugar percent for Ada 2017 are summarized in Table 27.

Table 27. Sugar beet yield, net sugar %, and recoverable sugar yield means for harvest at Ada 2017 trial ANOVA results.

Harvest Date	Yield Mg ha^{-1}*	Net Sugar %	Recoverable Sugar Yield Mg ha^{-1}*
September 19	76.24b	17.75a	12.74b
October 3	92.79a	17.68a	15.65a
LSD ($\alpha = 0.05$)	12.43	0.87	2.31

* CRD significant at the $P<0.05$. (N=8).

The RNDVI values had reached saturation at harvest dates and the VI values were all equal. There was therefore no relationship for YP and RSP. RENDVI also had no relationship with YP and RSP. This is probably due to the low number of samples (N=4). A higher number of samples could possibly improve the explanatory power of the VIs in relation to the yield and recoverable sugar. In addition to a low sample number the sample row length of five feet could also be increased. There was also high variance amongst the samples, which also reduced the R^2 values. Table 28 shows the regression analysis results.

Table 28. Regression coefficient (R^2 value) for the relationship between yield and recoverable sugar and two sensor readings for the sugar beet Ada 2017 harvest sensing. (YP=Yield prediction; RSP=Recoverable sugar prediction).

Harvest Date	RNDVI	RENDVI
YP September 19	-	0.656
YP October 3	-	0.385
RSP September 19	-	0.411
RSP October 3	-	0.326

* Regression significant at the P<0.05. (N=4).

Downer 2017 harvest study

Downer 2017 was planted on May 2 and was harvested on the two dates of September 19 and October 3. Yield, net sugar percent, and recoverable sugar yield were similar between the harvest dates.   The yield, recoverable sugar, and net sugar percent for Downer 2017 are summarized in Table 29.

Table 29. Sugar beet yield, net sugar %, and recoverable sugar yield means for harvest at Downer 2017 trial ANOVA results.

Harvest Date	Yield Mg ha^{-1}	Net Sugar %	Recoverable Sugar Yield Mg ha^{-1}
September 19	70.21a	18.65a	12.27a
October 3	82.71a	18.33a	14.38a
LSD ($\alpha = 0.05$)	13.55	1.35	2.57

* CRD significant at the P<0.05. (N=8).

The RNDVI values had reached saturation levels at the harvest dates leading to poor yield prediction and recoverable sugar prediction. The RENDVI gave generally poor results for both of the harvest dates. The RNDVI and RENDVI both generally produced poor results with the exception of the first RENDVI yield prediction. A higher number of samples could possibly improve the explanatory power of the VIs in relation to the yield and recoverable sugar. In

addition to a higher number of samples it may be advisable to increase the sample row length

greater than five feet. Table 30 shows the regression analysis results.

Table 30. Regression coefficient (R^2 value) for the relationship between yield and recoverable sugar and two sensor readings for the sugar beet Downer 2017 harvest sensing. (YP=Yield prediction; RSP=Recoverable sugar prediction).

Harvest Date	RNDVI	RENDVI
YP September 19	0.000	0.449
YP October 3	0.150	0.001
RSP September 19	0.111	0.163
RSP October 3	0.001	0.115

* Regression significant at the P<0.05. (N=4).

Prosper 2017 harvest study

Prosper 2017 was planted on May 1 and was harvested on the two dates of September 19

and October 3. The yield and recoverable sugar yield increased during the second harvest.

There was no difference in net sugar concentration between harvest dates. The yield,

recoverable sugar, and net sugar percent for Prosper 2017 are summarized in Table 31.

Table 31. Sugar beet yield, net sugar %, and recoverable sugar yield means for harvest at Prosper 2017 trial ANOVA results.

Harvest Date	Yield Mg ha^{-1}*	Net Sugar %	Recoverable Sugar Yield Mg ha^{-1}*
September 19	64.97b	19.00a	11.34b
October 3	89.23a	17.80a	14.90a
LSD ($\alpha = 0.05$)	15.18	1.64	2.97

* CRD significant at the P<0.05. (N=8).

Although RNDVI reached saturation levels the relationship between optical sensor

reading was significant for yield at the first sensing date. There were no significant regression

relationships of RNDVI with recoverable sugar concentration. The RENDVI was not related to

yield or recoverable sugar at either of the sensing dates. The sample size was small (N=4) and to

increase accuracy a higher number of samples might improve the relationships of optical

reflectance with yield, net sugar percent, and recoverable sugar. It may also be advisable to

increase the sample row length beyond the five feet that was used in this work. Table 32 shows

the regression analysis results.

Table 32. Regression coefficient (R^2 value) for the relationship between yield and recoverable sugar and two sensor readings for the sugar beet Prosper 2017 harvest sensing. (YP=Yield prediction; RSP=Recoverable sugar prediction).

Harvest Date	RNDVI	RENDVI
YP September 19	0.938*	0.264
YP October 3	0.383	0.383
RSP September 19	0.800	0.383
RSP October 3	0.398	0.398

* Regression significant at the P<0.05. (N=4).

The summary for the 2017 sugar beet harvest date study is presented in Table 33. At the

Ada and Prosper site there was an increase in both yield and recoverable sugar yield, while there

we no difference at the Downer site. There was no difference in net sugar percent due to harvest

timing at any of the three sites that were examined. Increased sample size and increased row

length sample are advisable to obtain higher quality data sets.

Table 33. Sugar beet yield, net sugar %, and recoverable sugar yield means 2017 harvest summary ANOVA results.

Site	Harvest Date	Yield Mg ha^{-1}	Net Sugar %	Recoverable Sugar Yield Mg ha^{-1}
Ada	September 19	76.24b*	17.75a	12.74b *
	October 3	92.79a *	17.68a	15.65a *
Downer	September 19	70.21a	18.65a	12.27a
	October 3	82.71a	18.33a	14.38a
Prosper	September 19	64.97b *	19.00a	11.34b *
	October 3	89.23a *	17.80a	14.90a*

* CRD significant at the P<0.05. (N=8).

The summary for the 2017 sugar beet harvest date study is presented in Table 34. There was no relationship between RNDVI and RENDVI and yield and recoverable sugar yield, with the one exception of Prosper RNDVI yield at the September 19 sensing date. Increased sample size and increased row length sample are advisable to obtain higher quality data sets.

Table 34. Regression coefficient (R^2 value) for the relationship between yield and recoverable sugar and two sensor readings sugar beet 2017 harvest sensing summary. (YP=Yield prediction; RSP=Recoverable sugar prediction).

Harvest	Ada		Downer		Prosper	
Date	RNDVI	RENDVI	RNDVI	RENDVI	RNDVI	RENDVI
YP September 19	-	0.656	0.000	0.449	0.938*	0.264
YP October 3	-	0.385	0.150	0.001	0.383	0.383
RSP September 19	-	0.411	0.111	0.163	0.800	0.383
RSP October 3	-	0.326	0.001	0.115	0.398	0.398

* Regression significant at the $P<0.05$. (N=4).

Ada 2018 harvest study

Ada 2018 was planted on May 3rd and was harvested on the three dates of August 21, September 4, and September 18. The yield and recoverable sugar both increased from the first harvest to the second harvest, but the third harvest yield and recoverable sugar yield were similar to the second harvest date. Net sugar percent was similar among all three sensing dates. The yield, recoverable sugar, and net sugar percent for Ada 2018 are summarized in Table 35.

Table 35. Sugar beet yield, net sugar %, and recoverable sugar yield means for harvest at Ada 2018 trial ANOVA results.

Harvest Date	Yield Mg ha^{-1}*	Net Sugar %	Recoverable Sugar Yield Mg ha^{-1}*
August 21	53.53b	18.30b	9.22b
September 4	72.97a	17.58a	12.12a
September 18	67.52a	18.10ba	11.56a
LSD ($\alpha = 0.05$)	11.77	0.67	1.68

* CRD significant at the $P<0.05$. (N=12).

There were no differences in the relationship of RNDVI or RENDVI with yield or recoverable sugar yield at the three harvest dates. This was likely due to the low number of samples, row length sample, and high variability in samples. Table 36 shows the regression analysis results.

Table 36. Regression coefficient (R^2 value) for the relationship between yield and recoverable sugar and two sensor readings for the sugar beet Ada 2018 harvest sensing. (YP=Yield prediction; RSP=Recoverable sugar prediction).

Harvest Date	RNDVI	RENDVI
YP August 21	0.647	0.136
YP September 4	0.274	0.075
YP September 18	0.697	-
RSP August 21	0.633	0.078
RSP September 4	0.393	0.095
RSP September 18	0.528	-

* Regression significant at the $P<0.05$. (N=4).

Casselton 2018 harvest study

Casselton 2018 was planted on May 21 and was harvested on the three dates of August 21, September 4, and September 18. The yield, net sugar percent, and recoverable sugar yield increased during the second harvest. The second and third harvests were the similar for yield, net sugar percent, and recoverable sugar yield. The yield, recoverable sugar, and net sugar percent for Casselton 2018 are summarized in Table 37.

Table 37. Sugar beet yield, net sugar %, and recoverable sugar yield means for harvest at Casselton 2018 trial ANOVA results.

Harvest Date	Yield Mg ha^{-1}*	Net Sugar %*	Recoverable Sugar Yield Mg ha^{-1}*
August 21	56.93b	16.30b	8.63b
September 4	77.20a	17.35a	12.57a
September 18	83.53a	18.00a	14.04a
LSD ($\alpha = 0.05$)	17.65	0.93	2.76

* CRD significant at the P<0.05. (N=12).

There were no differences in the relationship of RNDVI or RENDVI with yield or recoverable sugar yield at the three harvest dates. This was likely due to the low number of samples, row length sample, and high variability in samples. Table 38 shows the regression analysis results.

Table 38. Regression coefficient (R^2 value) for the relationship between yield and recoverable sugar and two sensor readings for the sugar beet Casselton 2018 harvest sensing. (YP=Yield prediction; RSP=Recoverable sugar prediction).

Harvest Date	RNDVI	RENDVI
YP August 21	0.542	0.010
YP September 4	0.319	0.003
YP September 18	0.717	0.200
RSP August 21	0.684	0.198
RSP September 4	0.250	0.000
RSP September 18	0.462	0.123

* Regression significant at the P<0.05. (N=4).

Glyndon 2018 harvest study

Glyndon 2018 was planted on May 2 and three harvests were made on August 21, September 4, and September 18. The yield, net sugar percent, and recoverable sugar yield all increased during the second harvest. There was no difference between the second and third

harvests. The yield, recoverable sugar, and net sugar percent for Glyndon 2018 are summarized

in Table 39.

Table 39. Sugar beet yield, net sugar %, and recoverable sugar yield means for harvest at
Glyndon 2018 trial ANOVA results.

Harvest Date	Yield Mg ha^{-1} *	Net Sugar %*	Recoverable Sugar Yield Mg ha^{-1}*
August 21	41.11b	19.33b	7.18b
September 4	80.43a	15.48a	11.40a
September 18	73.68a	16.58a	11.05a
LSD ($\alpha = 0.05$)	20.02	1.15	2.97

* CRD significant at the $P<0.05$. (N=12).

There were no differences in the relationship of RNDVI or RENDVI with yield or

recoverable sugar yield at the three harvest dates. This was likely due to the low number of

samples, row length sample, and high variability in samples. Table 40 shows the regression

analysis results.

Table 40. Regression coefficient (R^2 value) for the relationship between yield and recoverable
sugar and two sensor readings for the sugar beet Glyndon 2018 harvest sensing. (YP=Yield
prediction; RSP=Recoverable sugar prediction).

Harvest Date	RNDVI	RENDVI
YP August 21	0.400	0.087
YP September 4	0.319	0.081
YP September 18	0.000	0.000
RSP August 21	0.012	0.316
RSP September 4	0.361	0.066
RSP September 18	0.068	0.068

* Regression significant at the $P<0.05$. (N=4).

The summary for the 2018 sugar beet harvest date study is presented in Table 33. At the

Ada, Casselton, and Glyndon sites there was an increase in yield, net sugar percent, and

recoverable sugar yield at between the first and second harvest dates. The third harvest date was

similar to the second harvest date. Increased sample size and increased row length sample are

advisable to obtain higher quality data sets.

Table 41. Sugar beet yield, net sugar %, and recoverable sugar yield means 2018 harvest
summary ANOVA results.

Site	Harvest Date	Yield Mg ha^{-1}	Net Sugar %	Recoverable Sugar Yield Mg ha^{-1}
Ada	August 21	53.53b*	18.30b*	9.22b *
	September 4	72.97a *	17.58a *	12.12a*
	September 18	67.52a	18.10ba	11.56a
Casselton	August 21	56.93b *	16.30b *	8.63b *
	September 4	77.20a *	17.35a *	12.57a*
	September 18	83.53a	18.00a	14.04a
Glyndon	August 21	41.11b *	19.33b *	7.18b *
	September 4	80.43a *	15.48a *	11.40a*
	September 21	73.68a	16.58a	11.05a

* CRD significant at the $P<0.05$. (N=12).

The summary for the 2018 sugar beet harvest date study is presented in Table 42. There

was no relationship between RNDVI and RENDVI and yield and recoverable sugar yield.

Increased sample size and increased row length sample are advisable to obtain higher quality

data sets.

Table 42. Regression coefficient (R^2 value) for the relationship between yield and recoverable sugar and two sensor readings sugar beet 2018 harvest sensing summary. (YP=Yield prediction; RSP=Recoverable sugar prediction).

Harvest Date	Ada		Casselton		Glyndon	
	RNDVI	RENDVI	RNDVI	RENDVI	RNDVI	RENDVI
YP August 21	0.647	0.136	0.542	0.010	0.400	0.087
YP September 4	0.274	0.075	0.319	0.003	0.319	0.081
YP September 18	0.697	-	0.717	0.200	0.000	0.000
RSP August 21	0.633	0.078	0.684	0.198	0.012	0.316
RSP September 4	0.393	0.095	0.250	0.000	0.361	0.066
RSP September 18	0.528	-	0.462	0.123	0.068	0.068

* Regression significant at the $P<0.05$. (N=4).

CONCLUSIONS

Fertility experiments

Corn yield and sugar beet root and recoverable sugar yields in response to N were varied between sites. The regression relationships of corn yield to N were significantly positive, with an overall R^2 of ~0.76. In sugar beet, the regression relationships of root yield to N treatments were mostly significantly positive with R^2 values from 0.54 to 0.64, with the exception of Downer 2018. The regression relationship of sugar beet root yield with N was not significant, probably due to severe impacts of the confounding effects of sand syndrome, rhizoctonia root rot and early-season drought.

Sugar beet harvest date study

In general yield and recoverable sugar increased statistically during the harvest period from the first to second harvest, but not from the second to third harvest. Sugar concentration generally decreased between the first and second harvest, but not between the second and third harvest. There were no differences in the relationship between root yield, recoverable sugar yield and RNDVI and RENDVI at any harvest date. The relationship of RNDVI, RENDVI with sugar beet root yield and recoverable sugar yield was based on only four harvest samples from each experiment, which limited the ability of the statistical analysis to determine significance due to the low sample size in each comparison.

Final conclusions

Small unmanned aircraft systems (SUAS) equipped with remote sensors have the potential to improve the ability of farmers to better manage their N inputs. Massive amounts of data can be quickly captured and acted upon allowing for in-season corrections of many kinds. The positive relationships between N rate and sensor values obtained in this study support the

use of drone-based remote sensing use for directing in season N application through yield and quality prediction. To improve accuracy, improved height approximation techniques, utilization of active sensors as opposed to passive sensors, and improved wavelength capture of the sensor. The use of SUAS based remote sensors has potential to improve N use efficiency, increase farmer return on fertilizer investment, reduce environmental impacts, and predict crop yields.

REFERENCES

Albus, Walt, Besemann, Leonard, & Eslinger, Heidi. 2008. Strip-till, corn on corn, nitrogen
rate study. NDSU Carrington Research Center,
https://www.ag.ndsu.edu/carringtonrec/documents/agronomyrd/docs2008/Strip-till-
%20Corn%20on%20Corn-%20Nitrogen%20Rate%20Study.pdf/at_download/file

Alley, M. M., 2009. Nitrogen and phosphorus fertilization of corn. Virginia Coopertive
Extension, 2. https://doi.org/10.1111/ejss.12079

Amin, M. E.-M. H. 2011. Effect of different nitrogen sources on growth, yield and quality of
fodder maize (*Zea mays* L.). Journal of the Saudi Society of Agricultural Sciences, 10(1),
17–23. https://doi.org/10.1016/j.jssas.2010.06.003

Asrar, G., Fuchs, M., Kanemasu, E. 1984. Estimating absorbed photosynthetic radiation and
leaf area index from spectral reflectance in wheat. Agronomy Journal 76:300.
doi:10.2134/agronj1984.00021962007600020029x

Atzberger, C. 2013. Advances in remote sensing of agriculture: Context description, existing
operational monitoring systems and major information needs. Remote Sensing 5:13.
https://doi.org/10.3390/rs5020949

Awange, J. L., & Kyalo Kiema, J. B. 2013. Fundamentals of remote sensing. In Environmental
Science and Engineering (Subseries: Environmental Science) p. 111–118.
https://doi.org/10.1007/978-3-642-34085-7_7

Bender, R. R., Haegele, J. W., Ruffo, M. L., & Below, F. R. 2013. Modern corn hybrids'
nutrient uptake patterns. Better Crops, 97(1), 7–10.
https://doi.org/10.2134/agronj2012.0352

Biermacher, J. T., Epplin, F. M., Brorsen, B. W., Solie, J. B., & Raun, W. R. 2006. Precision nitrogen fertilization technology with micro grids. In American Agricultural Economics Association Annual Meetings. p.15. https://ageconsearch.umn.edu/bitstream/21046/1/sp06bi04.pdf

Blankenship, R. E. 2008. Molecular mechanisms of photosynthesis. Molecular Mechanisms of Photosynthesis. https://doi.org/10.1002/9780470758472

Bongiovanni, R., & Lowenberg-Deboer, J. 2004. Precision agriculture and sustainability. Precision Agriculture. https://doi.org/10.1023/B:PRAG.0000040806.39604.aa

Bu, H. 2014. Yield and quality prediction using satellite passive imagery and ground based active optical sensors in sugar beet, spring wheat, corn, and sunflower. NDSU thesis library.

Bu, H., Sharma, L. K., Denton, A., & Franzen, D. W. 2016. Sugar beet yield and quality prediction at multiple harvest dates using active-optical sensors. Agronomy Journal, 108(1), p. 273–284. https://doi.org/10.2134/agronj2015.0268

Campbell, L. G. 2002. Sugar beet quality improvement. Journal of Crop Production, 5(1–2), p. 395–413. https://doi.org/10.1300/J144v05n01_16

Campbell, L. G., & Fugate, K. K. 2002. Relationships among impurity components, sucrose, and sugarbeet processing quality. Journal of Sugar Beet Research, 52:2–21. https://doi.org/10.5274/jsbr.52.1.2

Canfield, D. E., Glazer, A. N., & Falkowski, P. G. 2010. The evolution and future of earth's nitrogen cycle. Science. https://doi.org/10.1126/science.1186120

Carlson, T. C., & Ripley, D. A. 1997. On the relationship between NDVI, fractional vegetation

cover, and leaf area index. Remote Sensing of Environment. 62:241–252.

https://doi.org/10.1016/S0034-4257(97)00104-1

Chatterjee, A., K. Subedi, D.W. Franzen, H. Mickelson, and N. Cattanach. 2018. Nitrogen

fertilizer optimization for sugarbeet in the red river valley of north dakota and

minnesota. Agron. J. 110:1554-1560. doi:10.2134/agronj2017.12.0694

Clevers, J. G. P. 1997. A simplified approach for yield prediction of sugar beet based on optical

remote sensing data. Remote Sensing of Environment, 61:221–228.

https://doi.org/10.1016/S0034-4257(97)00004-7

d'Amour, B, C., Reitsma, F., Baiocchi, G., Barthel, S., Güneralp, B., Erb, K.-H., Seto, K. C.

(2016). Future urban land expansion and implications for global croplands. Proceedings

of the National Academy of Sciences. https://doi.org/10.1073/pnas.1606036114

Department of Economic and Social Affairs. Population Division. 2017. World population

prospects: The 2017 Revision. United Nations.

https://doi.org/10.1017/CBO9781107415324.004

Department of Economic Development. 2017. Estimating Crop Yields; A Brief Guide.

agriculture.vic.gov.au/agriculture/grains-and-other-crops/crop-production/estimating-

crop-yields-a-brief-guide.

Dorsey, J., Rushmeier, H., & Sillion, F. 2008. Digital modeling of material appearance. Digital

Modeling of Material Appearance. https://doi.org/10.1016/B978-0-12-221181-2.X5001-0

Egli, D. B. (2008). Comparison of corn and soybean yields in the United States: Historical trends

and future prospects. Agronomy Journal. https://doi.org/10.2134/agronj2006.0286c

Elser, J. J. 2011. A world awash with nitrogen. Science.
https://doi.org/10.1126/science.1215567

El-Sarag, E. I., & Moselhy, S. H. 2013. Response of sugar beet quantity and quality to nitrogen
and potasium fertilization under sandy soils conditions. Asian Journal of Crop Science,
5(3):295–303. https://doi.org/10.3923/ajcs.295.303

Erisman, J. W., Sutton, M. A., Galloway, J., Klimont, Z., & Winiwarter, W. 2008. How a
century of ammonia synthesis changed the world. Nature Geoscience, 1(10):636–639.
https://doi.org/10.1038/ngeo325

Erdle, K., Mistele, B., & Schmidhalter, U. 2011. Comparison of active and passive spectral
sensors in discriminating biomass parameters and nitrogen status in wheat cultivars. Field
Crops Research. https://doi.org/10.1016/j.fcr.2011.06.007

Ertl, G. 2012. The arduous way to the haber-bosch process. Zeitschrift Fur Anorganische Und
Allgemeine Chemie, 638:(3–4), 487–489. https://doi.org/10.1002/zaac.201190458

Evans, J. R. 1989. Photosynthesis and nitrogen relationship in leaves of C3 plants. Oecologia,
78(1): 9–19. https://doi.org/10.1007/BF00377192

Fields, S. 2004. Global Nitrogen: Cycling out of control. Environmental Health Perspectives.
https://doi.org/10.1289/ehp.112-a556

Foley, J. a, Defries, R., Asner, G. P., Barford, C., Bonan, G., Carpenter, S. R., Snyder, P. K.
2005. Global consequences of land use. Science (New York, N.Y.), 309(5734):570–
574. https://doi.org/10.1126/science.1111772

Franzen, D. 2018. Fertilizing sugarbeet in North Dakota. NDSU Extension Services, North
Dakota State University Extension Bulletin SF-714 (Revised). North Dakota State Univ.

Fargo, ND.

https://www.ndsu.edu/fileadmin/soils/pdfs/Fertilizing_Sugarbeet_In_North_dakota.pdf

Franzen, D.W., M.D. Franzen, & Hongang B. 2017. North Dakota Corn Nitrogen Calculator.

NDSU Corn Nitrogen Calculator, www.ndsu.edu/pubweb/soils/corn/.

Fulton, J. P., Shearer, S. A., Higgins, S. F., & McDonald, T. P. 2013. A method to generate and

use as-applied surfaces to evaluate variable-rate fertilizer applications. Precision

Agriculture, 14(2):184–200. https://doi.org/10.1007/s11119-012-9286-1

Gabriel, J. L., Zarco-Tejada, P. J., López-Herrera, P. J., Pérez-Martín, E., Alonso-Ayuso, M., &

Quemada, M. 2017. Airborne and ground level sensors for monitoring nitrogen status in

a maize crop. Biosystems Engineering.

https://doi.org/10.1016/j.biosystemseng.2017.06.003

Gebbers, R., & Adamchuk, V. I. 2010. Precision agriculture and food security. Science.

https://doi.org/10.1126/science.1183899

Gehl, R. J., Schmidt, J. P., Maddux, L. D., & Gordon, W. B. 2005. Corn yield response to

nitrogen rate and timing in sandy irrigated soils. Agronomy Journal, 97(4):1230–1238.

https://doi.org/10.2134/agronj2004.0303

Gitelson, A., & Merzlyak, M. N. 1994. Quantitative estimation of chlorophyll-a using

reflectance spectra: Experiments with autumn chestnut and maple leaves. Journal of

Photochemistry and Photobiology, B: Biology, 22(3):247–252.

https://doi.org/10.1016/1011-1344(93)06963-4

Gitelson, A. A., & Merzlyak, M. N. 1998. Remote sensing of chlorophyll concentration in

higher plant leaves. Advances in Space Research, 22(5):689–692.

https://doi.org/10.1016/S0273-1177(97)01133-2

Gong, P., Pu, R., Biging, G. S., & Larrieu, M. R. 2003. Estimation of forest leaf area index using vegetation indices derived from Hyperion hyperspectral data. IEEE Transactions on Geoscience and Remote Sensing, 41(6 PART I):1355–1362. https://doi.org/10.1109/TGRS.2003.812910

Good, A. G., & Beatty, P. H. 2011. Fertilizing nature: A tragedy of excess in the commons. PLoS Biology, 9(8). https://doi.org/10.1371/journal.pbio.1001124

Grenzdörffer, G. J. 2014. Crop height determination with UAS point clouds. In International Archives of the Photogrammetry, Remote Sensing and Spatial Information Sciences - ISPRS Archives. 40:135–140. https://doi.org/10.5194/isprsarchives-XL-1-135-2014

Gu, C., Maggi, F., Riley, W. J., Hornberger, G. M., Xu, T., Oldenburg, C. M., Steefel, C. 2009. Aqueous and gaseous nitrogen losses induced by fertilizer application. Journal of Geophysical Research: Biogeosciences, 114(1). https://doi.org/10.1029/2008JG000788

Gutierrez-Rodriguez, M., Escalante-Estrada, J. A., & Rodriguez-Gonzalez, M. T. 2005. Canopy reflectance, stomatal conductance, and yield of *Phaseolus vulgaris* L. and *Phaseolus coccinues* L. Under Saline Field Conditions. International Journal of Agriculture & Biology, 7(2):491–494. https://doi.org/1560–8530/2005/07–3–491–494

Hajibabaee, M., Azizi, F., & Zargari, K. 2012. Effect of drought stress on some morphological, physiological and agronomic traits in various foliage corn hybrids. American-Eurasian Journal of Agriculture & Enviromental Science. https://doi.org/10.5829/idosi.aejaes.2012.12.07.1751

Hanway, J. J. 1962. Corn Growth and Composition in Relation to Soil Fertility: II. Uptake of N, P, and K and their distribution in different plant parts during the growing season.

Agronomy Journal, 54:217–222.

https://doi.org/10.2134/agronj1962.00021962005400030011x

Hasanuzzaman, M. 2015. Crop-weed competition, competition for nutrients. Crop-Weed

Competition. https://doi.org/10.1002/9780470015902.a0020477

Hatfield, J. L., & Follett, R. F. 2008. Nitrogen in the Environment. Nitrogen in the

environment. https://doi.org/10.1016/B978-0-12-374347-3.X0001-7

Hatfield, J. L., Gitelson, A. A., Schepers, J. S., & Walthall, C. L. 2008. Application of spectral

remote sensing for agronomic decisions. Agronomy Journal.

https://doi.org/10.2134/agronj2006.0370c

Hergert, G. W. 2010. Sugar Beet Fertilization. Sugar Tech. https://doi.org/10.1007/s12355-

010-0037-1

Horler, D. N. H., Dockray, M., Barber, J., & Barringer, A. R. 1983. Red edge measurements

for remotely sensing plant chlorophyll content. Advances in Space Research, 3(2):273–

277. https://doi.org/10.1016/0273-1177(83)90130-8

Huang, J., Wang, H., Dai, Q., & Han, D. 2014. Analysis of NDVI data for crop identification

and yield estimation. IEEE Journal of Selected Topics in Applied Earth Observations and

Remote Sensing, 7(11):4374–4384. https://doi.org/10.1109/JSTARS.2014.2334332

Humboldt State University. 2014. Electromagnetic Spectrum. Retrieved from

http://gsp.humboldt.edu/olm_2015/Courses/GSP_216_Online/lesson1-2/spectrum.html

Jenkinson, D. S. 2001. The impact of humans on the nitrogen cycle, with focus on temperate

arable agriculture. Plant and Soil, 228(1):3–15.

https://doi.org/10.1023/A:1004870606003

Jokela, W. E., & Randall, G. W. 1989. Corn yield and residual soil nitrate as affected by time and rate of nitrogen application. Agronomy Journal, 81(i):720. https://doi.org/10.2134/agronj1989.00021962008100050004x

Jordan, C. F. 1969. Derivation of Leaf-Area Index from Quality of Light on the Forest Floor. Ecology, 50(4):663–666. https://doi.org/10.2307/1936256

Kanter, D. R., Zhang, X., & Mauzerall, D. L. 2015. Reducing nitrogen pollution while decreasing farmers' costs and increasing fertilizer industry profits. Journal of Environment Quality, 44(2):325. https://doi.org/10.2134/jeq2014.04.0173

Khan, M. 2018. Sugar beet production guide, https://www.ag.ndsu.edu/publications/crops/2018-sugarbeet-production-guide/2018-Sugarbeet-production-guide.pdf

Lamb, J.A., A.L. Sims, L.J. Smith, and G.W. Rehm. 2001. Fertilizing sugarbeet in Minnesota and North Dakota. University of Minnesota Agriculture Extension. Available at http://www.extension.umn.edu/agriculture/sugarbeets

Lamb, D. W., Schneider, D. A., & Stanley, J. N. 2014. Combination active optical and passive thermal infrared sensor for low-level airborne crop sensing. Precision Agriculture, 15(5): 523–531. https://doi.org/10.1007/s11119-014-9350-0

Lamb, D. W., Steyn-Ross, M., Schaare, P., Hanna, M. M., Silvester, W., & Steyn-Ross, A. 2002. Estimating leaf nitrogen concentration in ryegrass (*Lolium* spp.) pasture using the chlorophyll red-edge: Theoretical modelling and experimental observations. International Journal of Remote Sensing, 23(18):3619–3648. https://doi.org/10.1080/01431160110114529

Lassaletta, L., Billen, G., Grizzetti, B., Anglade, J., & Garnier, J. 2014. 50 year trends in nitrogen use efficiency of world cropping systems: The relationship between yield and nitrogen input to cropland. Environmental Research Letters, 9(10). https://doi.org/10.1088/1748-9326/9/10/105011

Lawlor, D. W., Lemaire, G., & Gastal, F. 2001. Nitrogen, Plant Growth and Crop Yield. In Plant Nitrogen (pp. 343–367). https://doi.org/10.1007/978-3-662-04064-5_13

Li, F., Miao, Y., Feng, G., Yuan, F., Yue, S., Gao, X., Chen, X. 2014. Improving estimation of summer maize nitrogen status with red edge-based spectral vegetation indices. Field Crops Research, 157:111–123. https://doi.org/10.1016/j.fcr.2013.12.018

Liu, X. B., Zhang, X. Y., Wang, Y. X., Sui, Y. Y., Zhang, S. L., Herbert, S. J., & Ding, G. 2010. Soil degradation: A problem threatening the sustainable development of agriculture in Northeast China. Plant, Soil and Environment, 56(2):87–97.

Lowenberg-DeBoer, J. 2015. The Precision Agriculture Revolution. Foreign Affairs, 94(3): 105–112. https://doi.org/10.1016/j.pnsc.2008.07.020

Lu, C., & Tian, H. (2017). Global nitrogen and phosphorus fertilizer use for agriculture production in the past half century: Shifted hot spots and nutrient imbalance. Earth System Science Data. p. 185. https://doi.org/10.5194/essd-9-181-2017

Lutz, W., & Qiang, R. 2002. Determinants of human population growth. Philosophical Transactions of the Royal Society of London. Series B, Biological Sciences, 357:1197–1210. https://doi.org/10.1098/rstb.2002.1121

Malnou, C. S., Jaggard, K. W., & Sparkes, D. L. 2006. A canopy approach to nitrogen fertilizer recommendations for the sugar beet crop. European Journal of Agronomy, 25(3):254–263. https://doi.org/10.1016/j.eja.2006.06.002

93

Malveaux, C., Hall, S., & Price, R. R. 2014. Using drones in agriculture: Unmanned aerial
systems for agricultural remote sensing applications. American Society of Agricultural
and Biological Engineers Annual International Meeting 2014, 6(141911016):4075–4079.
https://doi.org/10.13031/aim.20141911016

Mamo, M., Malzer, G. L., Mulla, D. J., Huggins, D. R., & Strock, J. 2003. Spatial and temporal
variation in economically optimum nitrogen rate for corn. Agronomy Journal, 95(4):
958–964. https://doi.org/10.2134/agronj2003.9580

Maresma, Á. Ariza, M., Martínez, E., Lloveras, J., & Martínez-Casasnovas, J. A. 2016.
Analysis of vegetation indices to determine nitrogen application and yield prediction in
maize (zea mays l.) from a standard uav service. Remote Sensing, 8(12).
https://doi.org/10.3390/rs8120973

Martin, K., Raun, W., & Solie, J. 2012. By-plant prediction of corn grain yield using optical
sensor readings and measured plant height. Journal of Plant Nutrition, 35(9):1429–1439.
https://doi.org/10.1080/01904167.2012.684133

Mathews, M. C. 2001. Timing nitrogen applications in corn and winter forage. Proceedings
31st California Alfalfa and Forage Symposium December, 12–13. Retrieved from
http://groups.ucanr.org/LNM/files/6370.pdf

Mkhabela, M. S., Bullock, P., Raj, S., Wang, S., & Yang, Y. 2011. Crop yield forecasting on
the Canadian Prairies using MODIS NDVI data. Agricultural and Forest Meteorology,
151(3):385–393. https://doi.org/10.1016/j.agrformet.2010.11.012

Moosavi, S. G., Ramazani, S. H., Hemayati, S. S., & Gholizade, H. 2017. Effect of drought
stress on root yield and some morpho-physiological traits in different genotypes of sugar

beet (Beta vulgaris L.). Journal of Crop Science and Biotechnology, 20(3):167-174. doi:10.1007/s12892-017-0009-0

Mulla, D. J. 2013. Twenty five years of remote sensing in precision agriculture: Key advances and remaining knowledge gaps. Biosystems Engineering, 114(4):358–371. https://doi.org/10.1016/j.biosystemseng.2012.08.009

NCR 221. 1998. Recommended chemical soil test procedures for the north central region. Available online: http://extension.missouri.edu/p/sb1001

Nguy-Robertson, A., Gitelson, A., Peng, Y., Viña, A., Arkebauer, T., & Rundquist, D. 2012. Green leaf area index estimation in maize and soybean: Combining vegetation indices to achieve maximal sensitivity. Agronomy Journal. https://doi.org/10.2134/agronj2012.0065

Novoa, R., & Loomis, R. S. 1981. Nitrogen and plant production. Plant and Soil, 58(1–3):177–204. https://doi.org/10.1007/BF02180053

Oktem, A. G., & Emeklier, H. Y. 2010. Effect of nitrogen on yield and some quality parameters of sweet corn. Communications in Soil Science and Plant Analysis, 41(7): 832–847. https://doi.org/10.1080/00103621003592358

Paul, E. A. 2016. The nature and dynamics of soil organic matter: Plant inputs, microbial transformations, and organic matter stabilization. Soil Biology and Biochemistry. https://doi.org/10.1016/j.soilbio.2016.04.001

Pisani, O., Stricland, T.C., Hubbard, R.K., Bosch, D.D., Coffin, A.W., Endale, D.M., and Potter, T. L. 2017. Soil nitrogen dynamics and leaching under conservation tillage in the Atlantic Coastal Plain, Georgia, United States. Journal of Soil and Water Conservation, 72(5):519–529. https://doi.org/10.2489/jswc.72.5.519

Puri, V., Nayyar, A., & Raja, L. 2017. Agriculture drones: A modern breakthrough in precision agriculture. Journal of Statistics and Management Systems, 20(4):507–518. https://doi.org/10.1080/09720510.2017.1395171

Quemada, M., Gabriel, J. L., & Zarco-Tejada, P. 2014. Airborne hyperspectral images and ground-level optical sensors as assessment tools for maize nitrogen fertilization. Remote Sensing, 6(4):2940–2962. https://doi.org/10.3390/rs6042940

Ramakrishnan VV, G. A., & VV, R. 2015. Nitrogen sources and cycling in the ecosystem and its role in air, water and soil pollution: A Critical Review. Journal of Pollution Effects & Control, 03(02):1–26. https://doi.org/10.4172/2375-4397.1000136

Ranum, P., Peña-Rosas, J. P., & Garcia-Casal, M. N. 2014. Global maize production, utilization, and consumption. Annals of the New York Academy of Sciences, 1312(1): 105–112. https://doi.org/10.1111/nyas.12396

Raun, W. R., Solie, J. B., Johnson, G. V., Stone, M. L., Lukina, E. V., Thomason, W. E., & Schepers, J. S. 2001. In-season prediction of potential grain yield in winter wheat using canopy reflectance. Agronomy Journal, 93(1):131. https://doi.org/10.2134/agronj2001.931131x

Raun, W. R., Solie, J. B., & Stone, M. L. 2011. Independence of yield potential and crop nitrogen response. Precision Agriculture, 12(4):508–518. https://doi.org/10.1007/s11119-010-9196-z

Research and markets. 2018. Global Agriculture Drone Market Analysis & Trends - Industry Forecast to 2027.

Rouse, J. W., Haas, R. H., Schell, J. A., & Deering, D. W. 1973. Monitoring the vernal advancement and retrogradation (green wave effect) of natural vegetation. Progress Report RSC 1978-1:112. https://doi.org/19740008955

Sale, P. 2010. The use of nutrients in crop plants. Annals of Botany, 105(1), x–xi. https://doi.org/10.1093/aob/mcp227

Sankaran, S., & Ehsani, R. 2014. Introduction to the electromagnetic spectrum. In Imaging with Electromagnetic Spectrum: Applications in Food and Agriculture (Vol. 9783642548888:1–15). https://doi.org/10.1007/978-3-642-54888-8_1

Sawyer, J., Nafziger, E., Randall, G., Bundy, L., Rehm, G., & Joern, B. 2006. Concepts and rationale for regional nitrogen rate guidelines for corn concepts and rationale for regional nitrogen rate guidelines for corn. Iowa State University, University Extension.

Sharma, L. K., Bu, H., Franzen, D. W., & Denton, A. 2016. Use of corn height measured with an acoustic sensor improves yield estimation with ground based active optical sensors. Computers and Electronics in Agriculture, 124:254–262. https://doi.org/10.1016/j.compag.2016.04.016

Sharma, L. K., & Franzen, D. W. 2014. Use of corn height to improve the relationship between active optical sensor readings and yield estimates. Precision Agriculture, 15(3):331–345. https://doi.org/10.1007/s11119-013-9330-9

Sharma, L. K., Bu, H., Denton, A., & Franzen, D. W. 2015. Active-optical sensors using red NDVI compared to red edge NDVI for prediction of corn grain yield in North Dakota, U.S.A. Sensors (Switzerland), 15(11), 27832–27853. https://doi.org/10.3390/s151127832

Silva, J., & Uchida, R. 2000. Essential Nutrients for Plant Growth : Plant Nutrient Management in Hawaii's Soils, Approaches for Tropical and Subtropical Agriculture:31–55.

Sripada, R. P., Heiniger, R. W., White, J. G., & Meijer, A. D. 2006. Aerial color infrared

    photography for determining early in-season nitrogen requirements in corn. Agronomy

    Journal, 98(4):968–977. https://doi.org/10.2134/agronj2005.0200

Statista. 2017. World corn production by country 2017/2018,

    https://www.statista.com/statistics/254292/global-corn-production-by-country/

Statista. 2017. Sugar Beet Production in the U.S.,

    www.statista.com/statistics/191913/sugarbeets-production-in-the-us-from-2000/

Subedi, Keshab. 2016. Sugar beet yield and quality response to nitrogen fertilizer rate and in-

    season prediction of yield and quality using active-optical sensor. NDSU thesis library.

Suzuki, N., Rivero, R. M., Shulaev, V., Blumwald, E., & Mittler, R. 2014. Abiotic and biotic

    stress combinations. New Phytologist. https://doi.org/10.1111/nph.12797

Tagarakis, A. C., & Ketterings, Q. M. 2017. In-season estimation of corn yield potential using

    proximal sensing. Agronomy Journal, 109(4):1323–1330.

    https://doi.org/10.2134/agronj2016.12.0732

Tarkalson, D. D., Bjorneberg, D. L., & Moore, A. 2012. Effects of tillage system and

    nitrogen supply on sugarbeet production. Journal of Sugarbeet Research, 49(3):79-102.

    doi:10.5274/jsbr.49.3.79

Teal, R. K., Tubana, B., Girma, K., Freeman, K. W., Arnall, D. B., Walsh, O., & Raun, W. R.

    2006. In-season prediction of corn grain yield potential using normalized difference

    vegetation index. Agronomy Journal, 98(6):1488–1494.

    https://doi.org/10.2134/agronj2006.0103

Tripicchio, P., Satler, M., Dabisias, G., Ruffaldi, E., & Avizzano, C. A. 2015. Towards smart

    farming and sustainable agriculture with drones. In Proceedings - 2015 International

Conference on Intelligent Environments, IE 2015:140–143.

https://doi.org/10.1109/IE.2015.29

Toth, C., & Jóźków, G. 2016. Remote sensing platforms and sensors: A survey. ISPRS Journal
of Photogrammetry and Remote Sensing. https://doi.org/10.1016/j.isprsjprs.2015.10.004

Unger, M., Pock, T., Grabner, M., Klaus, A., & Bischof, H. 2009. A Variational Approach to
Semiautomatic Generation of Digital Terrain Models. In 5th Int. Symp. on Visual
Computing:1119–1130.

University of Minnesota. 2018. Fertilizer Recommendations for Agronomic Crops in
Minnesota, https://www.extension.umn.edu/agriculture/nutrient-management/nutrient-
lime-guidelines/fertilizer-recommendations-for-agronomic-crops-in-minnesota/sugar-
beet/

USDA, ERS. 2018. Corn and other feed grains background,
https://www.ers.usda.gov/topics/crops/corn-and-other-feedgrains/background

USDA, ERS. 2017. Sugar and Sweeteners Yearbook Tables. USDA ERS - Sugar and
Sweeteners Yearbook Tables, www.ers.usda.gov/data-products/sugar-and-sweeteners-
yearbook-tables.aspx

USDA, NASS. 2018. Charts and maps field crops.
https://www.nass.usda.gov/Charts_and_Maps/Field_Crops/cornprod.php

USDA, NASS. 2017. QuickStats Ad-Hoc Query Tool,
quickstats.nass.usda.gov/results/8B180A3B-0D63-363C-BD42-
9C90A7BFCDBB#F532339D-171F-3870-93EB-EFA514937D71

Van Alphen, B. J., & Stoorvogel, J. J. 2001. A methodology for precision nitrogen fertilization in high-input farming systems. Precision Agriculture, 2(4):319–332. https://doi.org/10.1023/A:1012338414284

Viña, A., Gitelson, A. A., Nguy-Robertson, A. L., & Peng, Y. 2011. Comparison of different vegetation indices for the remote assessment of green leaf area index of crops. Remote Sensing of Environment, 115(12):3468–3478. https://doi.org/10.1016/j.rse.2011.08.010

Von Wiren, N., Gazzarrini, S., & Frommer, W. B. 1997. Regulation of mineral nitrogen uptake in plants. Plant and Soil. https://doi.org/10.1023/A:1004241722172

Witte, C. P. 2011. Urea metabolism in plants. Plant Science. https://doi.org/10.1016/j.plantsci.2010.11.010

Yin, X., & Angela McClure, M. 2013. Relationship of corn yield, biomass, and leaf nitrogen with normalized difference vegetation index and plant height. Agronomy Journal, 105(4): 1005–1016. https://doi.org/10.2134/agronj2012.0206

Yin, X., McClure, M. A., Jaja, N., Tyler, D. D., & Hayes, R. M. 2011. In-season prediction of corn yield using plant height under major production systems. Agronomy Journal, 103(3): 923–929. https://doi.org/10.2134/agronj2010.0450

Yue, J., Yang, G., Li, C., Li, Z., Wang, Y., Feng, H., & Xu, B. 2017. Estimation of winter wheat above-ground biomass using unmanned aerial vehicle-based snapshot hyperspectral sensor and crop height improved models. Remote Sensing, 9(7). https://doi.org/10.3390/rs9070708

Xia, T., Miao, Y., Wu, D., Shao, H., Khosla, R., & Mi, G. 2016. Active optical sensing of spring maize for in-season diagnosis of nitrogen status based on nitrogen nutrition index. Remote Sensing, 8(7). https://doi.org/10.3390/rs8070605

Zhang, C., & Kovacs, J. M. 2012. The application of small unmanned aerial systems for precision agriculture: A review. Precision Agriculture. https://doi.org/10.1007/s11119-012-9274-5

Zhang, N., Wang, M., & Wang, N. 2002. Precision agriculture—a worldwide overview. Computers and Electronics in Agriculture, 36(2–3):113–132. https://doi.org/10.1016/S0168-1699(02)00096-0

Zhang, X., Mauzerall, D. L., Davidson, E. A., Kanter, D. R., & Cai, R. 2015. The economic and environmental consequences of implementing nitrogen-efficient technologies and management practices in agriculture. Journal of Environment Quality, 44(2):312. https://doi.org/10.2134/jeq2014.03.0129

APPENDIX

Table A1. Linear regression slope, intercept, R^2, and P values between corn yield and sugar beet recoverable sugar yield and optical reflectance and crop height.

Site Details				RNDVI				RENDVI				Crop Height			
Year	Crop	Site	GDD[†]	Slope	Intercept	R^2 Value	P Value	Slope	Intercept	R^2 Value	P Value	Slope	Intercept	R^2 Value	P Value
2017	Corn	Ada	730	-	-	-	N.S.*	-	-	-	N.S.	-	-	-	N.S.
2017	Corn	Ada	1219	122.3	-93.9	0.544	0.0002	-98.4	20.2	0.518	0.0004	7.72	-1.63	0.544	0.0002
2017	SB[‡]	Ada	1548	18.4	-1.11	0.706	<.0001	-	-	-	N.S.	26.8	6.12	0.461	0.0038
2017	SB	Ada	2450	26.0	-8.89	0.626	0.0003	-41.1	17.0	0.371	0.0123	10.4	11.2	0.426	0.0062
2017	SB	Downer	1680	50.5	-31.2	0.715	0.0005	-	-	-	N.S.	25.5	4.75	0.629	0.0021
2017	SB	Downer	2637	-	-	-	N.S	-	-	-	N.S.	19.6	6.57	0.543	0.0062
2018	Corn	Ada	312	-	-	-	N.S.	-	-	-	N.S.	-185.0	16.5	0.254	0.0464
2018	Corn	Ada	413	-	-	-	N.S.	-	-	-	N.S.	-	-	-	N.S.
2018	Corn	Ada	567	-	-	-	N.S.	-	-	-	N.S.	-	-	-	N.S.
2018	Corn	Ada	680	-	-	-	N.S.	-214.5	46.3	0.621	0.0003	-	-	-	N.S.
2018	Corn	Ada	831	56.8	-34.0	0.300	0.0282	-170.1	40.9	0.633	0.0002	41.2	2.93	0.587	0.0005
2018	Corn	Ada	972	137.1	-107.1	0.506	0.0020	-111.1	30.2	0.749	<.0001	8.10	8.98	0.278	0.0361
2018	Corn	Ada	1129	176.0	-143.1	0.689	<.0001	-71.1	27.0	0.740	<.0001	-	-	-	N.S.
2018	Corn	Ada	1239	245.6	-202.6	0.611	0.0004	-94.2	31.2	0.768	<.0001	3.52	9.60	0.257	0.0451
2018	Corn	Ada	1387	176.2	-137.8	0.594	0.0005	-88.9	29.6	0.759	<.0001	7.81	-0.144	0.596	0.0005
2018	Corn	Sabin	483	-	-	-	N.S.	-	-	-	N.S.	-	-	-	N.S
2018	Corn	Sabin	594	-	-	-	N.S.	-	-	-	N.S.	-	-	-	N.S
2018	Corn	Sabin	755	-	-	-	N.S.	-	-	-	N.S.	-	-	-	N.S
2018	Corn	Sabin	878	-	-	-	N.S.	-	-	-	N.S.	2817.4	168.1	0.281	0.0348
2018	Corn	Sabin	1037	-	-	-	N.S.	-	-	-	N.S.	-	-	-	N.S

Table A1. Linear regression slope, intercept, R^2, and P values between corn yield and sugar beet recoverable sugar yield and optical reflectance and crop height (continued).

Site Details				RNDVI				RENDVI				Crop Height			
Year	Crop	Site	GDD[†]	Slope	Intercept	R² Value	P Value	Slope	Intercept	R² Value	P Value	Slope	Intercept	R² Value	P Value
2018	Corn	Sabin	1189	-	-	-	N.S.	-	-	-	N.S.	-	-	-	N.S
2018	Corn	Sabin	1360	-	-	-	0.0292	-104.6	30.5	0.629	0.0002	-	-	-	N.S
2018	Corn	Sabin	1478	-	-	-	N.S.	-98.6	29.0	0.790	<.0001	-	-	-	N.S
2018	Corn	Sabin	1632	-	-	-	N.S.	-55.3	25.8	0.780	<.0001	-	-	-	N.S
2018	SB	Ada	704	-	-	-	N.S.	-	-	-	N.S.	-	-	-	N.S.
2018	SB	Ada	914	-	-	-	N.S.	-	-	-	N.S.	-	-	-	N.S.
2018	SB	Ada	1191	14.9	5.72	0.558	0.0053	79.7	-5.07	0.515	0.0086	-	-	-	N.S.
2018	SB	Ada	1400	10.4	6.28	0.3640	0.0378	90.8	-4.12	0.451	0.0168	34.9	12.4	0.348	0.0434
2018	SB	Ada	1663	-	-	-	N.S.	-	-	-	N.S.	-	-	-	N.S.
2018	SB	Ada	1916	-	-	-	N.S.	-	-	-	N.S.	-	-	-	N.S.
2018	SB	Ada	2185	-	-	-	N.S.	-	-	-	N.S.	-	-	-	N.S.
2018	SB	Ada	2389	-	-	-	N.S.	-	-	-	N.S.	-	-	-	N.S.
2018	SB	Ada	2679	-	-	-	N.S.	-	-	-	N.S.	-	-	-	N.S.
2018	SB	Downer	862	-	-	-	N.S.	-	-	-	N.S.	-	-	-	N.S.
2018	SB	Downer	1085	-	-	-	N.S.	-	-	-	N.S.	-	-	-	N.S.
2018	SB	Downer	1373	-	-	-	N.S.	-	-	-	N.S.	-	-	-	N.S.
2018	SB	Downer	1592	-	-	-	N.S.	-	-	-	N.S.	-	-	-	N.S.
2018	SB	Downer	1863	-	-	-	N.S.	-	-	-	N.S.	-	-	-	N.S.
2018	SB	Downer	2127	-	-	-	N.S.	-	-	-	N.S.	-	-	-	N.S.
2018	SB	Downer	2410	-	-	-	N.S.	-	-	-	N.S.	-	-	-	N.S.

Table A1. Linear regression slope, intercept, R^2, and P values between corn yield and sugar beet recoverable sugar yield and optical reflectance and crop height (continued).

Site Details				RNDVI				RENDVI				Crop Height			
Year	Crop	Site	GDD[†]	Slope	Intercept	R^2 Value	P Value	Slope	Intercept	R^2 Value	P Value	Slope	Intercept	R^2 Value	P Value
2018	SB	Downer	2624	-	-	-	N.S.	-	-	-	N.S.	-	-	-	N.S.
2018	SB	Downer	2921	-	-	-	N.S.	-	-	-	N.S.	-	-	-	N.S.

* Indicates regression analysis is not significant at the P<0.05.
† Growing degree days.
‡ Sugar beet.
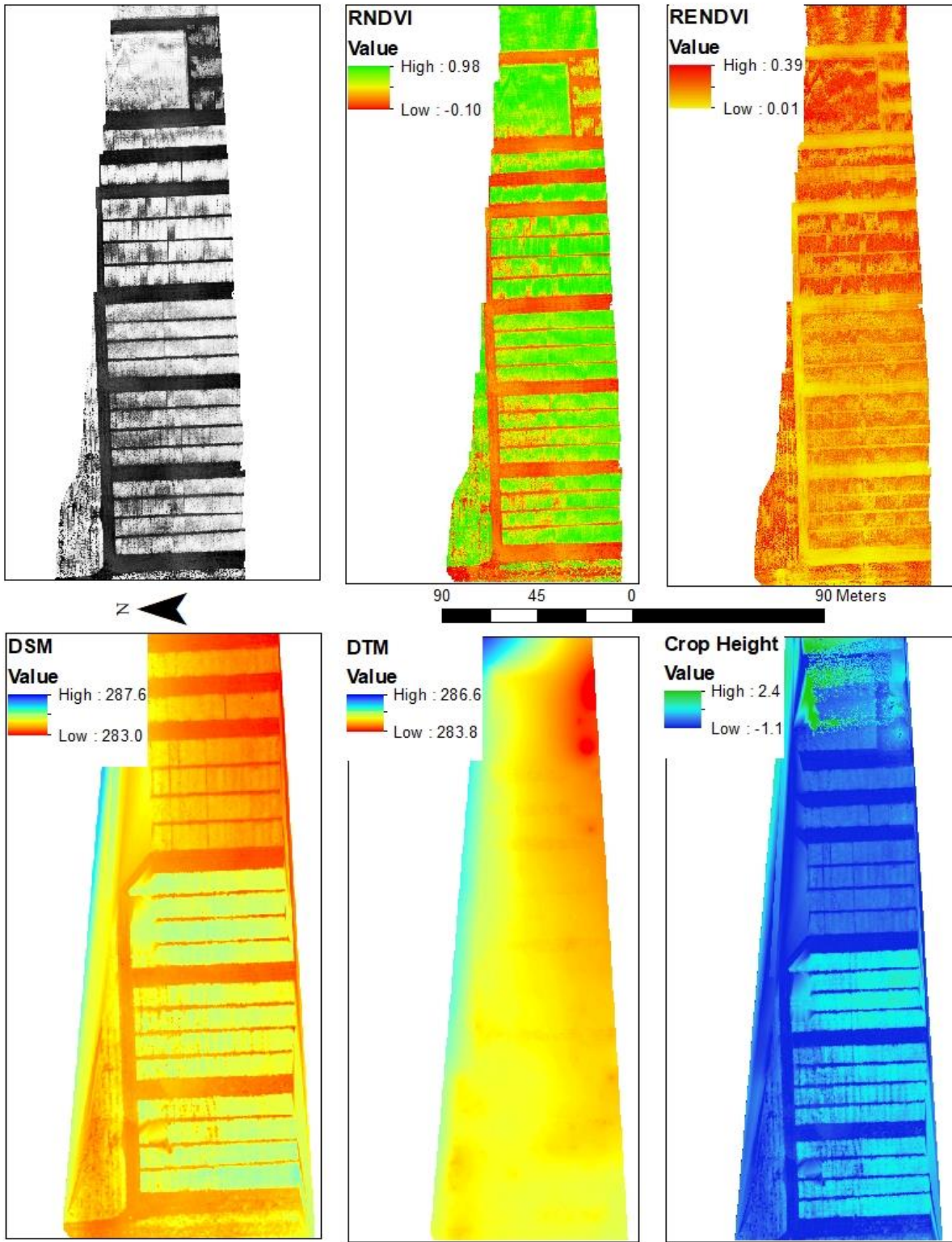
Figure A1. Ada June 30 2017 experimental site SUAS imagery produced with Pix4D and ArcGIS (Black/White; RNDVI; RENDVI: DSM (Meters); DTM (Meters); Crop Height (Meters)).
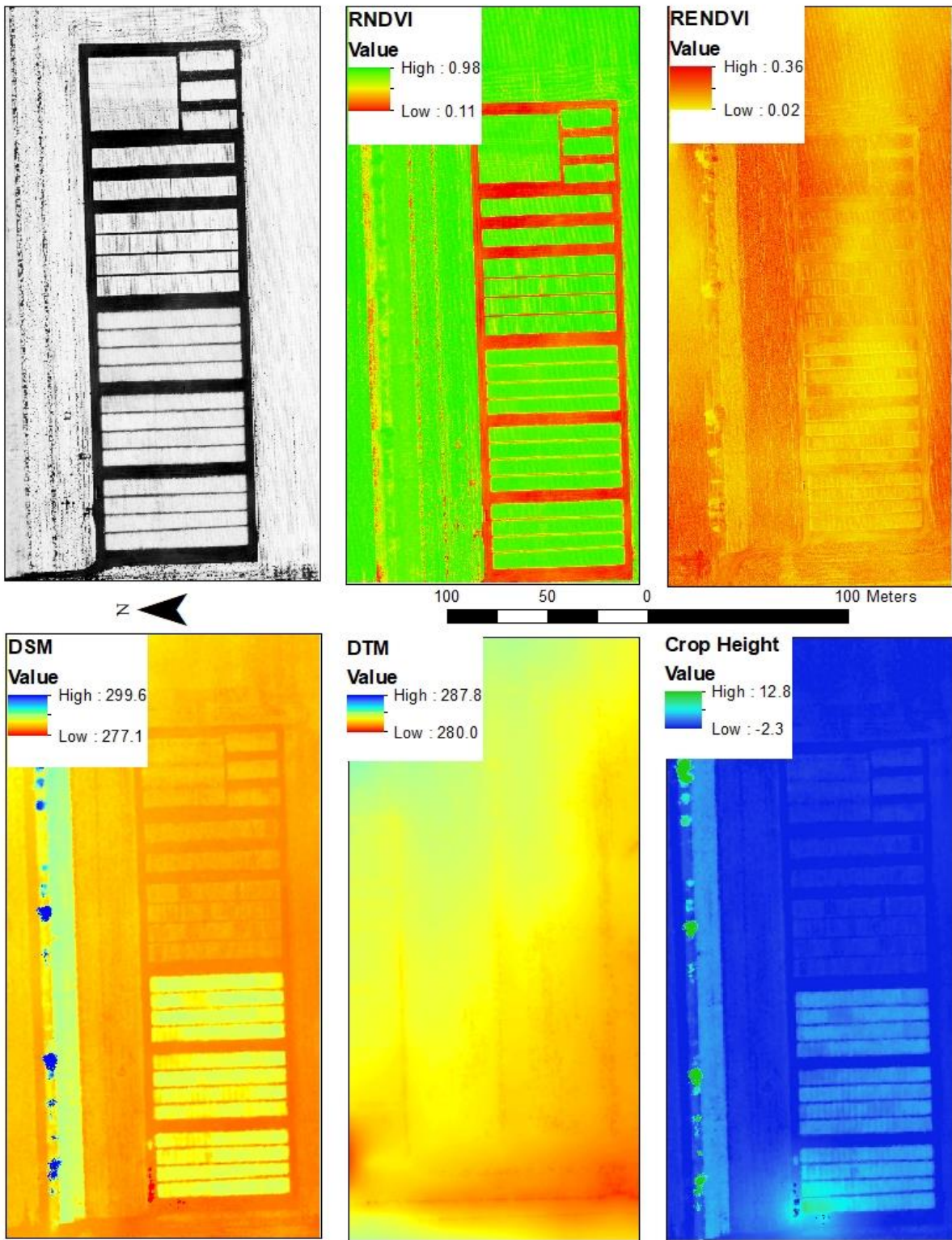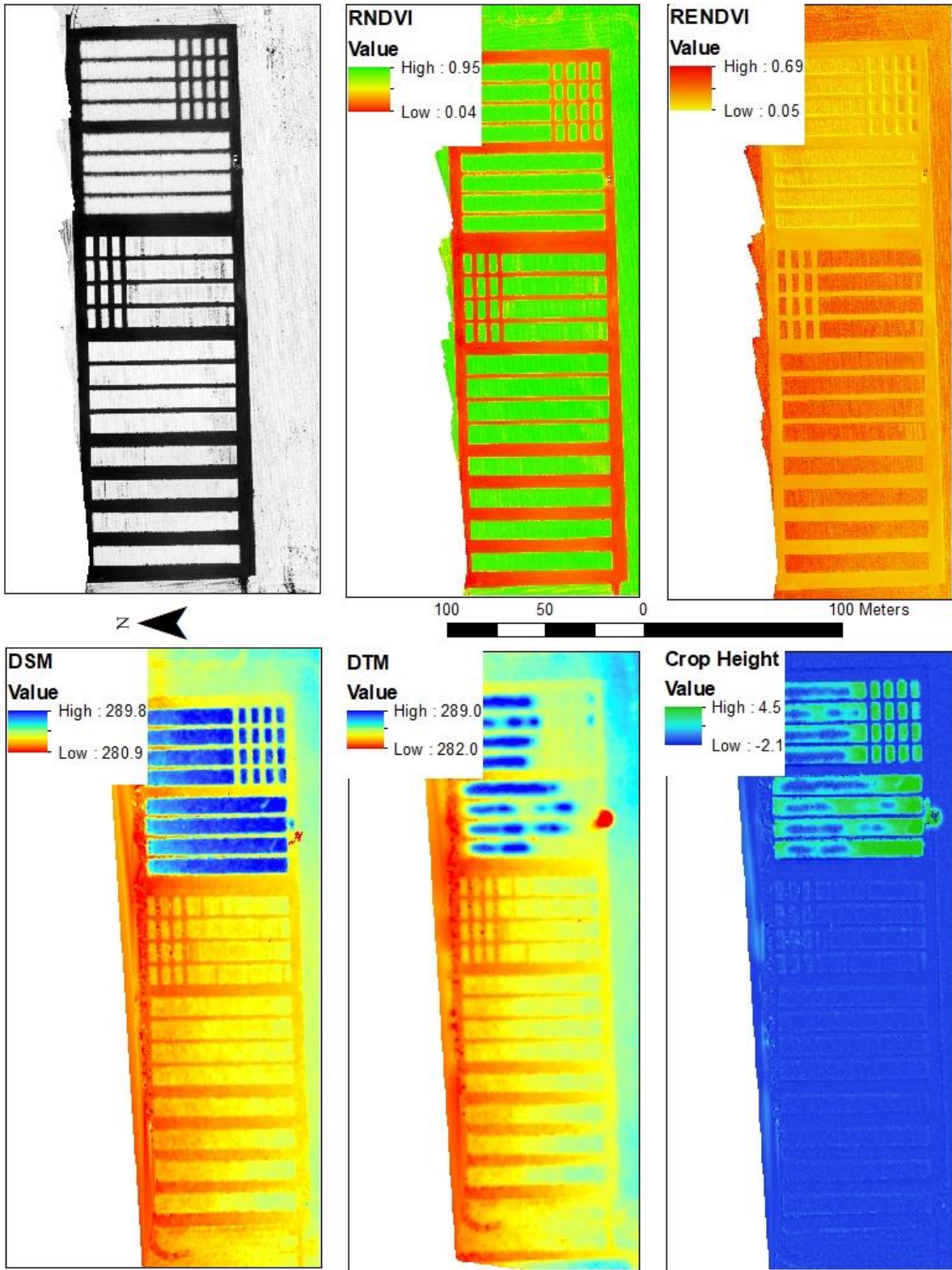
Figure A2. Ada July 26 2017 experimental site SUAS imagery produced with Pix4D and ArcGIS (Black/White; RNDVI; RENDVI: DSM (Meters); DTM (Meters); Crop Height (Meters)).
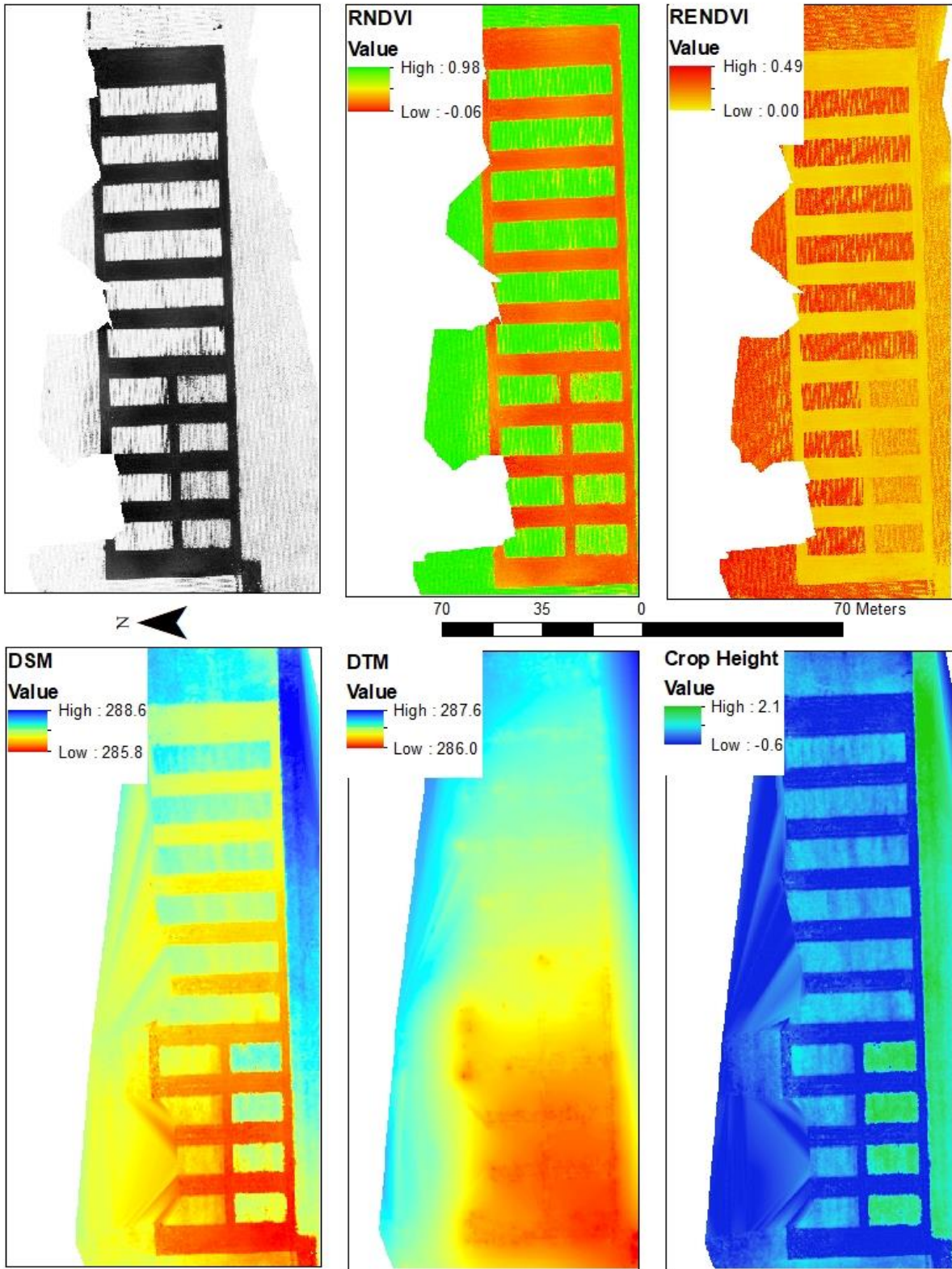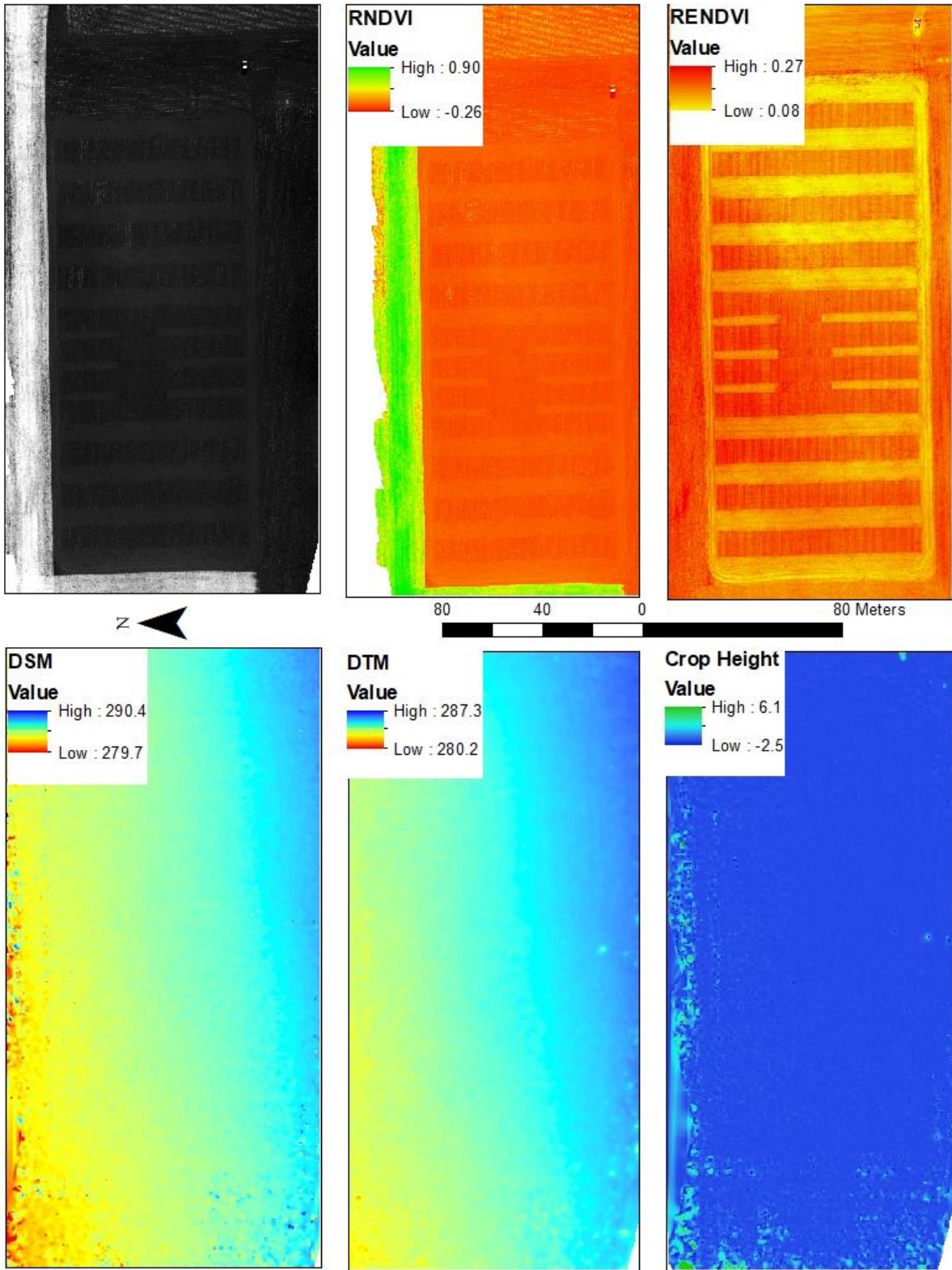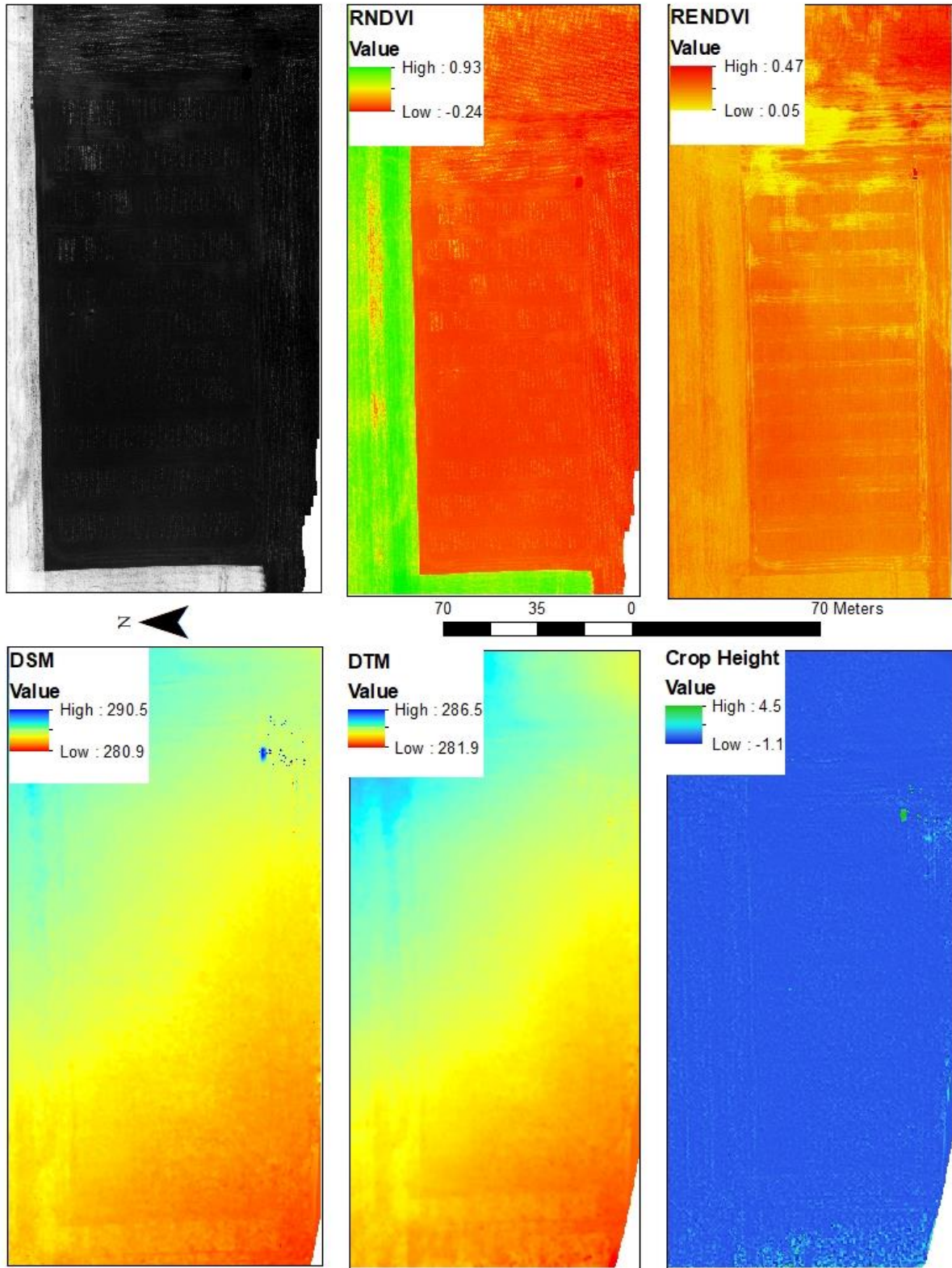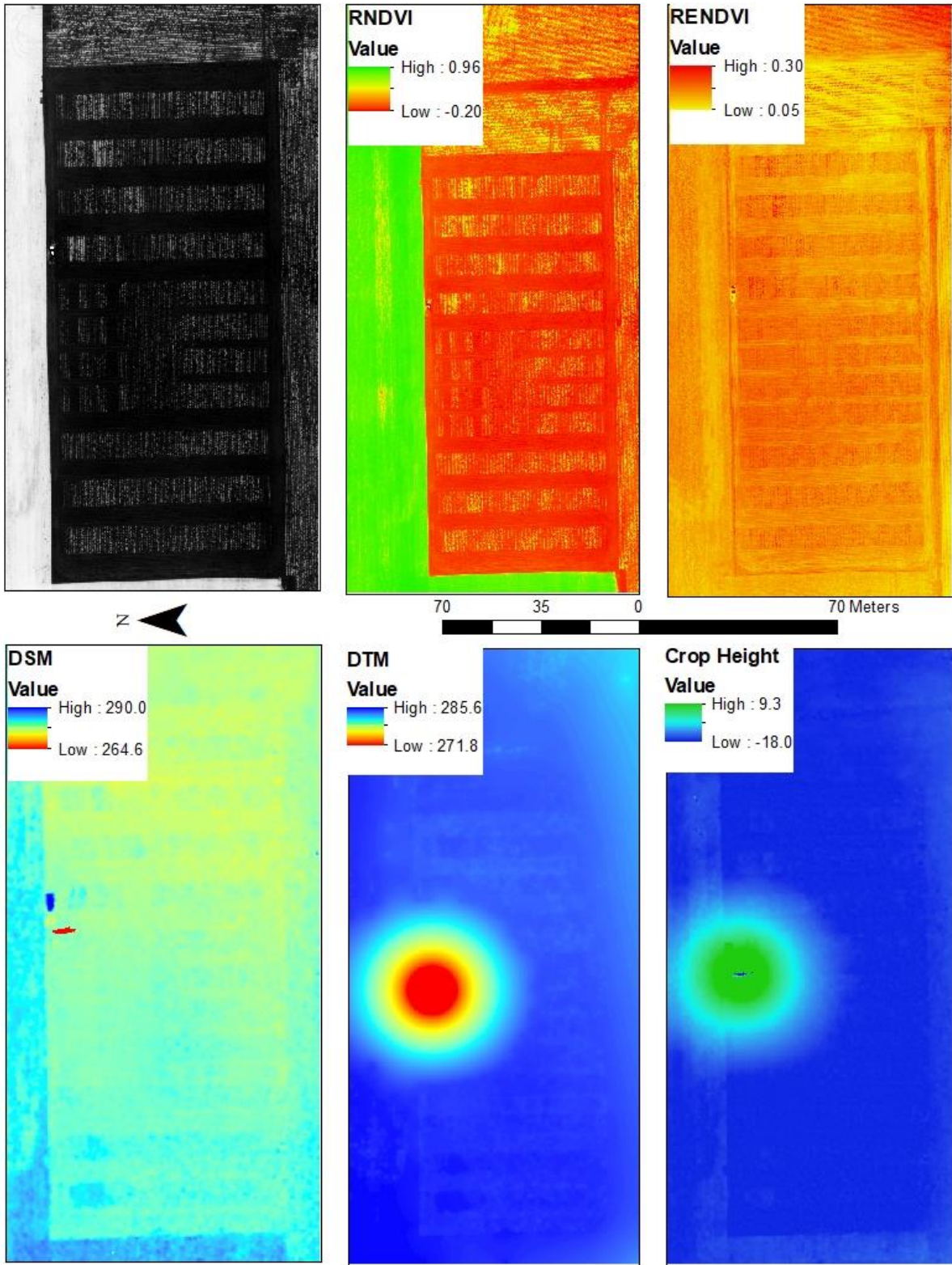
Figure A3. Downer June 29 2017 experimental site SUAS imagery produced with Pix4D and ArcGIS (Black/White; RNDVI; RENDVI: DSM (Meters); DTM (Meters); Crop Height (Meters)).
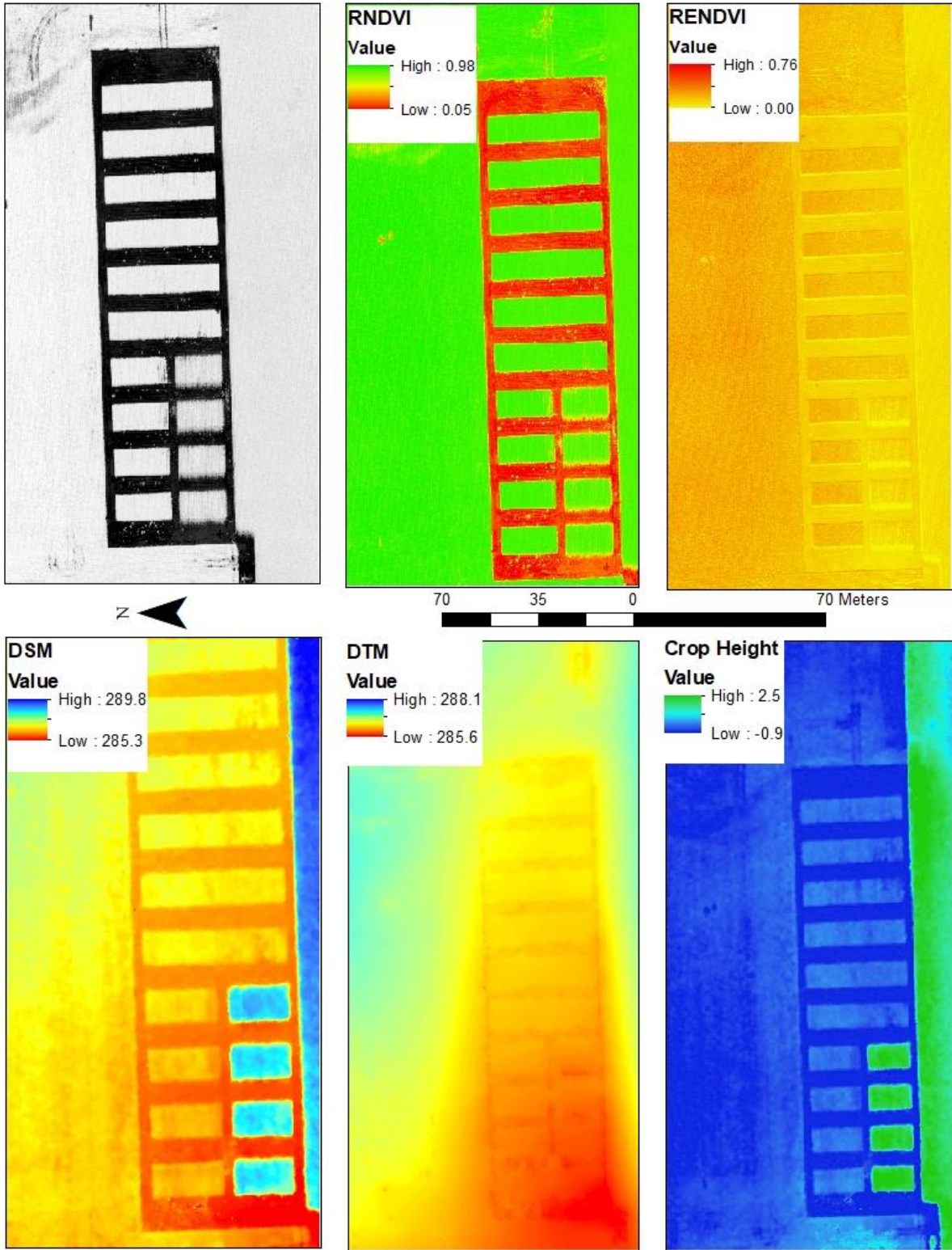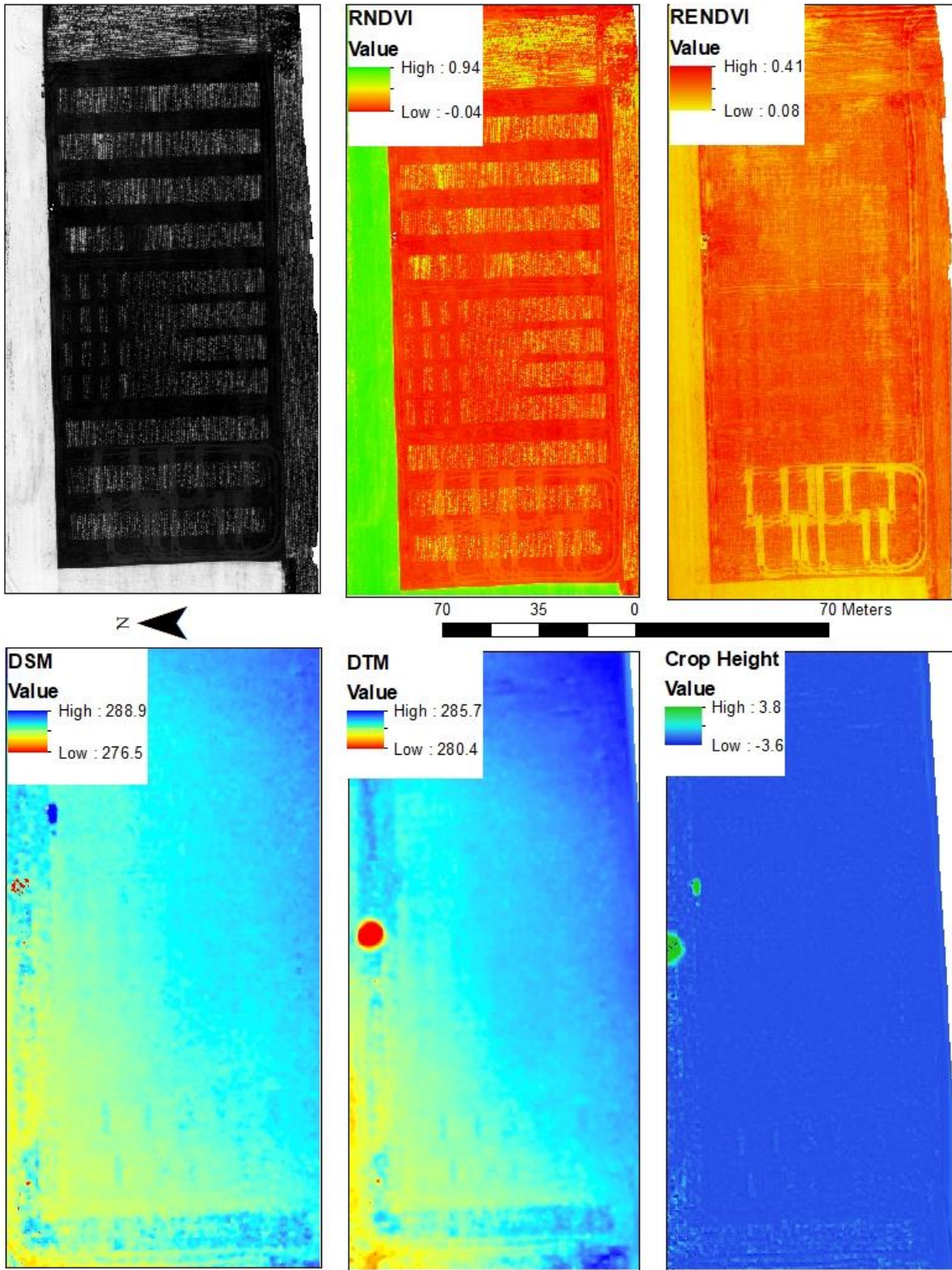
Figure A4. Downer July 26 2017 experimental site SUAS imagery produced with Pix4D and ArcGIS (Black/White; RNDVI; RENDVI: DSM (Meters); DTM (Meters); Crop Height (Meters)).
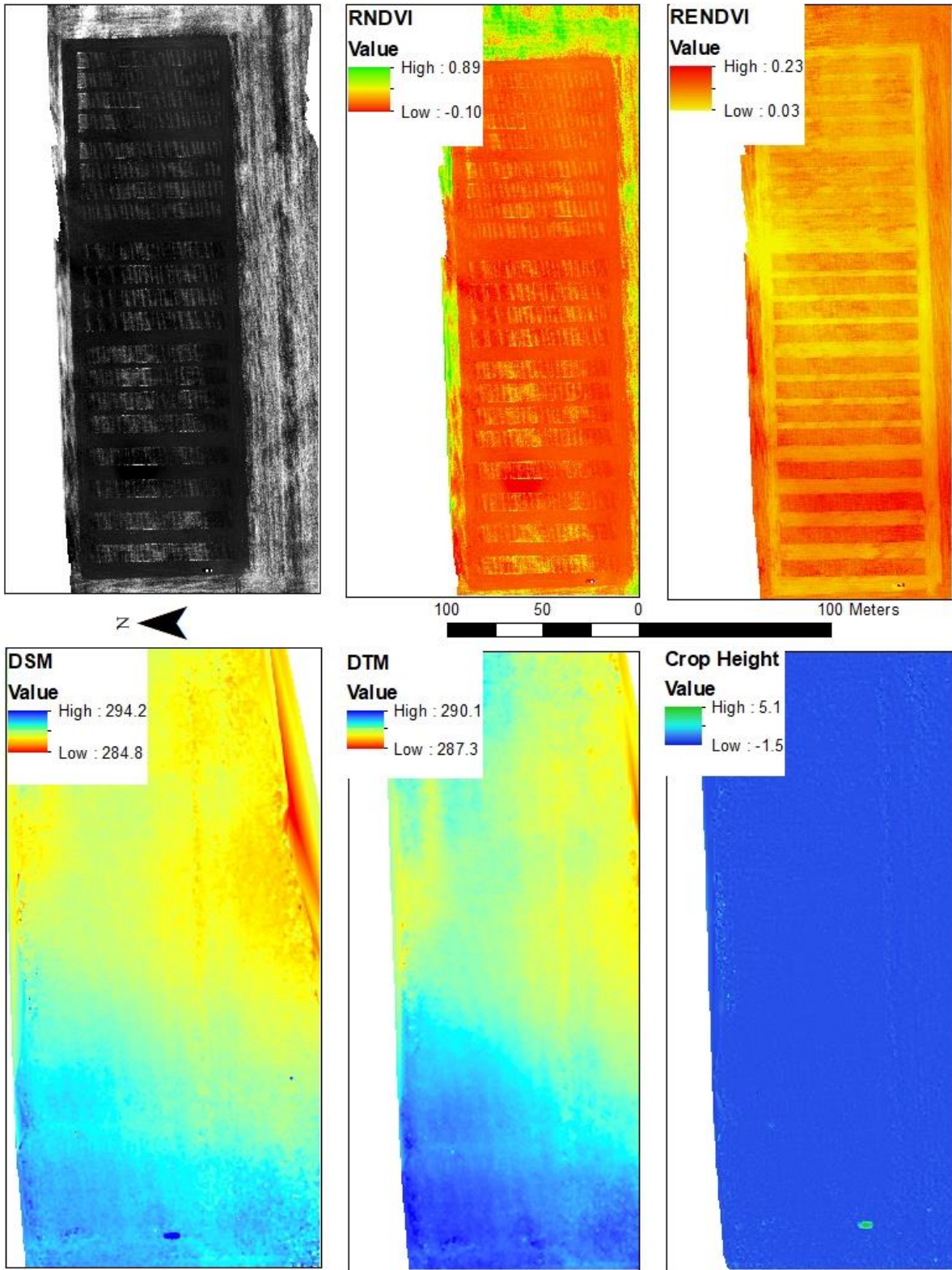
Figure A5. Ada May 31 2018 experimental site SUAS imagery produced with Pix4D and ArcGIS (Black/White; RNDVI; RENDVI: DSM (Meters); DTM (Meters); Crop Height (Meters)).
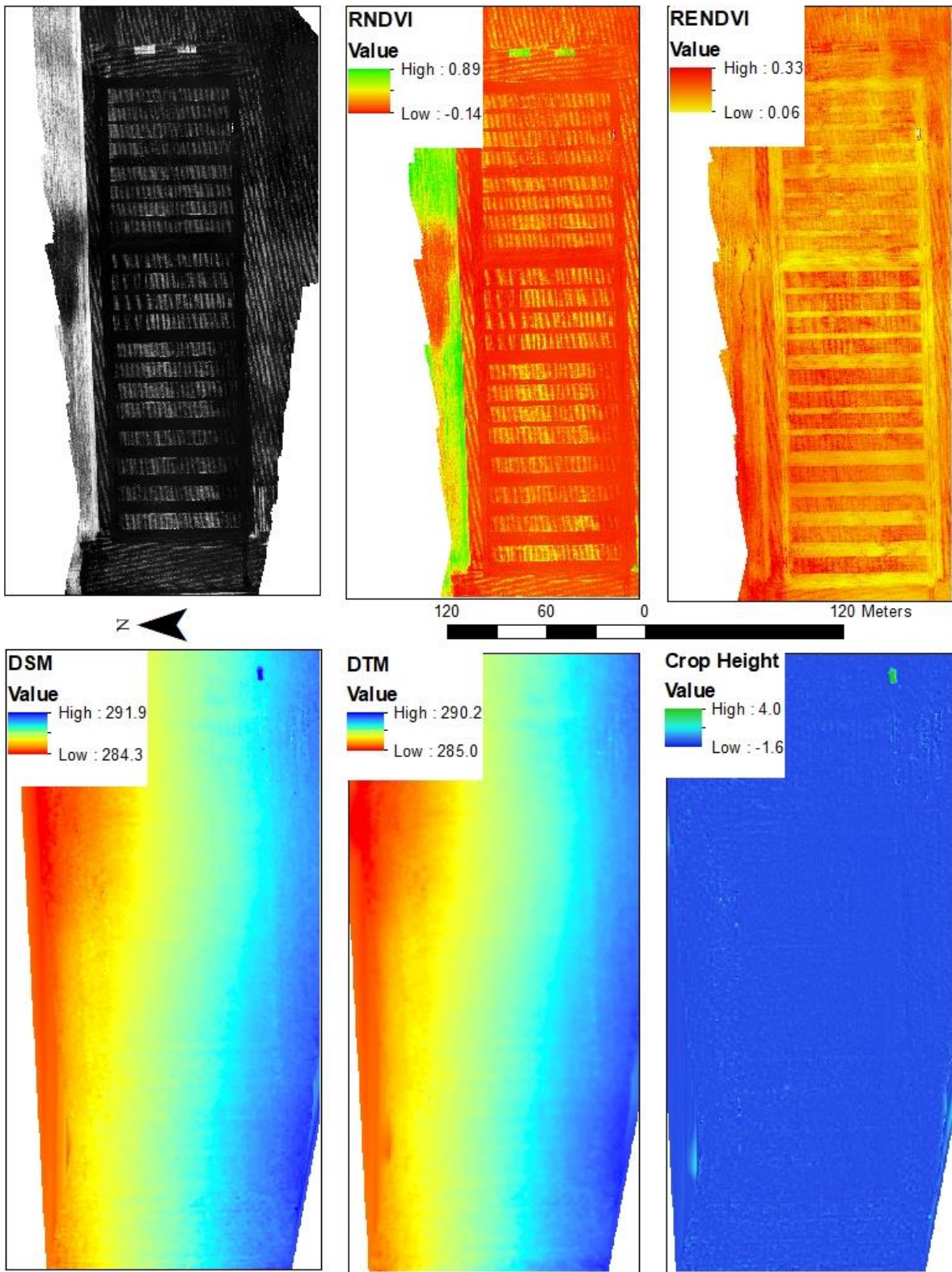
Figure A6. Ada June 7 2018 experimental site SUAS imagery produced with Pix4D and ArcGIS (Black/White; RNDVI; RENDVI: DSM (Meters); DTM (Meters); Crop Height (Meters)).

111
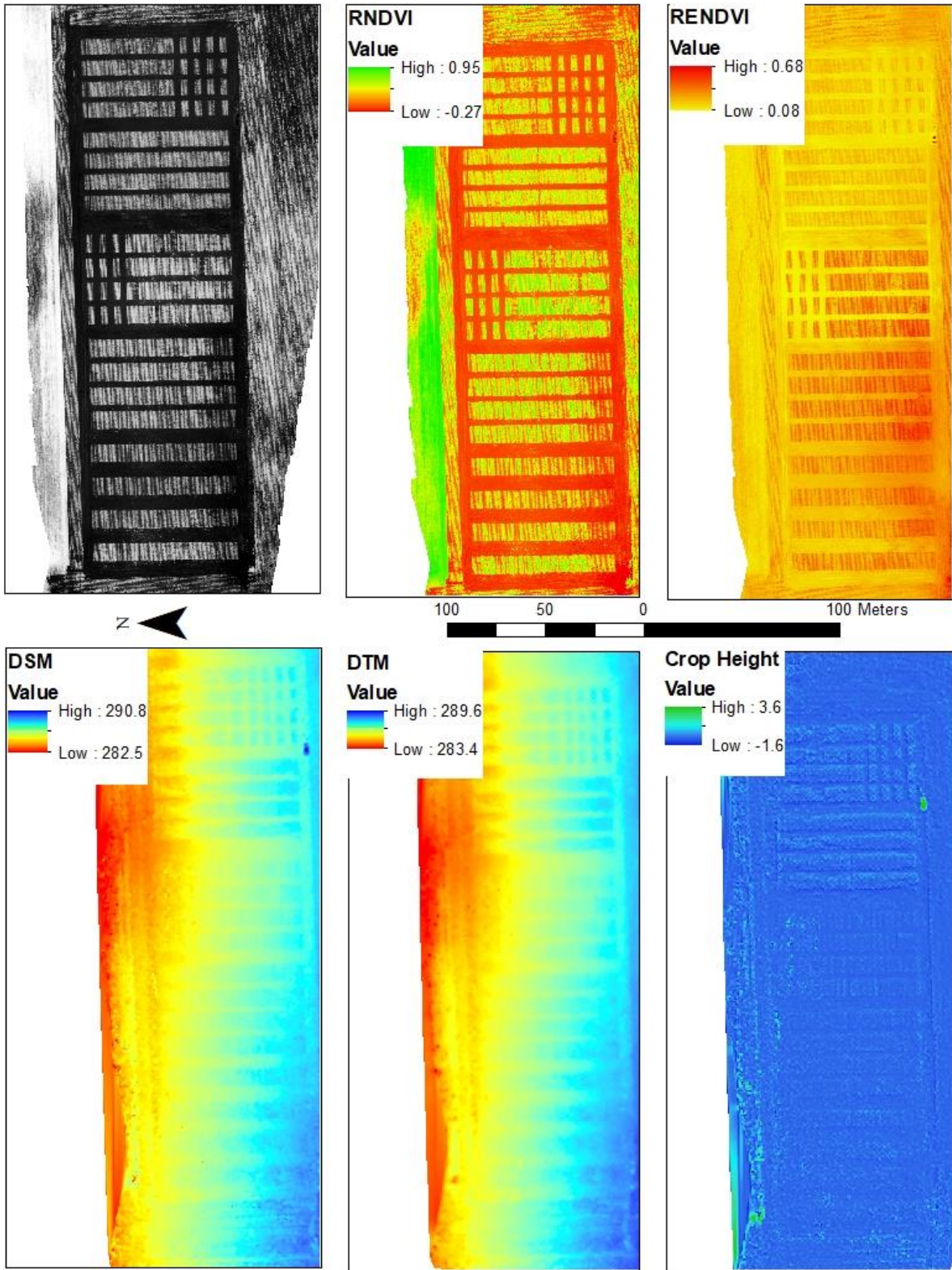
Figure A7. Ada June 15 2018 experimental site SUAS imagery produced with Pix4D and ArcGIS (Black/White; RNDVI; RENDVI: DSM (Meters); DTM (Meters); Crop Height (Meters)).
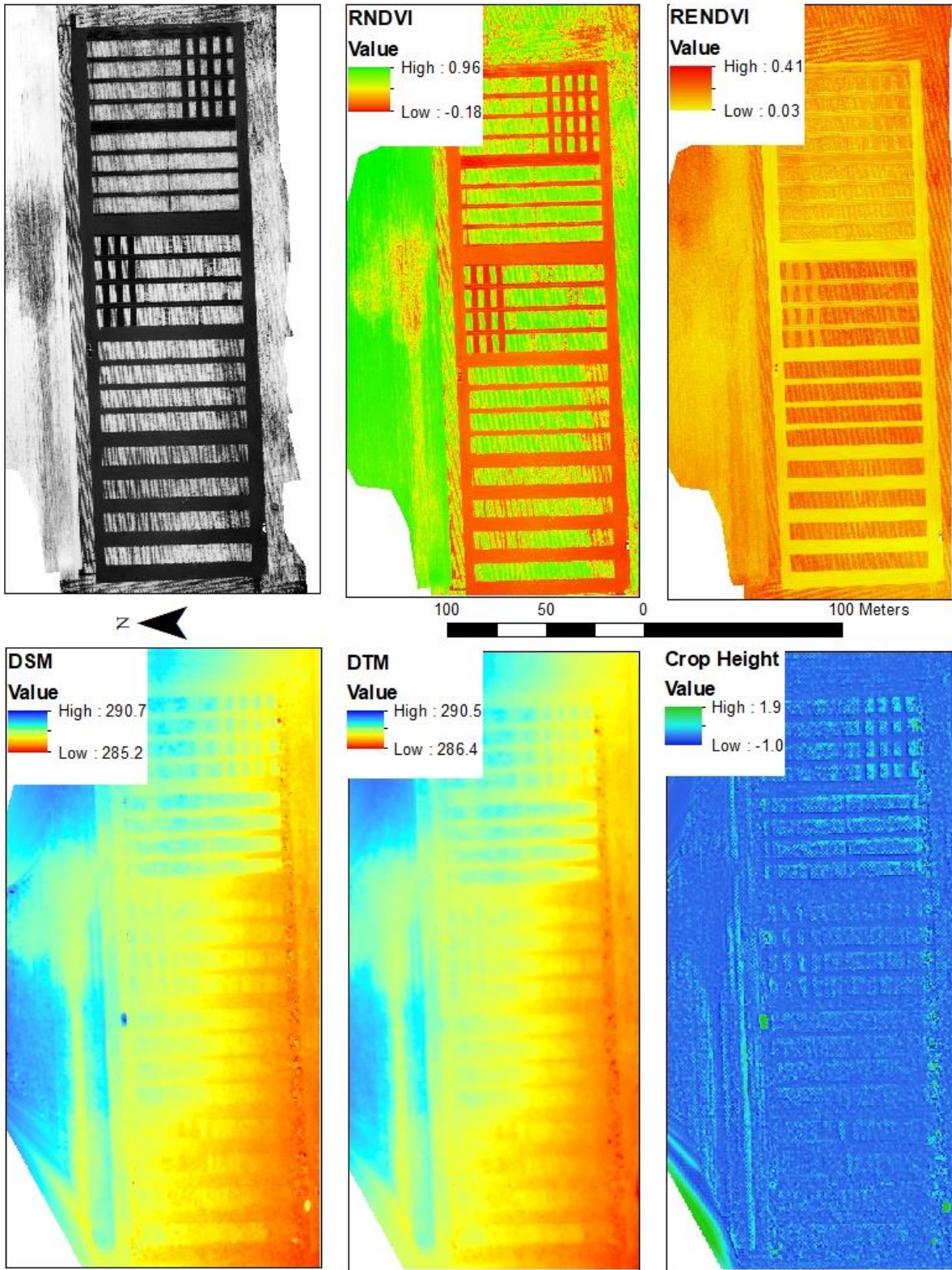
Figure A8. Ada June 21 2018 experimental site SUAS imagery produced with Pix4D and ArcGIS (Black/White; RNDVI; RENDVI: DSM (Meters); DTM (Meters); Crop Height (Meters)).
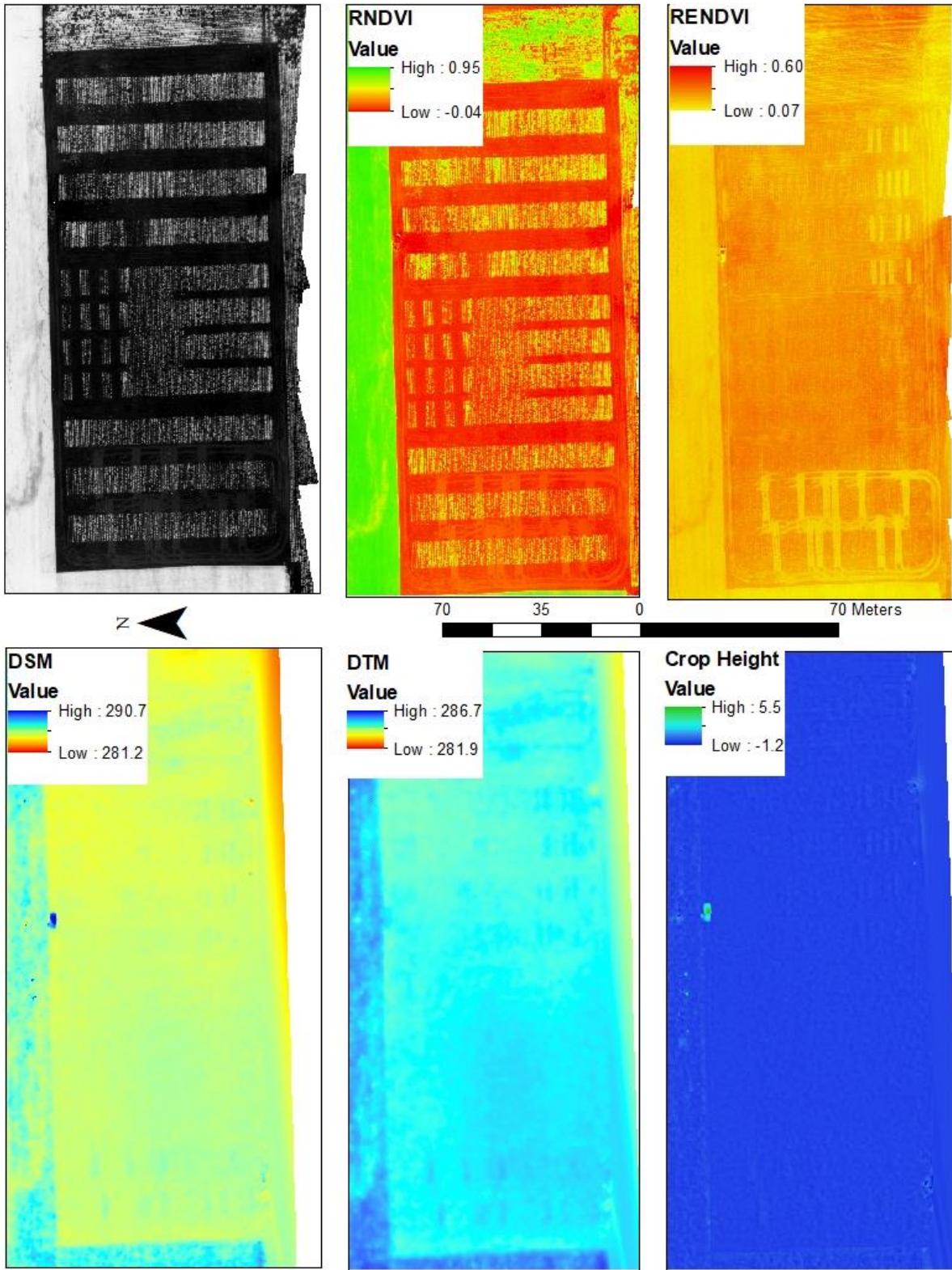
113
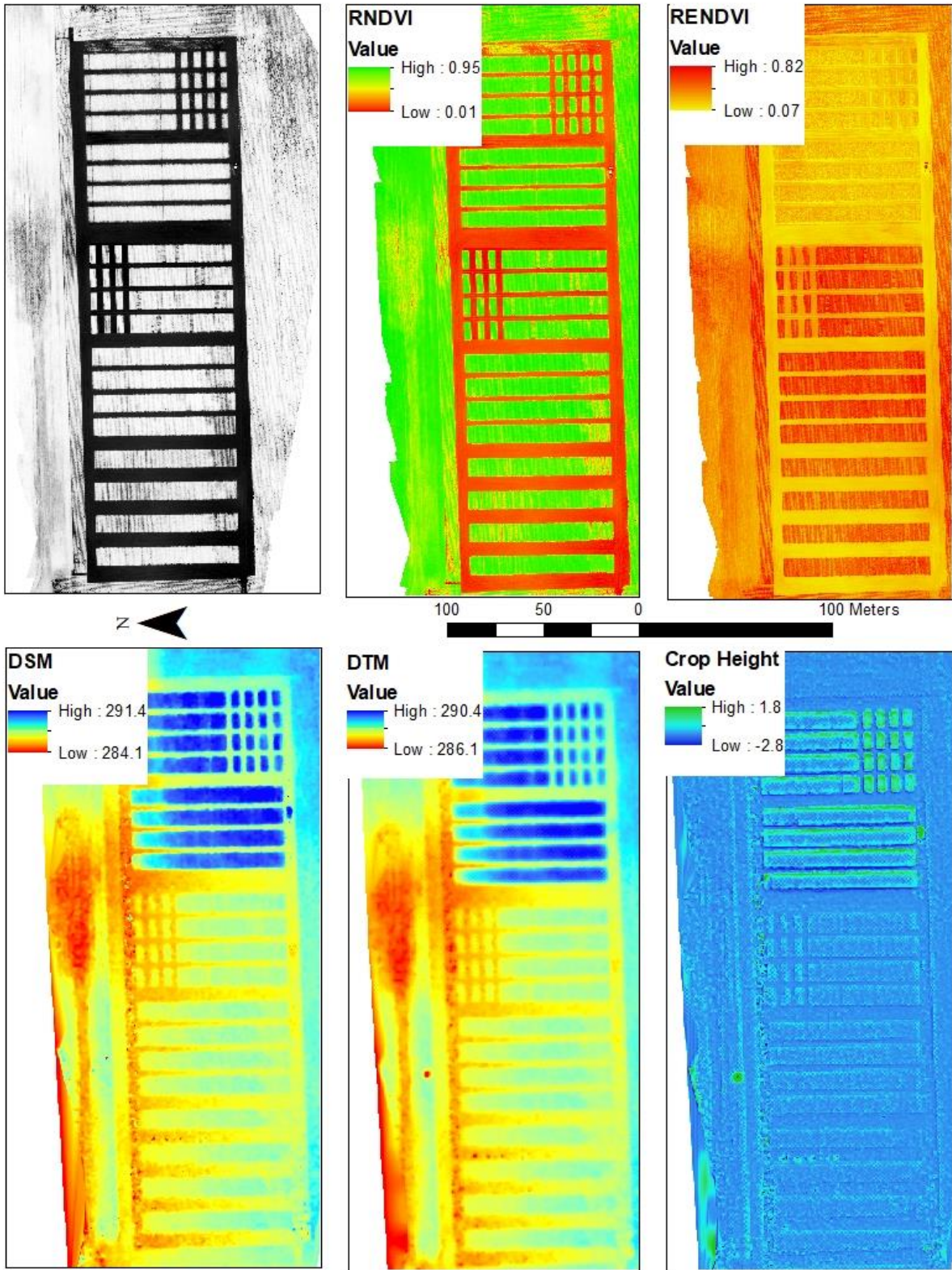
Figure A9. Ada June 28 2018 experimental site SUAS imagery produced with Pix4D and ArcGIS (Black/White; RNDVI; RENDVI: DSM (Meters); DTM (Meters); Crop Height (Meters)).
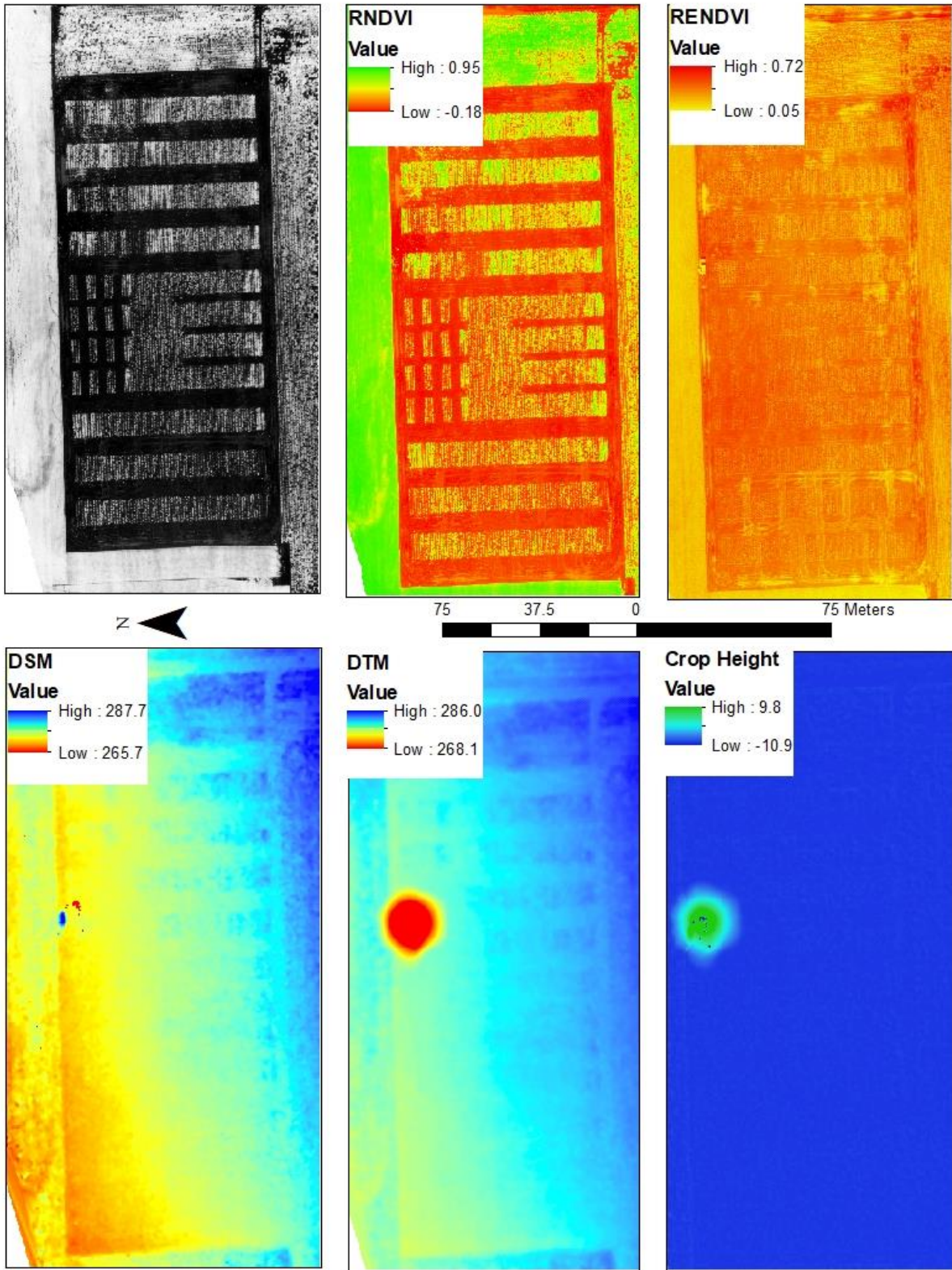
114
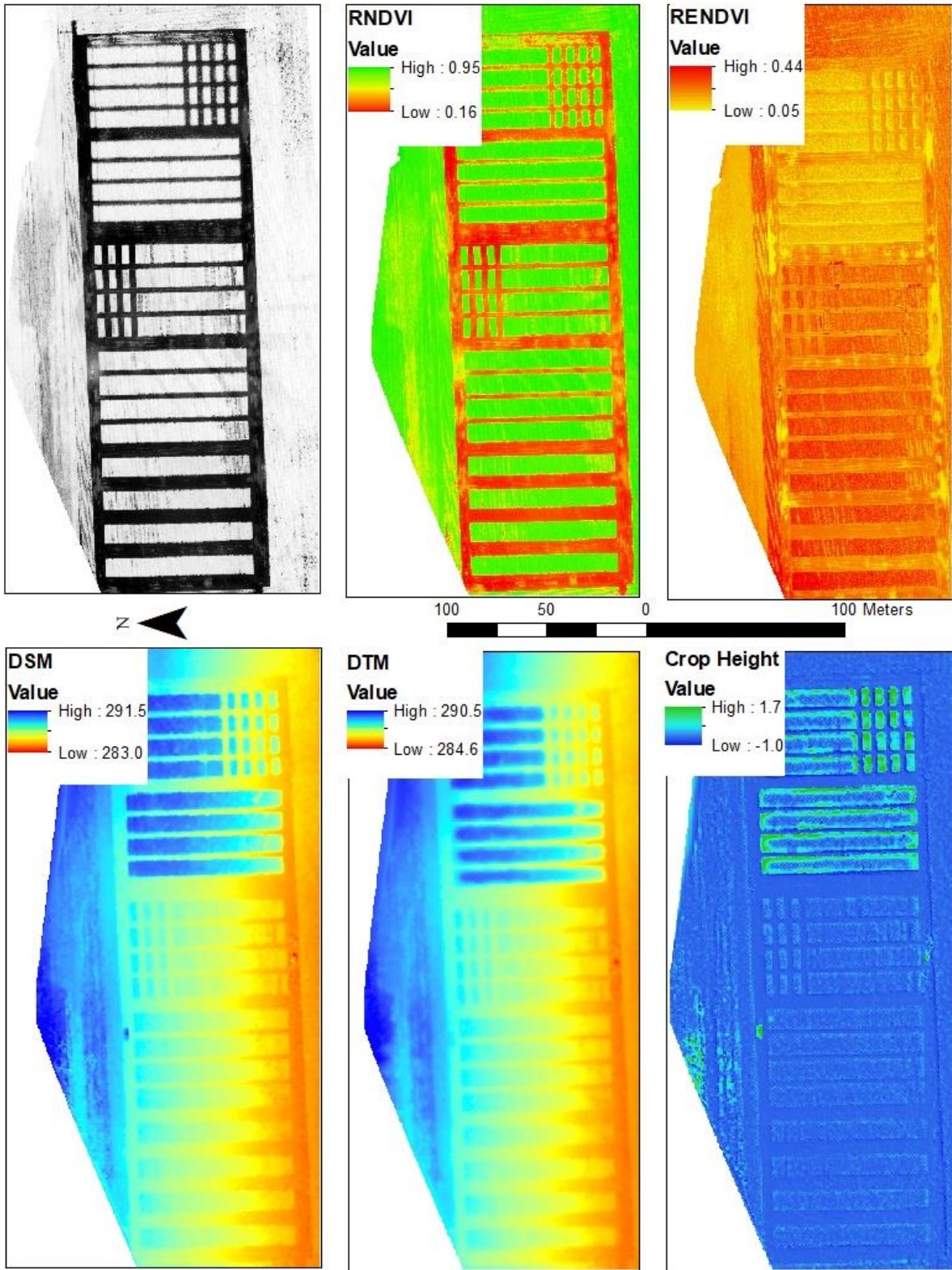
Figure A10. Ada July 5 2018 experimental site SUAS imagery produced with Pix4D and ArcGIS (Black/White; RNDVI; RENDVI: DSM (Meters); DTM (Meters); Crop Height (Meters)).
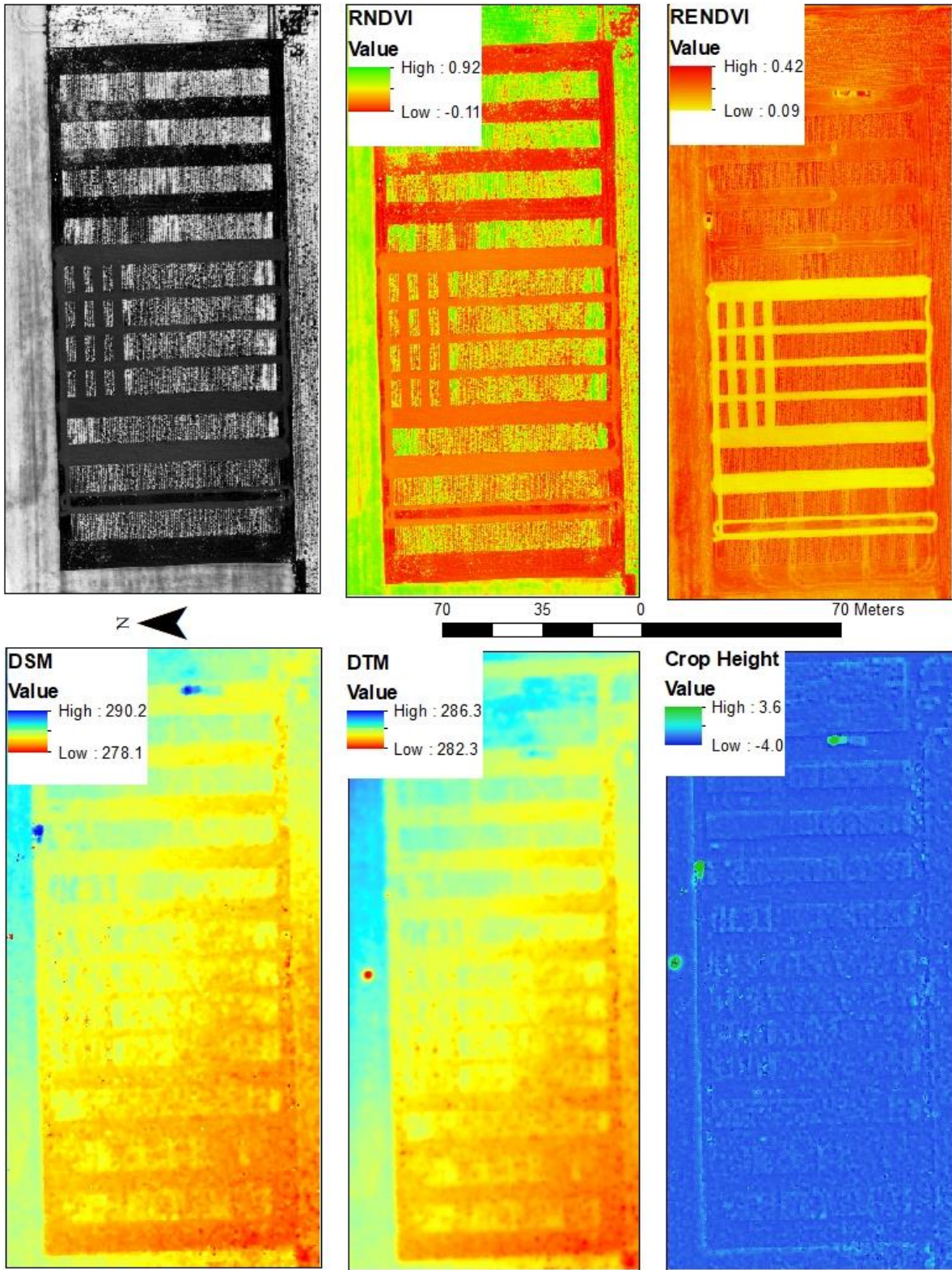
115
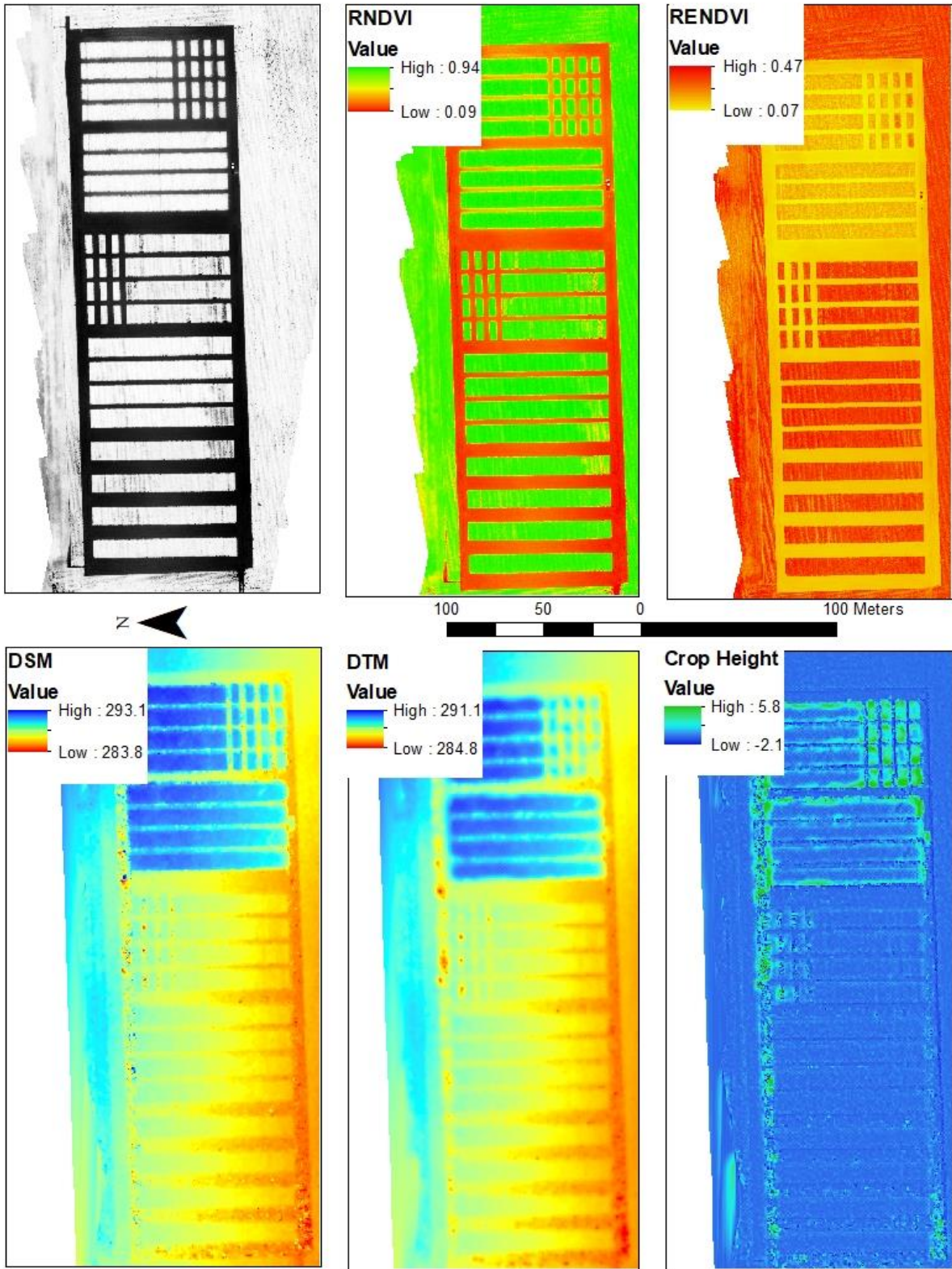
Figure A11. Ada July 12 2018 experimental site SUAS imagery produced with Pix4D and ArcGIS (Black/White; RNDVI; RENDVI: DSM (Meters); DTM (Meters); Crop Height (Meters)).

116
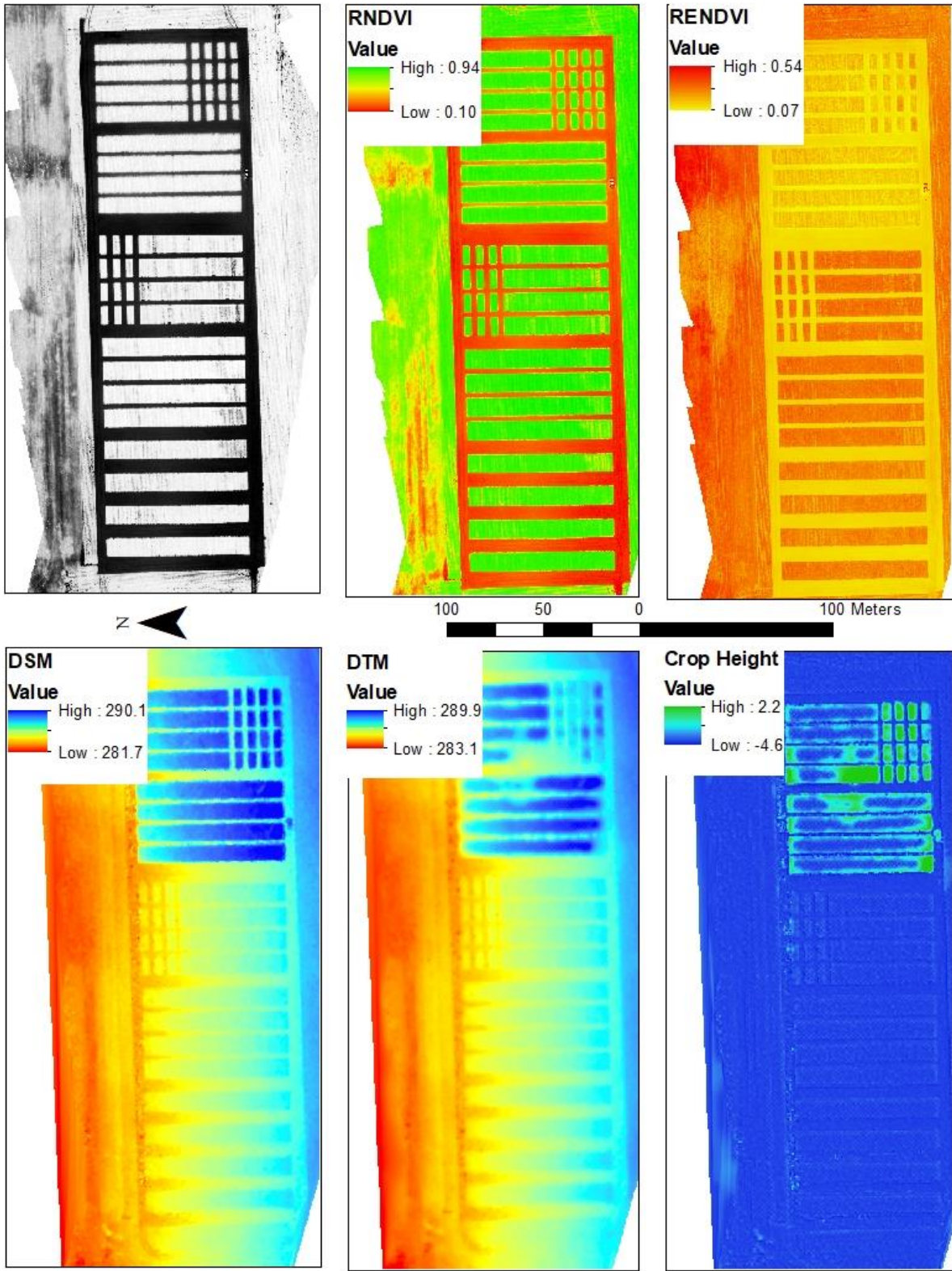
Figure A12. Ada July 18 2018 experimental site SUAS imagery produced with Pix4D and ArcGIS (Black/White; RNDVI; RENDVI: DSM (Meters); DTM (Meters); Crop Height (Meters)).
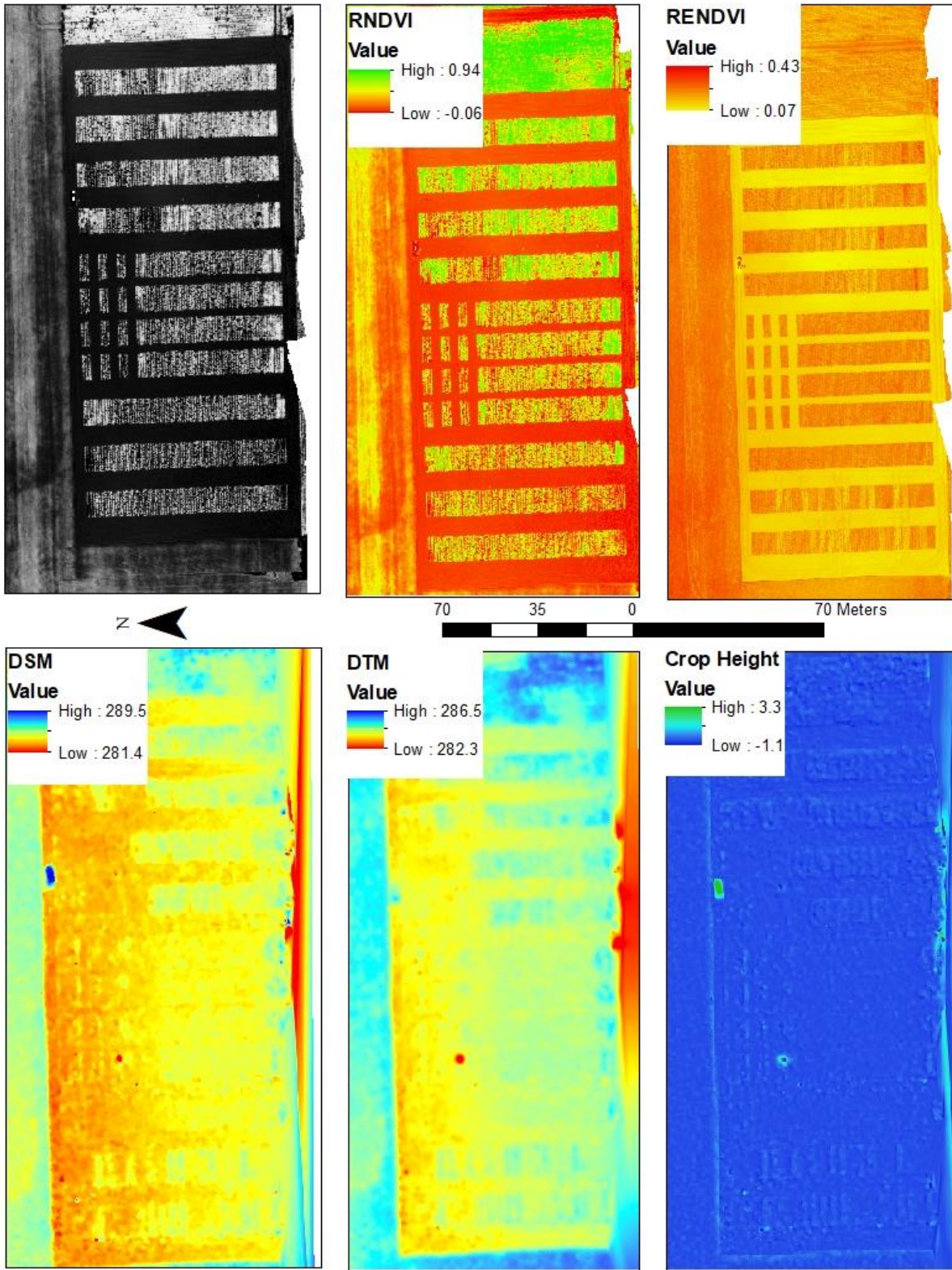
Figure A13. Ada July 27 2018 experimental site SUAS imagery produced with Pix4D and ArcGIS (Black/White; RNDVI; RENDVI: DSM (Meters); DTM (Meters); Crop Height (Meters)).

Figure A14. Downer May 31 2018 experimental site SUAS imagery produced with Pix4D and ArcGIS (Black/White; RNDVI; RENDVI: DSM (Meters); DTM (Meters); Crop Height (Meters)).
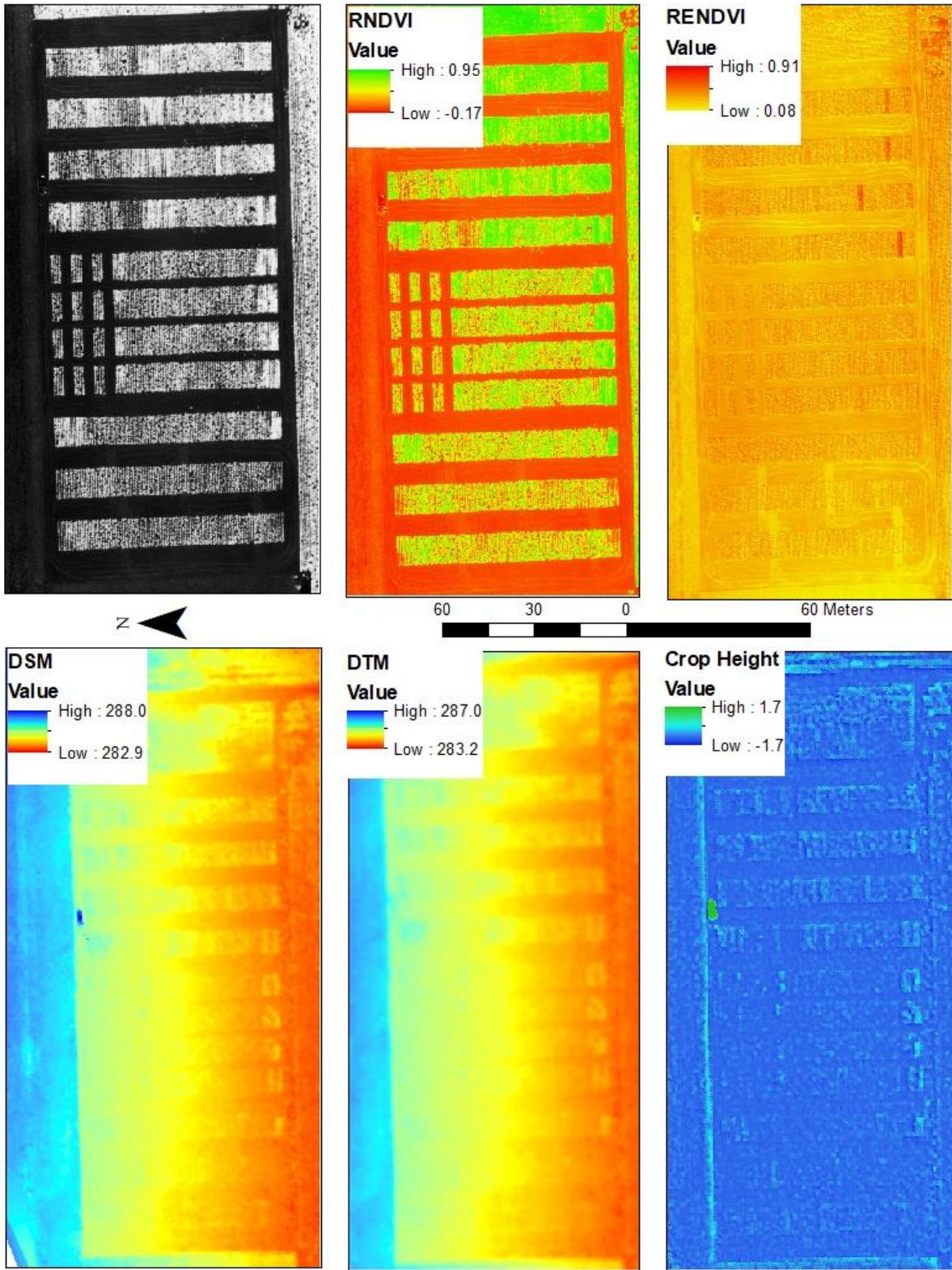
119

Figure A15. Downer June 7 2018 experimental site SUAS imagery produced with Pix4D and ArcGIS (Black/White; RNDVI; RENDVI: DSM (Meters); DTM (Meters); Crop Height (Meters)).

Figure A16. Downer June 15 2018 experimental site SUAS imagery produced with Pix4D and ArcGIS (Black/White; RNDVI; RENDVI: DSM (Meters); DTM (Meters); Crop Height (Meters)). An error occurred in the DTM generation which rendered crop height unusable.
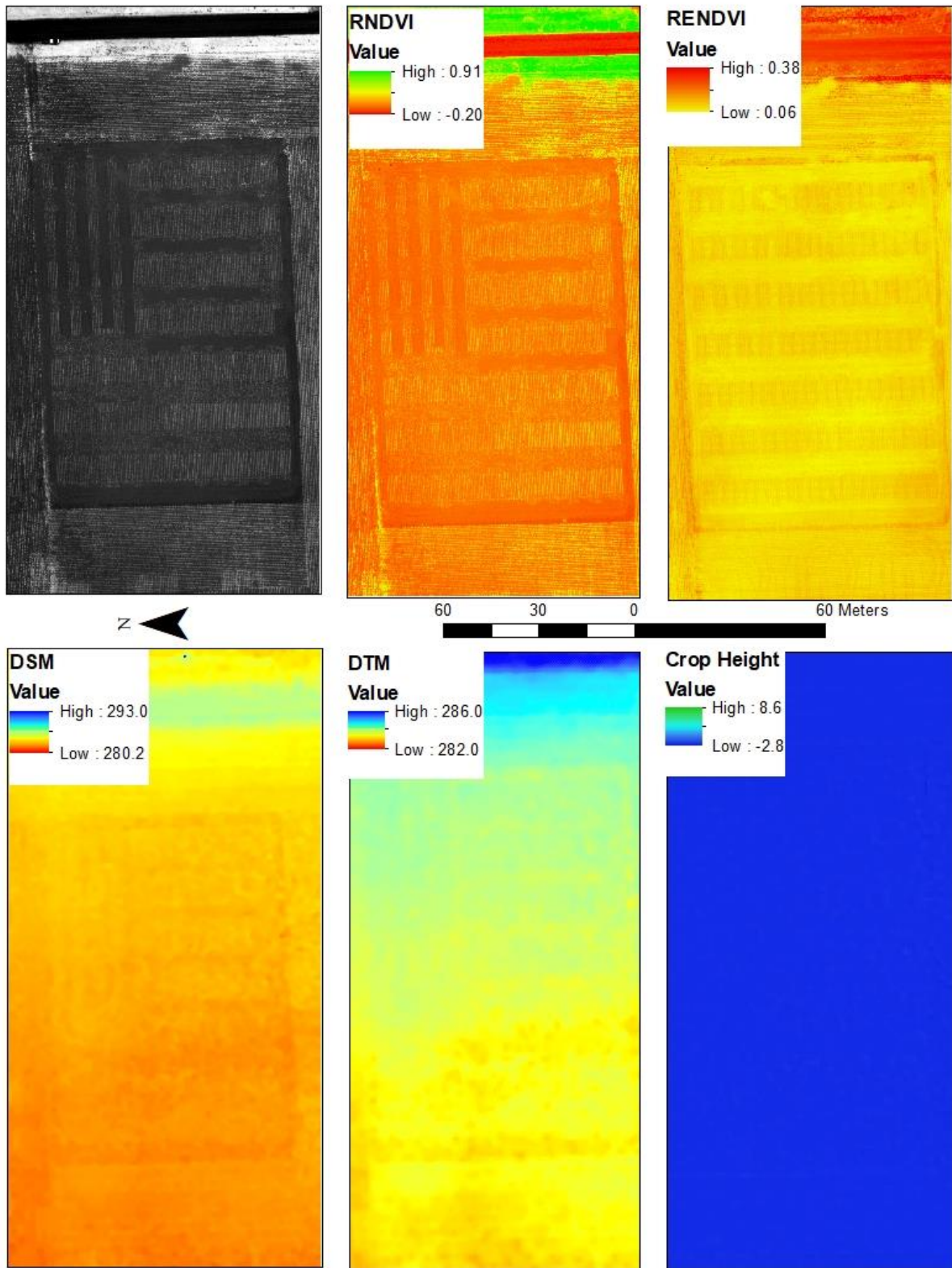
121

Figure A17. Downer June 21 2018 experimental site SUAS imagery produced with Pix4D and ArcGIS (Black/White; RNDVI; RENDVI: DSM (Meters); DTM (Meters); Crop Height (Meters)).
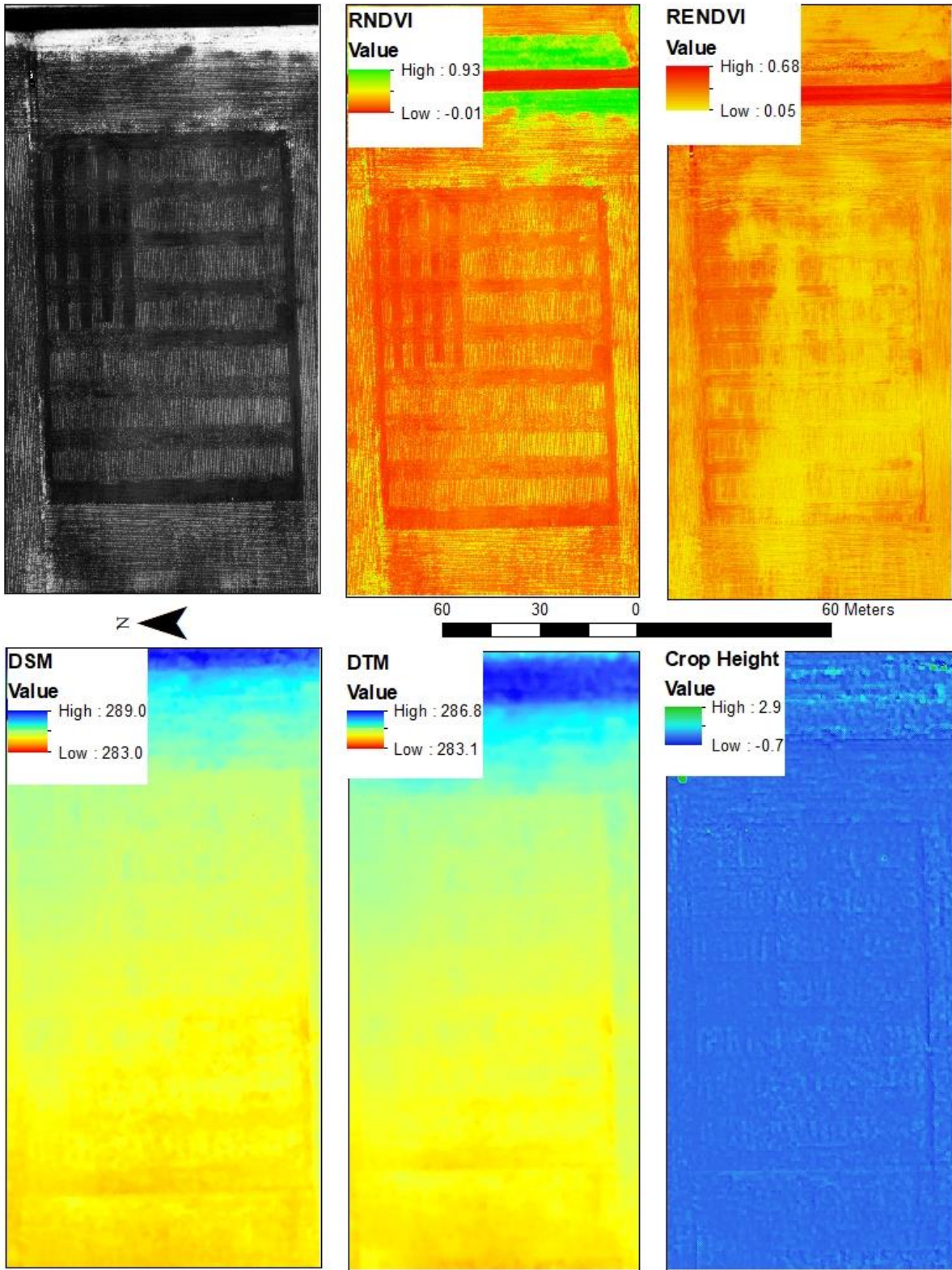
Figure A18. Downer June 28 2018 experimental site SUAS imagery produced with Pix4D and ArcGIS (Black/White; RNDVI; RENDVI: DSM (Meters); DTM (Meters); Crop Height (Meters)).

123

Figure A19. Downer July 5 2018 experimental site SUAS imagery produced with Pix4D and ArcGIS (Black/White; RNDVI; RENDVI: DSM (Meters); DTM (Meters); Crop Height (Meters)).

124

Figure A20. Downer July 12 2018 experimental site SUAS imagery produced with Pix4D and ArcGIS (Black/White; RNDVI; RENDVI: DSM (Meters); DTM (Meters); Crop Height (Meters)).
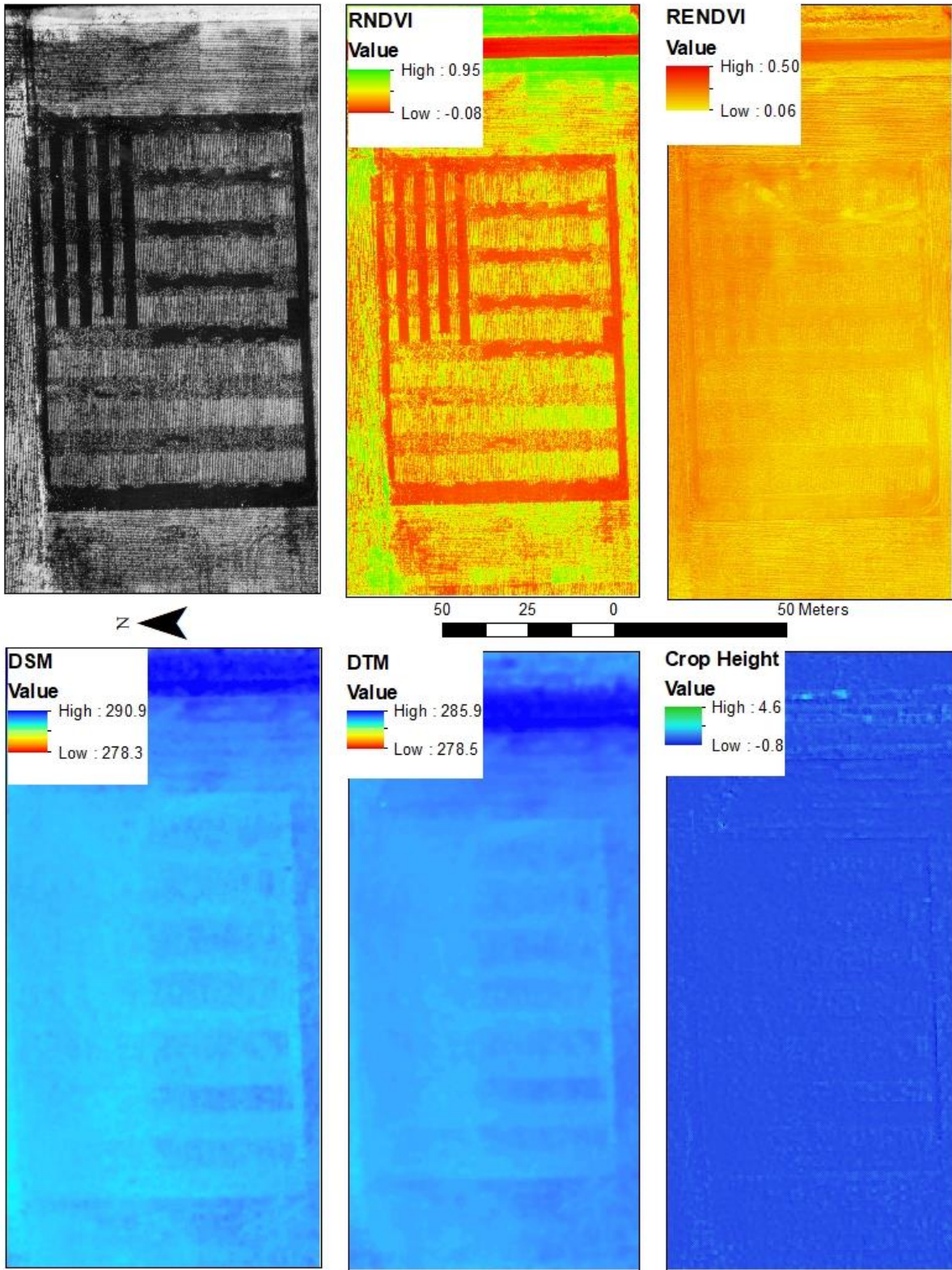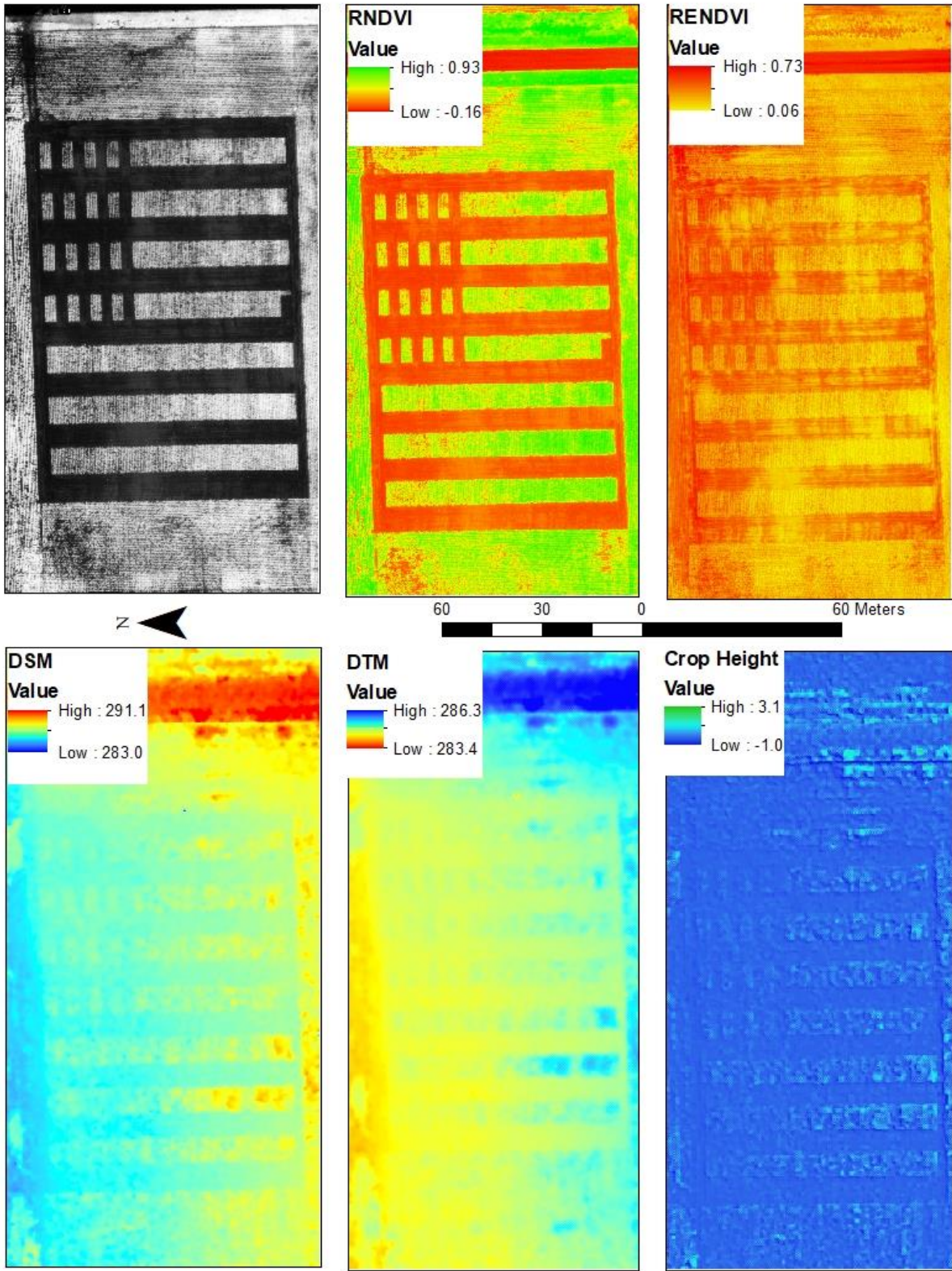
Figure A21. Downer July 18 2018 experimental site SUAS imagery produced with Pix4D and ArcGIS (Black/White; RNDVI; RENDVI: DSM (Meters); DTM (Meters); Crop Height (Meters)).

126

Figure A22. Downer July 27 2018 experimental site SUAS imagery produced with Pix4D and ArcGIS (Black/White; RNDVI; RENDVI: DSM (Meters); DTM (Meters); Crop Height (Meters)).

127

Figure A23. Sabin May 31 2018 experimental site SUAS imagery produced with Pix4D and ArcGIS (Black/White; RNDVI; RENDVI: DSM (Meters); DTM (Meters); Crop Height (Meters)).
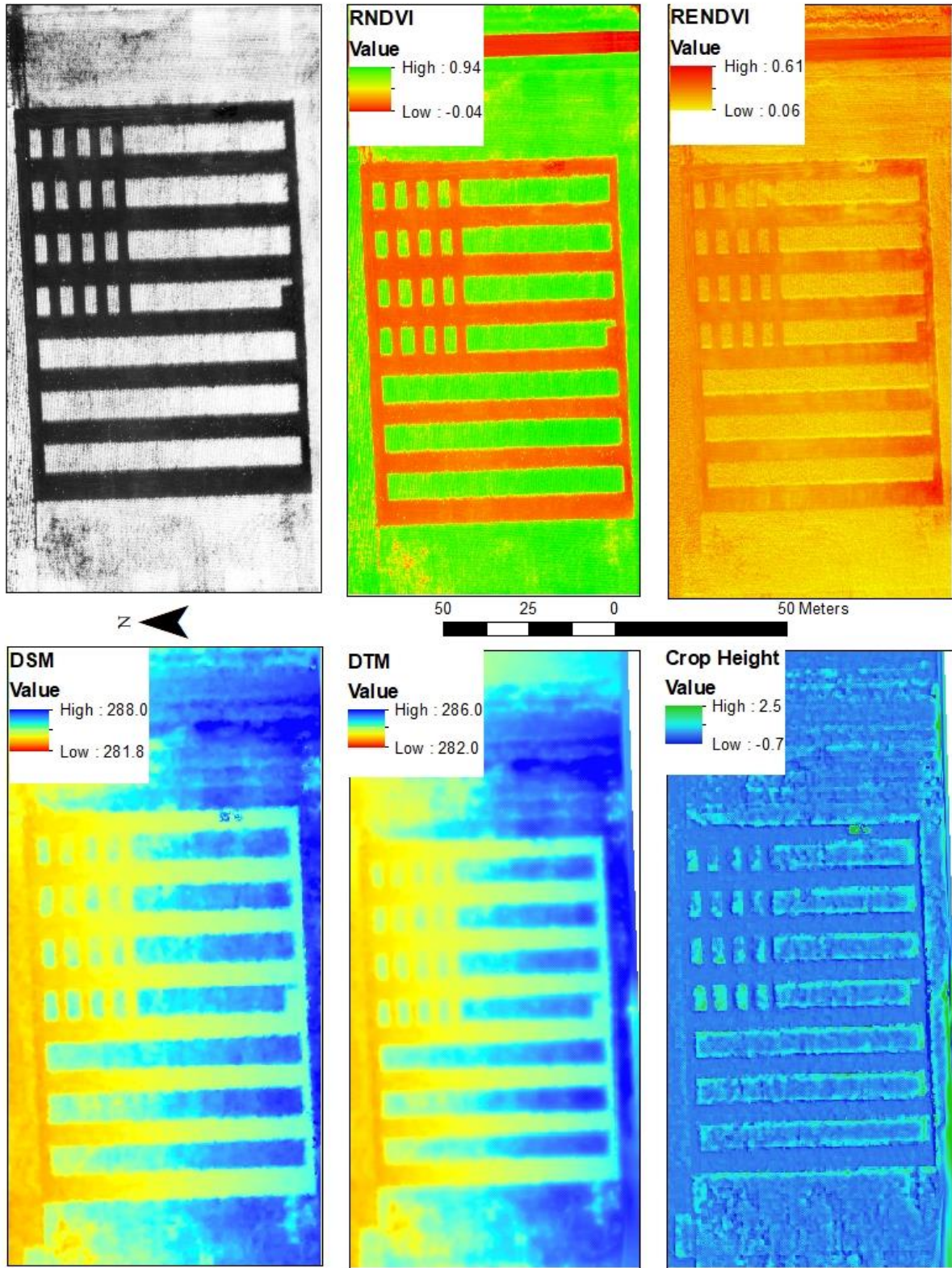
128

Figure A24. Sabin June 7 2018 experimental site SUAS imagery produced with Pix4D and ArcGIS (Black/White; RNDVI; RENDVI: DSM (Meters); DTM (Meters); Crop Height (Meters)).
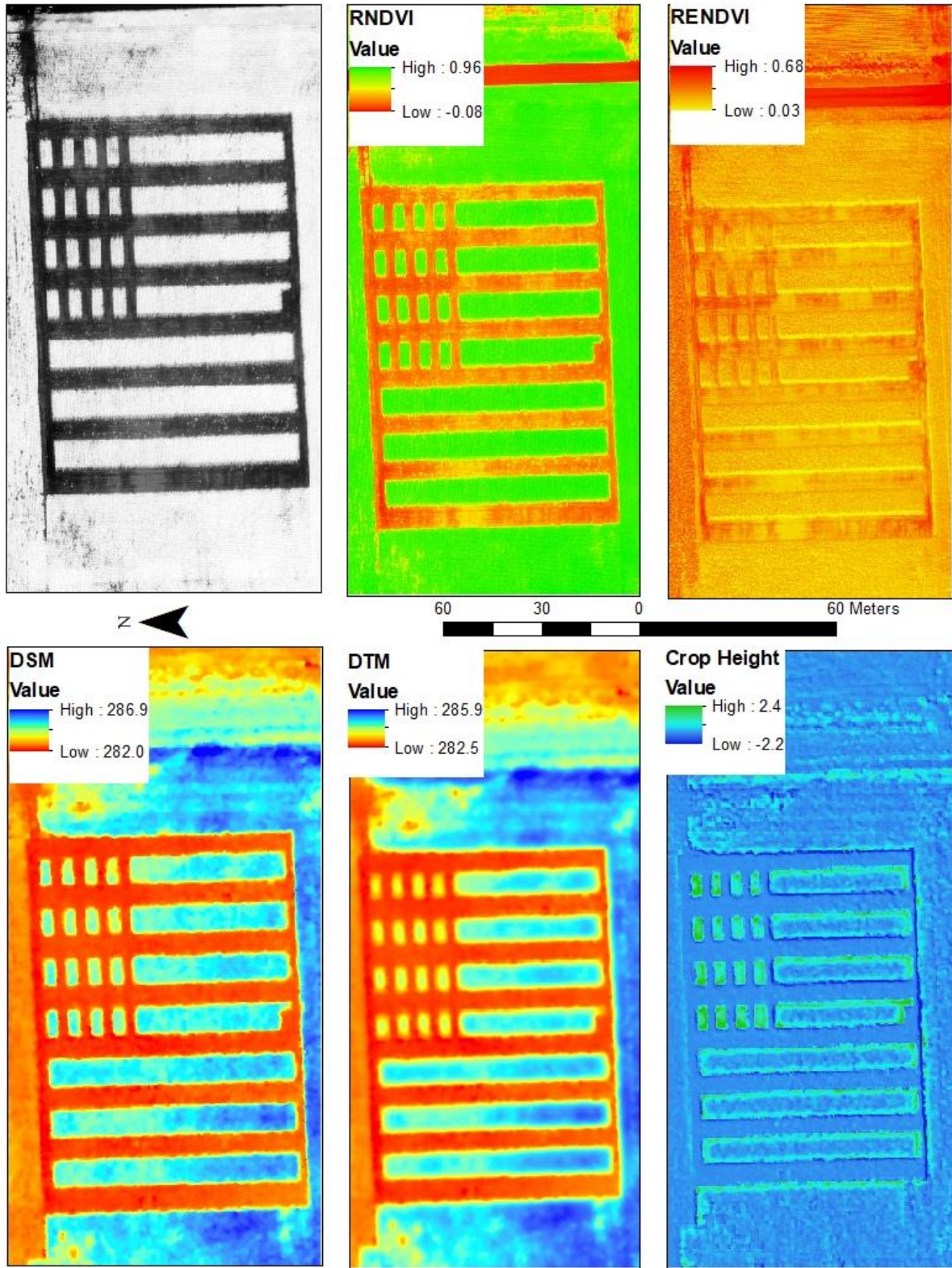
Figure A25. Sabin June 15 2018 experimental site SUAS imagery produced with Pix4D and ArcGIS (Black/White; RNDVI; RENDVI: DSM (Meters); DTM (Meters); Crop Height (Meters)).

Figure A26. Sabin June 21 2018 experimental site SUAS imagery produced with Pix4D and ArcGIS (Black/White; RNDVI; RENDVI: DSM (Meters); DTM (Meters); Crop Height (Meters)).
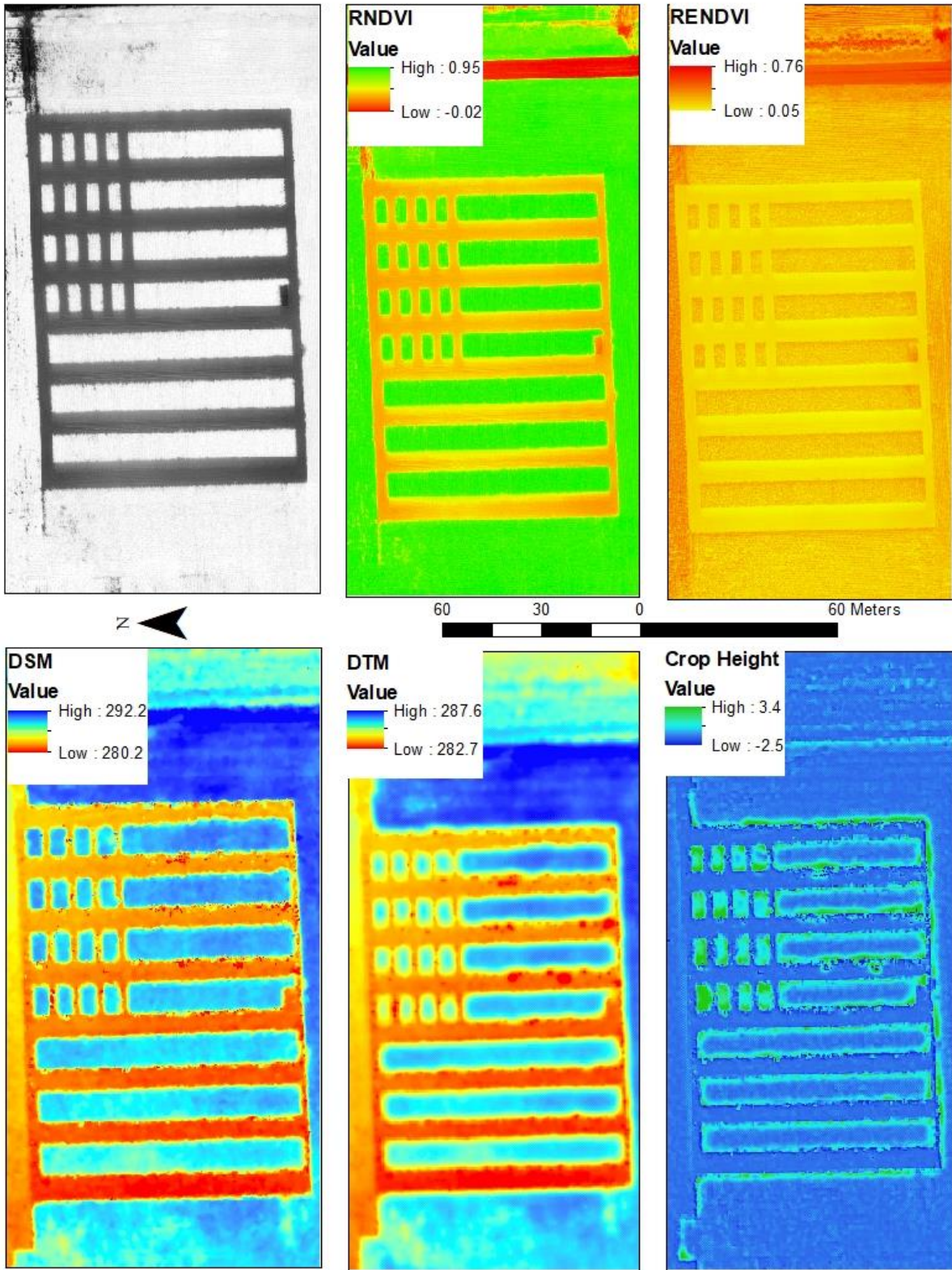
131

Figure A27. Sabin June 28 2018 experimental site SUAS imagery produced with Pix4D and ArcGIS (Black/White; RNDVI; RENDVI: DSM (Meters); DTM (Meters); Crop Height (Meters)).

Figure A28. Sabin July 5 2018 experimental site SUAS imagery produced with Pix4D and ArcGIS (Black/White; RNDVI; RENDVI: DSM (Meters); DTM (Meters); Crop Height (Meters)).

Figure A29. Sabin July 12 2018 experimental site SUAS imagery produced with Pix4D and
ArcGIS (Black/White; RNDVI; RENDVI: DSM (Meters); DTM (Meters); Crop Height
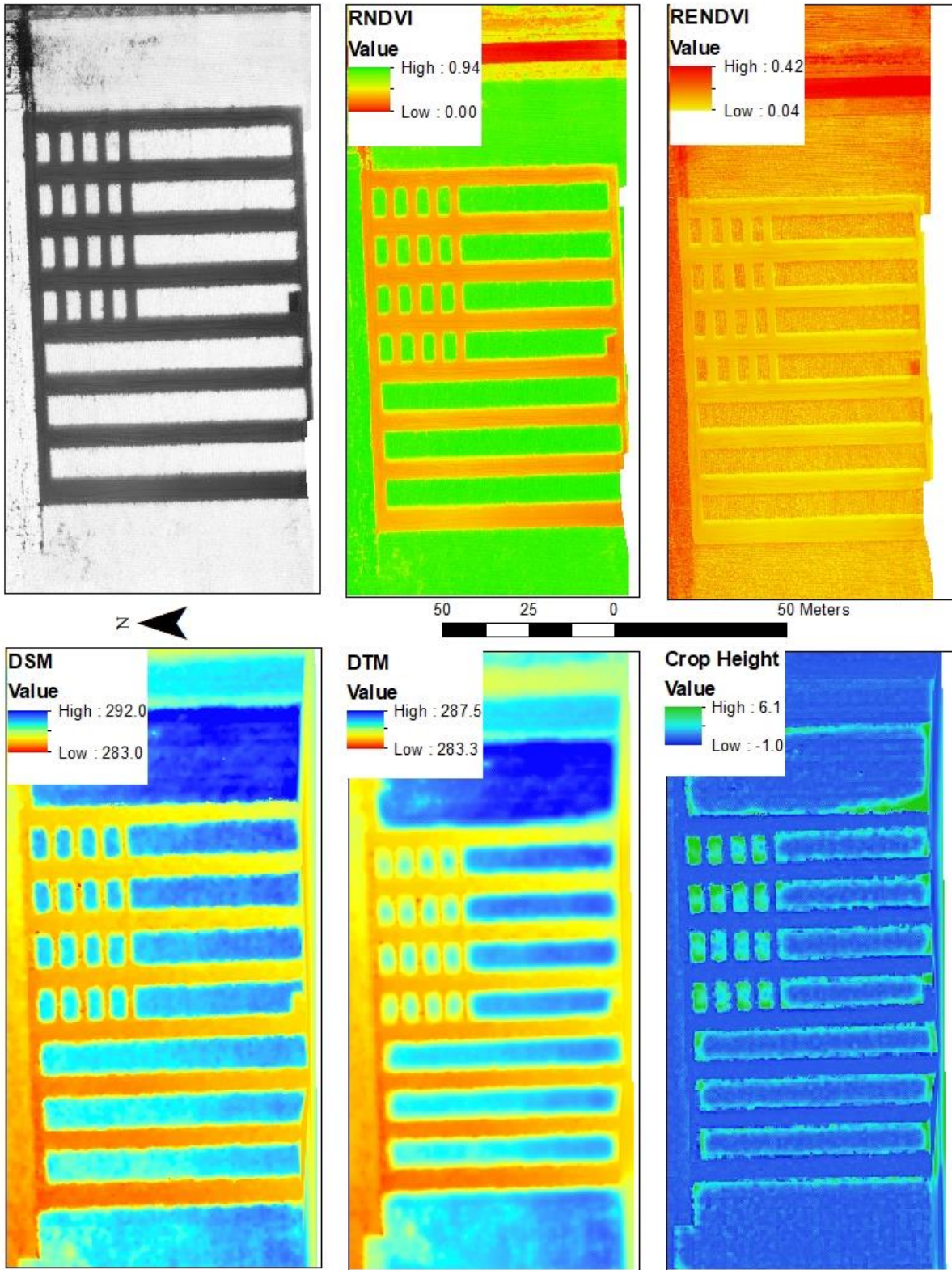(Meters)).

134

Figure A30. Sabin July 18 2018 experimental site SUAS imagery produced with Pix4D and ArcGIS (Black/White; RNDVI; RENDVI: DSM (Meters); DTM (Meters); Crop Height (Meters)).
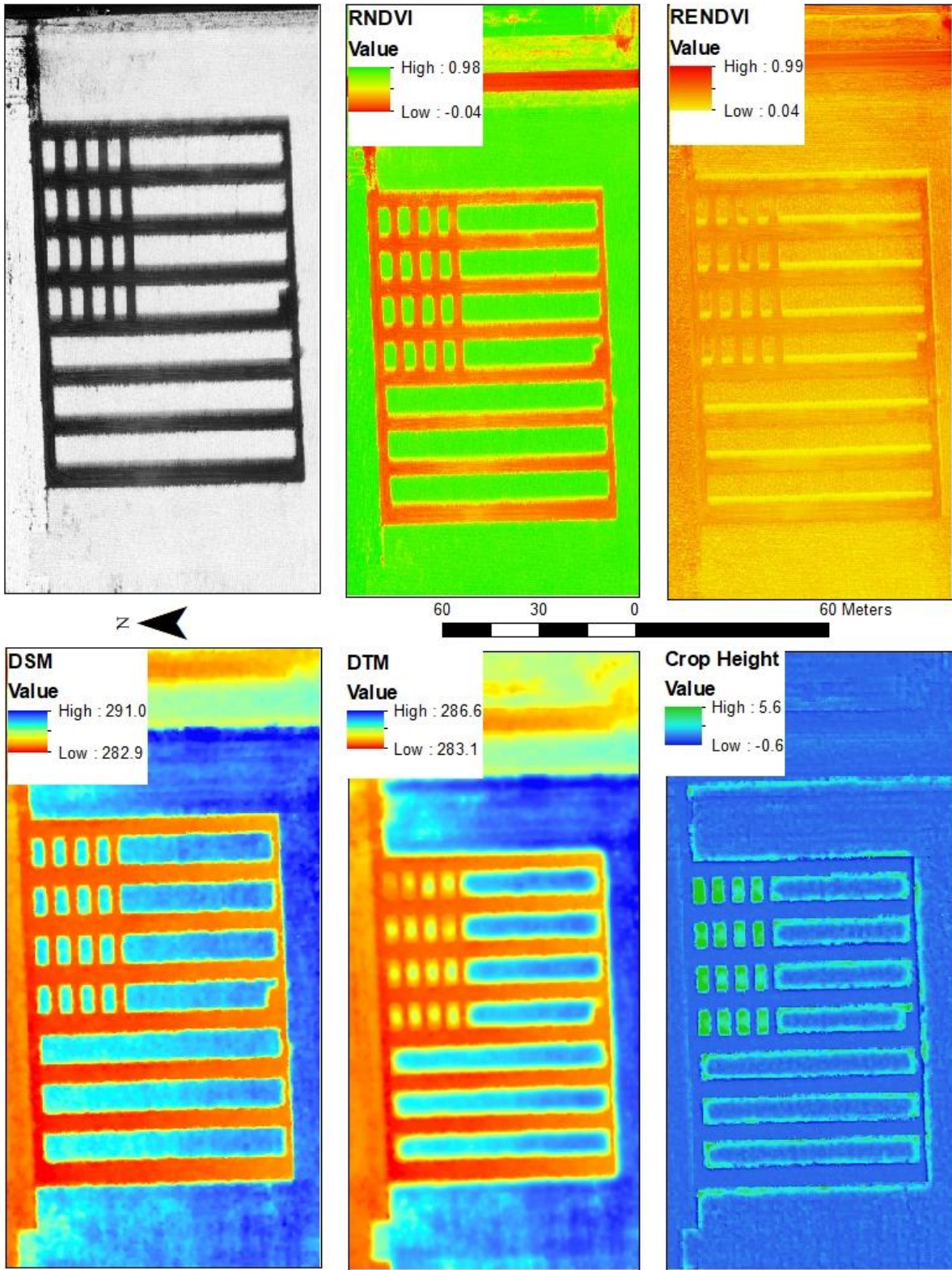
135

Figure A31. Sabin July 27 2018 experimental site SUAS imagery produced with Pix4D and ArcGIS (Black/White; RNDVI; RENDVI: DSM (Meters); DTM (Meters); Crop Height (Meters)).